Chemotaxis and phototaxis of gametes in brown algae having two heterogeneous flagella

（2 本の異質鞭毛を有する褐藻配偶子の走化性と走光性）

by

Nana Terauchi

Division of Biosphere Science,

Graduate school of Environmental Science,

Hokkaido University

Contents

Acknowledgements

Special thanks go to my supervisor Prof. Taizo Motomura (Graduate school of Environmental Science, Hokkaido University) for guiding me through algal culturing, TEM, SEM, IMF and providing me many equipment that I need for my work. More than anything, I would like to thank for giving me advises on my works, encouraging me to do research. Another special thanks go to Associate Prof. Chikako Nagasato (Graduate school of Environmental Science, Hokkaido University) for providing me helpful suggestions, caring me in daily life and reading of this thesis. I also would like to appreciate to Prof. Etsuro Yamaha (Graduate school of Environmental Science, Hokkaido University) and Prof. Takeo Horiguchi (Department of Biological Sciences, Faculty of Science, Hokkaido University) for their valuable suggestions and critical reading of this thesis.

Especially, in technical ways, I am deeply grateful to Assistant Prof. Kogiku Shiba and Prof. Kazuo Inaba (Shimoda Marine Research Center, Tsukuba University) who taught me high-speed video recording techniques and gave me helpful suggestions through all my works. I also thank to Associate Prof. Taiki Umezawa (Graduate school of Environmental Science, Hokkaido University) for providing me synthesized sex pheromones of brown algae, technician Mr. Toshiaki Ito (Electron Microscope Laboratory, Research Faculty of Agriculture, Hokkaido University) who taught and helped me about electron tomography, Dr. Osamu Kutomi (Yamanashi University) for giving me suggestions on the observation media, Prof. Mineo Iseki (Toho University) for advising on the illumination system, Prof. Tatsuya Togashi (Chiba University) for helpful discussions about phototaxis, Mr. Toyoki Iwao (Fisheries Science Center of Toba) and Prof. Akira Kurashima (Mie University) for collecting *Mutimo cylindricus*.

All my work would not have been accomplished without a number of people who gave me invaluable comments. It is not just about my work but also to my daily life of my PhD. Particular thanks go to my seniors Dr. Fu Gang (University of Texas Southwestern Medical Center, USA) and Dr. Makoto Terauchi (Kobe University) who guided me through molecular works and gave me helpful discussions and suggestions. My deepest appreciation also goes to other lab members and

visitors, Dr. Tatyana Klochkova (Kamchatka State Technical University, Russia), Dr. Kazumasa Yamada (Prefectural University of Kumamoto), Mr. Yuki Katayama, Mr. Hiroki Kawamoto, Mr. Shen Yuan, Assistant Prof. Hisanori Iwai (Osaka Prefecture University), Ms. Laure Mignerot (Station Biologique de Roscoff, France) for their kindness and giving me a peace of mind. I also appreciate the staffs in Muroran Marine Station, Ms. Saeko Kitabayashi, Mr. Teruo Tomioka, Assistant Prof. Atsuko Tanaka (Ryukyu University), Ms. Hiromi Kato, Ms. Naoko Hashizume for caring me in my daily life and heartfelt supports.

Finally, my deep thanks goes to my parents, Ms. Miki Kinoshita and Dr. Yoshihiro Kinoshita for their financial and mental supports in my whole life.

General introduction

Most brown algae (Phaeophyceae, Heterokontophyta) live in marine habitats (Plates 1, 2). They are multicellular photosynthetic eukaryotes belonging to the stramenopiles, which are phylogenetically distant from the opisthokonts (animals and fungi) and the archaeplastida (land plants, green and red algae and glaucophytes) (Adl et al. 2012). Brown algae exhibit three types of sexual reproduction: isogamy (equally sized male and female gametes), anisogamy (female gametes larger than male gametes), and oogamy (sperm and eggs) (Wynne and Loiseaux 1976; Luthringer et al. 2014). Evolutionary pathways of isogamy to anisogamy and oogamy have been widely accepted, especially in the volvocine green algae (Nozaki et al. 2014). However, in the phylogenetic analysis of brown algae, the patterns of sexual reproduction have changed multiple times during their evolution (Silberfeld et al. 2010).

Brown algae usually undergo alterations of their generations between sporophytes and gametophytes (Plate 3). Both generations produce reproductive cells, unispores or tetraspores, with meiosis from the sporophytes, and male and female gametes (sperm and eggs) from the gametophytes. In contrast to the unicellular phytoplankton, brown algal swarmers can swim for a short time after liberation from the mother thalli. For example, zoospores of the laminarialean species swim for at least 24 hours under suitable conditions (Henry and Cole 1982a), while male and female gametes of *Cutleria multifida* swim for almost 20 h and 5 min to 2 h, respectively (Yamanouchi 1912).

Brown algal swarmers take the advantage of several kinds of taxis against physico-chemical signals (Plate 4). For example, Amsler and Neushul (1989, 1990) reported that zoospores of *Macrocystis pyrifera* swam towards ammonium, glycine, aspartate, iron, boron, cobalt, and manganese to find adaptive habitats for gametophyte generations. Male gametes (or sperm) need to find and fuse to female gametes (or eggs), whereas to find a partner or adaptive habitat, brown algal swarmers and many motile microorganisms have been known to respond to a variety of physical and chemical parameters in their environment: light, chemicals, temperature gradients, and the earth's magnetic and gravitational fields (Nultsch and Häder 1988).

Ultrastructures of flagella in brown algae

Swimming direction and reactions to physico-chemical stimuli (phototaxis and chemotaxis) of unicellular flagellates, including animal sperm, are driven by the bending waves of flagella. The flagellar axonemes show a well-conserved structure in many eukaryotes: 9+2 microtubules, axonemal dynein, and regulatory structures such as a central apparatus and radial spokes (Gibbons 1981) (Plate 5). Flagellar bending is generated by the propagation of sliding of doublet microtubules by axonemal dyneins (Gibbons and Gibbons 1973; Brokaw 1979; Brokaw and Kamiya 1987; Inaba 2003; Lindemann 2004; Inaba 2011). The swarmers of stramenopiles, including brown algae, generally possess two heterogenous flagella elongated from a pair of flagellar basal bodies at the ventral side of the cell (Andersen 2004). The anterior flagellum (AF) possesses tubular hairs (tripartite mastigonemes) and elongates towards the forward direction (Jahn et al. 1964; Holwill and Sleigh 1967; Bouck 1969). Composed proteins of the mastigonemes (OCM family) were identified in the chrysophycean unicellular alga, *Ochromonas danica* (Yamagishi et al. 2007, 2009). The posterior flagellum (PF) elongates towards the backward direction. In several cases, the basal part of the PF becomes swollen, which is called the paraflagellar body (Kawai 1992a; Maier 1995; Kawai and Kreimer 2000). Zoospores and gametes of brown algae usually have a long AF and a short PF. However, sperm of Laminariales, Sporochnales, Desmarestiales, and some Fucales characteristically have a longer PF than AF (Kawai 1992a). The sperm in Dictyotales are an exceptional case as they have only an AF.

The structural information of flagellar apparatus is very important for thinking about flagellar waveforms and to know the precise positions of proteins. However, many of the works about structures of flagellar apparatus had been accumulated, still the precise positions and the shape of complex structures connecting to basal bodies had not been clearly revealed.

Recognition of male and female gametes

In isogamous species, female gametes initially settle down on the substratum, become round by drawing the flagella into the cell, and secrete the sex pheromone which attracts male gametes (Müller 1977, 1979) (Plate 14). After gathering around female gametes, male gametes anchor

themselves to the surface of the female gamete with the tip of the AF and one of them usually fuses with the female gamete (Müller and Falk 1973; Müller 1978; Geller and Müller 1981). On their tip, the AF and PF have a thin whiplash called the acronema, which is composed of an elongation of two central microtubules of the flagellar axoneme (Henry and Cole 1982a, b). The acronema of the AF in particular is very long (10–13 μm long) and is easily detached by fixation. Cell-cell recognition between male and female gametes was reported to be mediated by the N-acetylglucosamin-containing glycoprotein on the plasma membrane of the female gametes and the lectin-like sugar binding protein on the tip of the AF of male gametes (Schmid 1993; Schmid et al. 1994). Maier and Schmid (1995) performed an immunological labeling on binding sites of various lectins, and revealed that concanavalin A (Con A) and aleuria aurantia agglutinin (AAA) strongly binded to the AF of *Ectocarpus* gametes. In the comparative transcriptome analysis of male and female gametes, and immature gametophytes and sporophytes of *Ectocarpus*, 109 male gamete-specific genes were identified (Lipinska et al. 2016). Among 109 genes coding for extracellular or cell surface proteins, 12 genes were identified as putative gamete recognition genes. Lipinska et al. (2016) also suggested a candidate gene (Esi0130_0068), which functions in gamete recognition in *Ectocarpus siliculosus*. This contained six or seven transmembrane domains, and had an REG (receptor for egg jelly) and GPS (G-protein-coupled receptor proteolytic site) domain, and PCC (polycystin cation channel) family.

In anisogamy, fertilization occurs in the mostly same manner as isogamy (Kitayama et al. 1992; Nagasato et al. 1998). In oogamy, eggs started to release the sex pheromone after they were released from the oogonia in the Laminariales (Müller et al. 1979; Lüning 1981), and the sex pheromone, lamoxiren, could induce the liberation of sperm from the antheridia (Maier and Müller 1982).

Twelve sex pheromones of brown algae have been identified, and these are, more or less, unsaturated C8- and, more commonly, C11-hydrocarbons (Plate 13). The pheromones are not always specific at the species and genus levels, but are probably specific for higher taxonomic categories like families and orders (Kochert 1978; Maier 1993; Maier 1995). The model of the green alga *Chlamydomonas reinhardtii* is well-studied and lacks the sex pheromone, therefore the mating

process depends on successful random encounters between compatible cells. However, the oogamous species of *Chlamydomonas* is known to release a sex pheromone (lurlenic acid, lurlenol) (Frenkel et al. 2014). The receptor for the sperm attractant (resact) in sea urchins was identified and characterized as a transmembrane-type guanylylcyclase (GC) (Singh et al. 1988), as was the receptor for the sperm attractant (asterosap) of the starfish (Nishigaki et al. 2000). These receptors are almost localized exclusively on the flagella (Cardullo et al. 1994; Nishigaki et al. 2000). In brown algae, the receptors in male gametes that receive the female gamete sex pheromones remain unknown.

Locomotion responses of male gametes to the sex pheromone in brown algae

In brown algae, the swimming path and flagellar waveforms of male gametes change in response to sex pheromones from female gametes during fertilization. In isogamy, male gametes initially change their swimming patterns from free to thigmotactic swimming in the presence of the sex pheromone. Free-swimming is when the male gametes swim without touching anything by rotating their cell body, while thigmotactic swimming is when they swim near the substratum without rotating their cell body (Müller 1978). The asymmetry rates of the AF waveforms increase, and the unilateral beats of PF frequently occur by the sex pheromone (Geller and Müller 1981). Consequently, the male gametes showing thigmotactic swimming form small clock-wise circular paths, viewing from the ventral side of their cell bodies. Exact locomotion response in anisogamous species is not clarified. Sperm in oogamous species such as *Laminaria digitata, Fucus spiralis*, have a longer PF than AF, show a characteristic turning when they sense a "gradient decrease" in the sex pheromone (Maier and Müller 1986; Maier and Müller 1990). Similar to isogamy, the sperm of *Hormosira banksii*, with a longer AF than PF, also showed characteristic turning (Maier et al. 1992).

Basic information of locomotion response in male gametes to the sex pheromone is accumulated, except anisogamous species. However, further works such as physiological experiments need more precise quantitative data.

Blue-light reception of brown algal swarmers

In intertidal habitats, brown algae use the limited range of light wavelength from blue light to a

shorter wavelength that penetrates deeper into seawater (Plate 4). Many studies have been conducted on the blue light response of brown algae. For example, in the laminarialean species, blue light induces the maturation of male and female gametophytes (Dring and Lüning 1975; Dring 1988). Moreover, in *Silvetia compressa*, blue and green lights induce the release of gametes (Pearson et al. 2004). Phototaxis of brown algal swarmers is induced by blue light. Under blue light excitation, a strong green auto-fluorescence can be observed on the PF, especially near the paraflagellar body, in various brown algal swarmers (Table 1). Swarmers having an eyespot (stigma) in the chloroplast and PF having the green autofluorescence, exhibit phototaxis (Müller et al. 1987; Coleman 1988; Kawai 1988; Fu et al. 2016). This substance was suggested to be flavin-binding protein (Müller et al. 1987; Kawai 1992b). Consequently, the blue light receptor has been hypothesized to be a flavoprotein that is present in the PF. The swollen paraflagellar body of PF is closely associated with the concaved stigma, and is composed of two parts: electron dense material and crystalized material (Maier 1997a, b; Fu et al. 2013, 2014). The stigma of swarmers is visible as an orange spot under the light microscope, and is presumed to reflect and focus light on the photoreceptor (Kreimer et al. 1991).

From an analysis of isolated flagella of brown algal swarmers, *Scytosiphon lomentaria*, Fujita et al. (2005) suggested a candidate blue light photoreceptor, a 41-kDa flavoprotein, which is homologous to the Old yellow enzyme. Later, from a proteome analysis using flagella of *Colpomenia bullosa*, Fu et al. (2014) revealed another candidate photoreceptor, a 167-kDa LOV (Light-oxygen-voltage-sensing)/RGS (Regulators of G protein signaling) containing protein, helmchrome, which was detected in the PF fraction, and its localization in the PF was confirmed by an immunological experiment. Moreover, helmchrome was found in the PF of various phototactic species of brown algal swarmers (Fu et al. 2016). The LOV domain is a ubiquitous class of photoreceptors for sensing blue light, which can be detected in various organisms (Glantz et al. 2016; Takahashi 2016). However, in brown algal swarmers, the function of any photoreceptor related to phototaxis has not been characterized in vivo.

Locomotion responses to light in brown algal swarmers

The behaviors of microorganisms, including brown algal swarmers, in the natural habitat, are the

result of a delicate balance between positive (movement toward the light source) and negative phototaxis (away from the light source) (Häder 1988) (Plate 4). For example, bi-flagellated male and female gametes of the green alga, *Monostroma angicava*, show a positive phototaxis towards the water surface to increase the rate of fertilization (Togashi and Bartelt 2011). After fertilization (planogamy), quadri-flagellated zygotes show a negative phototaxis for settlement on the substratum. Although planogamy is widely documented in green algae, this does not occur in brown algae (Maier 1995). According to field experiments using non-phototactic brown algal swarmers of *Macrocystis pyrifera* and *Pterygophora californica* and positively phototactic swarmers of *Ectocarpus siliculosus*, the latter were more dispersed than the former and contributed to increase in diffusion and expansion of the habitat of brown algae (Reed et al. 1988). However, negative phototaxis of swarmers probably leads to an attachment to the substratum (Amsler et al. 1992; Fletcher and Callow 1992).

The analysis of the action spectrum on the phototactic response of brown algal swarmers showed that the major peaks are ca. 430 and 460 nm in *E. siliculosus* gametes (Kawai et al. 1990), ca. 420 and 460 nm in *Pseudochorda gracilis* zoospores (Kawai et al. 1991), and 450 nm in *S. lomentaria* and *Petalonia fascia* (Flores-Moya et al. 2002). Thus, it is believed that a blue light perceiving system (photoreceptor) for phototaxis exists in brown algae. Light triggered-transitory flagellar motions of swarmers in *S. lomentaria* were studied using infrared high-speed microscopy (Matsunaga et al. 2010). An obvious change in the swimming direction of swarmers was observed 100–160 ms after the onset of unidirectional blue light (437 nm). During this period, a brief cessation of AF movement and the large unilateral bend of the PF were observed after which, swarmers moved towards the light source (positive phototaxis). Unfortunately, the signaling pathway that converts photoreception to flagellar waveforms remains unclear at present.

In the green alga *C. reinhardtii*, the sign (negative or positive) of phototaxis is affected by several extracellular factors such as light intensity (Feinleib and Curry 1971) and extracellular calcium ion (Ca^{2+}) concentration (Morel-Laurens 1987). Moreover, intracellular conditions such as photosynthetic activity (Takahashi and Watanabe 1993) and reduction-oxidation poise (Wakabayashi et al. 2011) change the sign of phototaxis. In *Ochromonas danica*, the sign of

phototaxis is affected by light intensity (Häder et al. 1981). However, in brown algae, light intensity ($4 \cdot 10^{-3}$–$3.6 \cdot 10^{3}$ μmol photons $m^{-2}s^{-1}$) and wavelength (350–650 nm) did not affect the sign of phototaxis in the gametes of *E. siliculosus* (Kawai et al. 1990). Under too low (＜10 μmol photons m^{-2} s^{-1}) or too high (>190 μmol photons m^{-2} s^{-1}) light intensity, swarmers of *S. lomentaria* do not show phototaxis (Flores-Moya et al. 2002). Although balance between positive and negative phototaxis is very important factor for survival of brown algae, the factors that alter the sign of phototaxis in brown algal swarmers have not been reported.

In this study, using several kinds of brown algal gametes (Plates 1, 2), followings were analyzed:

Chapter 1 To make the basic structural information of flagella and basal bodies in male gametes of the isogamous brown alga, I firstly defined the precise position and association of several structures, such as microtubular flagellar rootlets, bands, and fibrous structures, existing near basal bodies, using *Ectocarpus* gametes by electron tomography.

Chapter 2 To reveal the precise chemotactic behaviors of male gametes in isogamy (Part 2. 1), anisogamy (Part 2. 2) and oogamy (Part 2. 3), quantitative analysis of their locomotion and flagellar waveforms were performed using a high-speed video recording system, and comparative analysis of them and other organisms were conducted.

Chapter 3 To clarify the regulation of phototactic sign, especially focusing on relation to Ca^{2+} (Part 3. 1) and sex pheromone (Part 3. 2), phototactic behaviors of male gametes were quantitatively analyzed. Finally, general conclusions on these results and perspectives for the future studies were described.

Chapter 1

Three-dimensional organization of flagellar basal apparatus in *Ectocarpus* gametes

Introduction

Sophisticated flagellum and basal apparatus regulate the locomotion of swarmers, including various unicellular algae, protozoa, gametes and zoospores of algae, and animal sperm. Motile gametes and zoospores of brown algae usually have two different flagella: the anterior flagellum and the posterior one (Kawai 1992a) (Plate 5a). Flagella of brown algal gametes are crucial for phototaxis (Kawai and Kreimer 2000; Matsunaga et al. 2010), chemotaxis (Geller and Müller 1981; Maier and Müller 1990; Kreimer 1994), and the first contact between male and female gametes (Müller and Falk 1973).

The ultrastructure of flagella and basal apparatus of the brown algae has been examined extensively (Manton 1956, 1957, 1959, 1964; Manton and Clarke 1950, 1951, 1956; Cheignon 1964; Henry and Cole 1982a, b; O'Kelly and Floyd 1984; Motomura 1989; O'Kelly 1989; Maier 1997a, b). The flagellar basal apparatus of *Laminaria digitata* (Hudson) J. V. Lamouroux zoospores and *Ectocarpus siliculosus* (Dillwyn) Lyngbye male gametes were observed by O'Kelly and Floyd (1984), O'Kelly (1989) and Maier (1997b), respectively, who made schematic representations with the number of microtubules (MTs) in each of the microtubular flagellar rootlets and the morphology of several bands connecting two flagellar basal bodies. Moestrup (2000) proposed a new numbering system of the flagellar basal bodies and the rootles in various algal groups. These authors obtained basic structural information on flagellar basal apparatus of the brown algal swarmers using conventional transmission electron microscopy and chemical fixation methods. However, such methods have a limited resolution, and a higher resolution would be necessary to observe the microstructural features in detail.

It is known that numbering system for doublet MTs of the axoneme can provide a better understanding of the spatial arrangement of flagellum and basal apparatus, as well as the flagellar movement (Wooly 2010). In this study, electron tomography to re-observe the spatial relation of each flagellar component in *E. siliculosus* gametes under a high-resolution was performed. Moreover, a numbering system comprising nine triplet MTs of basal bodies was adapted to identify the precise

position of these flagellar components.

Materials and Methods

Plant material and laboratory culture

A gametophyte of *E. siliculosus* (Es400 male) was obtained from Dr. A. F. Peters (Bezhin Rosko, France) and was cultured in half strength PES medium (Provasoli 1968) under cool-white fluorescent lamps (30–40 μmol m^{-2} s^{-1}) at 15°C in long day condition (14 h light:10 h dark). To induce the release of gametes, fertile gametophytes bearing mature plurilocular gametangia were transferred to Petri dishes filled with new culture medium. After 2–3 days, gametes were released from plurilocular gametangia 2 h after light on. Liberated gametes were collected into 1.5 mL microtubes using a micropipette.

Transmission electron microscopy

Freeze fixation and freeze substitution were conducted as previously described by Nagasato and Motomura (2002) and Ueki et al. (2008) with some modifications. Released male gametes were spun down (6000 *g*, 1 min, 4°C) (Himac CF 15R, Hitachi, Tokyo, Japan) and the pellet of gametes was placed on formvar-coated gold loops (5–10 mm diameter). Samples were rapidly frozen by placing the loop into liquid propane pre-cooled to -180°C. The loop was transferred to liquid nitrogen, and then submerged in cooled acetone (-85°C) containing 4% OsO_4. After 2 days, the samples were transferred to -20°C for 2 h, followed by 4°C for 2 h, and finally to the room temperature. They were detached from the formvar-coated gold loops, washed several times with acetone at room temperature, and infiltrated with Spurr's epoxy resin at room temperature using the following conditions: 20% resin in acetone for 12 h; 30% for 5 h; 40% for 5 h; 50% for 12 h; 70% for 5 h; 80% for 5 h; and 100% for 2 days. The final two steps of infiltration were carried out in desiccators. Samples were finally embedded in Spurr's epoxy resin on dishes made of aluminum foil. Successfully frozen samples were selected using a light microscope, and serial sections were cut using a diamond knife (Micro Star, Micro Star Tech, TX, USA) on an ULTRACUT ultramicrotome (Reichert-Jung, Depew, NY, USA). The serial sections were mounted on formvar-coated slot grids,

stained with TI blue (Nisshin EM Corporation, Tokyo, Japan) for 40 min at room temperature, followed by lead citrate (Reynolds 1963) for 10 min at room temperature. Finally, they were observed using JEM-1011 electron microscope (JEOL, Tokyo, Japan).

Electron tomography

Serial sections (90–190 nm) were cut for JEM-2100 electron microscope (JEOL, Tokyo, Japan). The sections were mounted on formvar-coated one-slot grid and stained with 5% hafnium tetrachloride in 100% methanol for 40 min, followed by lead citrate staining for 10 min at room temperature, or stained with 2% uranyl acetate for 1 h at 60°C and lead citrate for 3 min at room temperature. After staining, the side of the grid carrying sections was coated with formvar to sandwich them. Then, 15 nm colloidal gold particles were attached to both sides of the grid, and the grids were coated with carbon on both sides. These samples were used to obtain tilted images for tomographic analysis.

Image acquisition and analysis

Samples were placed on a tilt-rotate specimen holder and observed using the JEM-2100 electron microscope with 200 kV acceleration voltages. Specimens were oriented from -60° to 60° at 1° interval and images were captured using a Veleta digital camera with a resolution of 2,048 × 2,048 pixels (Olympus Soft Imaging Solutions, Münster, Germany) at ×50,000, ×80,000 and ×100,000 magnification, and the pixel sizes were 1.254 nm, 0.784 nm and 0.627 nm, respectively. Dual-axis electron tomography was performed around two orthogonal axes in order to obtain high resolution images and to reduce the "missing wedge" artifact (Mastronarde 1997).

Using the colloidal gold particles as fiducial markers, the tilt series (2D images) were aligned and combined to reconstruct a double-axis tomogram using the computer software IMOD (Kremer and Mastronarde 1996).

Results and discussion

In this study, the ultrastructure of the flagellar basal body in *E. siliculosus* from 23 tomograms was observed. The schematic representation of the flagellar apparatus is shown in Plate 6. The

terminology by O'Kelly and Floyd (1984), Maier (1997b) and Moestrup (2000) were adopted for the components of the flagellar basal apparatus. The flagellar basal body was located at the center of the cell's ventral surface, in close association with the nucleus, chloroplast, and Golgi body. The longitudinal axes of two basal bodies, as well as the anterior flagellar basal body (AB) and the posterior flagellar basal body (PB) were arranged more or less parallel to the ventral surface of the cell, but not on the co-planar position (Plates 7–10). When viewed from the dorsal face of the cell, the PB always appeared to the left of the AB (Plate 8a–h). The PB was dorsally shifted by approximately one-third of the basal body diameter (Plate 8i–k).

The spatial arrangements of all rootles were analyzed using more than three tomograms. All microtubular rootlets, a major anterior rootlet (MAR, R3), a minor anterior rootlet (mar, R4), a major posterior rootlet (MPR, R2), a minor posterior rootlet (mpr, R1), and a bypassing rootlet (BR), were closely associated with AB and PB (Plate 8a–h). The mar, which was composed of a single microtubule (MT), originated from the left side of AB and extended anterior along the left side of AB (Plate 8d, e) from the dorsal view. The angle between the longitudinal axis of AB and the mar measured about 20°, and the basal part of the mar directly attached to the proximal part of the AB and PB (Plate 8d, e). Cap structure could not be detected at the basal end of MT of the mar. The mpr, which was composed of a single MT, originated from a deltoid striated band (DB) (O'Kelly and Floyd 1984; Maier 1997b), and extended toward the left side of the cell at an angle of about 10° to the longitudinal axes of PB (Plate 8d–g). The original MAR component was composed of approximately 8 MTs and attached to AB with darkly stained material (Maier 1997b). This structure could be clearly observed by electron tomography (Plate 8d, e, double arrowheads). Connecting structures of AB-BR and AB-mar were detected (Plate 8i–k). The MPR originated at the posterior fibrous band (pfb) near the PB and was composed of three MTs (O'Kelly and Floyd 1984; Maier 1997b) (Plate 8h, Plate 9b, c).

When viewed from the dorsal side, striated strap-shaped band (SB) was observed. It spread from the proximal parts of AB to PB (Plates 8b, c, 10a–d), and the darkly stained V-shaped segment was conspicuous (Plate 8b, c). The deltoid striated band (DB) was observed between AB and PB (Plates 8f, 9d, 10f–h). It was mainly attached to the proximal part of PB and mpr. It showed a regular

striation pattern, which had a periodicity in the range of 29–44 nm from analyses of two tomographs. All flagellar rootlets were attached to these bands and connected to AB or PB. Therefore, these bands might have a role to maintain spatial arrangement of AB, PB, and the rootlet MTs. A connecting structure between PB and the chloroplast was observed in two tomograms (Plate10i–k). Katsaros et al. (1993) suggested that in *E. siliculosus* gametes nucleus-basal body connector, DB and SB contained centrin, which is Ca^{2+}-mediated contractile protein (Salisbury et al. 1984, 1988). Nagasato and Motomura (2004) reported that centrin was localized between the proximal sites of AB and PB in gametes of *Scytosiphon lomentaria* (Lyngbye) Link.

Basal plates of AB and PB showed the same appearance and existed at their distal parts. They were plate-like structures with small holes attached to the plasma membrane. Moreover, electron dense material accumulated at the center of the plate, and attached to the central pair of flagellar axoneme (Plates 8f, g, 9c, d).

There are two numbering systems for designating doublet MTs in the flagellar axonemes (Lin et al. 2012). In sea urchin sperm flagella, axoneme of doublet No. 1 was decided as a doublet MT that located at an equal distance from the central pair, and numbering proceeded in the direction of the dynein arms (Afzelius 1959; Sale 1986). The remaining eight doublets were consecutively numbered in a clockwise direction when observing the flagellum from the proximal to the distal sides. A bridge exists between doublet MTs No. 5 and No. 6. Another numbering system is based on the flagella of the green alga *Chlamydomonas reinhardtii* Dangeard (Hoops and Witman 1983; Bui et al. 2009). In *Chlamydomonas* flagella, beak-like structure can be detected in three out of nine doublet MTs. One of these three doublet MTs, marked as No.1, characteristically lack outer dynein arm, and eight doublets were consecutively labeled in clockwise direction, similar to the case of sea urchin's sperm. There is a bridge between No.1 and No. 2 doublet MTs. Melkonian (1984) widely adopted this flagellar numbering system for the green algae. However, flagellar axoneme of the brown algal swarmers does not possess morphologically distinct doublet MTs. Fu et al. (2013) defined doublet No. 1 as a line extending through the central pair of MTs of the axoneme, at the level of the paraflagellar body of PF, and consecutively labeled the rest of the doublet MTs in a clockwise direction, when observing the flagellum from the distal to the proximal sides. In the

present study, doublet MTs in a clockwise direction were consecutively labeled when observing the flagellum from the proximal side to the distal one, after doublet No. 1 was decided as a doublet MT that located at an equal distance from the central pair (Afzelius 1959).

A numbering system of the basal body triplets could be adopted by tracing flagellar axonemal doublets in serial sections (Plate11). PB existed against the side of No. 7–9 triplet MTs of AB (Plate 11e, f). The MAR and BR were passing near the side of No. 2–4 of AB and No. 5–7 of AB, respectively (Plate11c, e, f). The mar existed between No. 8 and No. 9 of AB (Plate11f). The MPR and BR were passing near the side of No. 5–7 of PF (Plate11g). The DB and SB were attached to No. 7–8 and No. 9–1 of AB, respectively (Plate11e, f). Fibrous material was elongated from a part of the chloroplast to No. 1 of PB (Plate 11h). Eyespot and crystallized material region in the paraflagellar body (Fu et al. 2013) were facing to the side of No. 6–9 of PF (Plate 11i). These data will facilitate the precise mapping of previously identified structures, as well as novel basal apparatus proteins.

Chapter 2 Chemotactic behaviors of male gametes in brown algae

Part 2. 1 Chemotaxis in the isogamous brown alga *Ectocarpus siliculosus*

Introduction

Motile gametes of the brown algae usually have two heterogeneous flagella, a long anterior flagellum (AF) and a short posterior flagellum (PF) (Clayton 1989; O' Kelly 1989; Anderson 2004) (Plate12). The AF is decorated with mastigonemes and generates a force for moving forward of gametes (Jahn et al. 1964; Holwill and Sleigh 1967; Bouck 1969). The PF frequently has a basal swelling part (paraflagellar body), and provides rapid lateral beats for changing the direction of the cell movement (Maier 1995; Kawai and Kreimer 2000).

Chemotactic responses of male gametes to a sex pheromone from settled female gametes have been studied for many years in the isogamous brown alga, *Ectocarpus siliculosus* (Müller and Falk 1973; Müller 1978; Geller and Müller 1981). First, female gametes shortly settle on the substratum and secrete the sex pheromone 'ectocarpen' (Müller 1967; Müller et al. 1971) (Plates 13, 14). Second, free-swimming male gametes began to swim in close contact with the surface of slide glass or cover slip. This response is enhanced by the presence of the sex pheromone from the female gamete, and is regarded as thigmotaxis (Müller 1978; Geller and Müller 1981). The swimming velocity of male gametes decreased, and the swimming radius became smaller. Third, the male gamete changes the AF waveform, which causes the cell body to move in circular paths under existence of the sex pheromone. This behavior of the male gamete is regarded as chemokinesis (Maier 1993, 1995). PF of the male gamete performs fast, unilateral beating, when it detects a decrease of the sex pheromone concentration gradients. This PF behavior results in a reorientation towards the pheromone source and is defined as chemoklinotaxis (Maier 1993, 1995). Afterwards, the male gamete anchors itself with the tip of the AF on the surface of the female gamete, and finally, the male gamete fuses to the female one (Müller and Falk 1973) (Plate 15). Therefore, the AF and PF of male gametes have crucial roles in approach and contact with female gametes.

Geller and Müller (1981) firstly reported that the AF of male gametes in *E. siliculosus* perform asymmetric bending in the presence of the sex pheromone, which shows a negative linear

correlation between the average of deflection angle of the AF from the cell axis and the radius of the track of the male gametes during chemokinesis. Their analysis was based on measuring the deflection of the first visible bend of the AF from the cell axis**.** However, information on the flagellar waveform of brown algae has been limited compared to the case of metazoa (Gibbons 1981; Inaba 2003) and the green alga, *Chlamydomonas* (Mitchell 2000). Analyses of flagellar waveforms in sperm of marine invertebrates using high-speed camera revealed that flagellar waveforms became asymmetric when sperm changed the swimming direction toward the sex pheromone source. Their flagellar waveforms remained symmetric when sperm swam directly toward the pheromone source (Miller and Brokaw 1970; Miller 1975, 1977). It has been reported that Ca^{2+} was a primary factor regulating the symmetry and asymmetry of flagellar waveforms (Kaupp et al. 2008; Yoshida and Yoshida 2011).

In this part, swimming paths and two heterogeneous flagellar waveforms of male and female gametes of the brown alga *E. siliculosus* were quantitatively analyzed using a high-speed camera, focusing on free- and thigmotactic-swimming male and female gametes and chemotactic-swimming male gametes to understand the more precise relationship between AF and PF waveforms of male gametes during fertilization in brown algae.

Materials and Methods

Preparation of gametes

Male and female gametophytes (strain Ec32m and Ec25f) of *Ectocarpus siliculosus* were gifts from Drs Peters, A. F. (Bezhin Rosko, France) and Coelho, S. M. (UMR 7139 CNRS-UPMC, Station Biologique de Roscoff, France). These gametophytes were cultured in the half strength PES medium (Provasoli 1968) under cool white fluorescent lamps (30–40 μmol m^{-2} s^{-1}) at 15 ˚C in long day conditions (14 h light:10 h dark). Two days after changing to new medium, gametes were released from plurilocular gametangia within 2 h of light irradiation. They showed a strong negative phototaxis and gathered at the opposite side of culture dishes from the light source.

Observations and recording

Thirty µl of culture medium containing freshly liberated male and female gametes was added in an observation chamber (90 µm depth). This observation chamber was made of double-faced adhesive tape between a slide glass and a cover slip. Images of flagellar waveforms were recorded with a phase contrast microscope (BX51, Olympus, Tokyo, Japan) with a 40× objective (UPlan FLN, Olympus) connected to a high-speed CCD camera (HAS220, Ditect, Tokyo, Japan) at 200 or 600 fps (frames per s) and 1/1000 s shutter speed. Observations were carried out using an R-58 red cut-off glass filter (S-058, HOYA, Tokyo, Japan) in the dark room at room temperature (ca. 20ºC), for preventing the effect of blue light on phototaxis of *E. siliculosus* (Kawai et al. 1990). Image analyses of flagellar waveforms were executed only on planner bending waveforms.

Data analysis

Swimming velocities, swimming path curvatures, flagellar curvatures and the deflection angle of gametes were analyzed by Bohboh software (Bohboh Soft, Tokyo, Japan). Images of the cell body of gametes were automatically tracked, and the swimming velocities were measured along the zigzag trajectory of the cell bodies during flagellar beating cycles (trajectory swimming velocity). The path curvature, which is the reciprocal of the radius of curvature (ρ) of the circular swimming path, was also calculated (Plate 16). Trajectories in a clockwise direction were defined as a plus and trajectories in a counter-clockwise direction were defined as a minus. The flagellar waveforms of gametes were automatically traced. The flagellar curvature (Plate 16), which is the reciprocal of the radius of curvature (r) of the flagellar waveform, was calculated based on the method of Baba and Mogami (1985). Flagellar asymmetry was expressed as the ratio of the maximal curvature of P bend (Principal bend) and that of R bend (Reverse bend) (P bend Max / R bend Max). The ratio should be equal to one when the flagella show completely symmetric bending, and is should be greater than one when they show an asymmetric waveform. This ratio is referred to as the asymmetric index (Shiba et al. 2008).

The angle of the tangent to the flagellar shaft was measured with respect to the direction of the axis of the cell body. It was referred to the deflection angle (Plate 16). The right side was defined as plus and the left side was defined as minus, when the AF was localized to the direction of forward

movement and viewed from the ventral side of the gametes. The anterior end of cell body was defined as zero with respect to the deflection angle of the AF and the posterior end of cell body was defined as zero in with respect to the deflection angle of the PF. The points which tended to take on large values in maximum and minimum of the deflection angle was 8 μm from the tip of the AF and 1 μm from the tip of the PF.

Results

Locomotion of free- and thigmotactic-swimming gametes

Two patterns of swimming were observed in male and female gametes of *E. siliculosus*. The first observed pattern was that the gametes freely swam with helical rotations of the cell body without touching anything. Trajectories of these gametes showed spiral or undulating lines (Plate 17a). The second observed pattern was that they swam just on the substratum by eliminating the helical rotation of the cell bodies. These thigmotactic-swimming male and female gametes followed straight to large circular paths (Plate 17b).

Just after adding 30 μl of culture medium containing freshly liberated male or female gametes to a chamber, about 20% of gametes showed thigmotaxis and 80% of gametes freely swam. After three min, about 50% of gametes showed thigmotactic-swimming. The number of thigmotactic-swimming gametes gradually increased.

The swimming velocity was 205.2 ± 49.5 μm s^{-1} (n = 95) in free-swimming male gametes and 131.5 ± 24.1 μm s^{-1} (n = 115) in thigmotactic-swimming gametes, and there were a significant difference ($P < 0.001$) between the two values (Table 2). In female gametes, the swimming velocity was 191.0 ± 48.4 μm s^{-1} (n=90) in free-swimming gametes and 151.8 ± 38.6 μm s^{-1} (n = 115) in thigmotactic-swimming gametes. There was also a significant difference ($P < 0.001$) between these values. No significant difference was observed between the swimming patterns of male and female gametes.

The path curvature, which is the reciprocal number of the radius of curvature (ρ) of the circular-swimming gametes, was calculated. Trajectories in a clockwise rotation were defined as plus and those in a counter-clockwise direction were defined as minus. Thigmotactic-swimming

male gametes showed highly linear to large circular paths without a pheromone source, and 66% of the path curvature values ranged from -0.02 to 0.02 μm^{-1} (n = 115) (Plate 17c). Similar tendencies were also observed in female gametes.

AF movements of free- and thigmotactic-swimming gametes

Flagellar waveform of free- and thigmotactic-swimming male and female gametes, which showed typical swimming velocities and path curvatures, were quantitatively analyzed. The AF showed periodic oscillations, but the PF showed only irregular oscillations in *Ectocarpus* gametes. Therefore, flagellar curvature, asymmetric index and beat frequency were analyzed only in the AF.

AF movements of free-swimming gametes were composed of symmetric and asymmetric waveforms (Plate 18a, c). The AF of thigmotactic-swimming gametes usually showed asymmetric waveforms (Plate 18b, c). In the case of free-swimming male gametes, which showed the highly linear paths (path curvature -0.01–0.009 μm^{-1}) (n = 5), maximum values of P-bend and R-bend in the AF were 1.13 ± 0.09 and 1.08 ± 0.06, respectively. The asymmetric index (P bend / R bend) of the AF was 1.05 ± 0.03 as the whole region (Plate 18d). The slightly curved free-swimming male gametes (>0.012 μm^{-1}) had an asymmetric waveform which was similar to those of thigmotactic-swimming gametes (not shown). The AF of thigmotactic-swimming male gametes, which showed highly linear paths (from -0.008 to 0.008 μm^{-1}, n = 7), displayed asymmetric waveforms (Plate 18d). The maximum values of P-bend and R-bend were 1.16 ± 0.13 and 0.98 ± 0.12, respectively. Next, the asymmetric index at the base was separately measured, middle and tip regions of AF (Plate 18d) for examining which part of AF showed a conspicuous asymmetry. The asymmetric indices were 1.05 ± 0.07 at the base (0–5 μm), 1.19 ± 0.045 at the middle (6–10 μm), 1.42 ± 0.15 at the tip (11–14 μm), and 1.24 ± 0.075 as the whole region (0–14 μm). The AF waveform of these two types of gametes, which showed highly linear paths, were significantly different in asymmetric index, especially between the tip region and the whole region ($P < 0.001$) (Plate 18d). Female gametes also showed similar patterns of AF waveforms. The asymmetric waveform in AF was observed in both free- and thigmotactic-swimming gametes; however, the symmetric waveform in the AF was observed only in free-swimming gametes during straight

swimming.

The deflection angle between the flagellum and the axis of cell body was obtained. The average values of the deflection angle in the AF of free- and thigmotactic-swimming male gametes, which showed a highly linear path, were 6.3° ± 8.0° (max 102.6°, min 80.8°) and -22.9° ± 4.5° (max 45.2°, min -106.6°), respectively (Plate 18e). There was a statistically significant difference between these two values ($P < 0.001$). The deflection angle of the AF, of thigmotactic-swimming male gametes moving in an almost linear direction, was similar to that of slightly curved free-swimming gametes (not shown). Beat frequencies of free- and thigmotactic-swimming gametes were nearly the same (53–54 Hz), and there was no difference between male and female gametes. While, maximum amplitudes of AF, which were measured from the traces of AF waveforms, were 6.3 ± 0.6 μm (n=5) in free-swimming male gametes and 5.2 ± 0.6 μm (n=5) in thigmotactic-swimming ones.

PF movements of free- and thigmotactic-swimming gametes

PF waveforms of free-swimming gametes showed continuous oscillations, with the deflection angle ranging from -20.6° to 29.8° (Plate 19a, b). While, those of thigmotactic-swimming ones usually showed no motion, or occasional small beats with the deflection angle ranging between 22.3° and 24.0° (Plate 19a, b). A similar tendency was observed in female gametes. It was suggested that not only AF waveforms but also PF waveforms were different between free and thigmotactic-swimming gametes.

Chemoorientation of male gametes

When adding male gametes to settled female gametes, about 50% of male gametes rapidly showed thigmotactic-swimming pattern. The trajectories of these male gametes were converted from linear paths to middle and small circular paths (Plate 20b). Swimming path curvatures of these male gametes (within 150 μm from settled female gametes) were mainly between 0.04–0.2 μm^{-1} (n = 115) (Plate 20c). Most of them put their ventral side on the surface of the substratum and swam in clockwise circle. Free-swimming male gametes did not show small circular paths, rather they swam in spirals or undulating lines (Plate 20a). Namely, flagellar behaviors of free-swimming male

gametes were not affected by the absence or presence of the sex pheromone from settled female gametes. Swimming velocities of thigmotactic-male gametes during chemotaxis were 78.1 ± 14.3 μm s^{-1} (n = 108), and significantly decreased compared to the control ($P < 0.001$). Although, the average swimming velocity of free-swimming male gametes was 199.8 ± 48.4 μm s^{-1} (n = 83). A significant difference in this value was not observed when compared to the control. The AF beat frequencies of the male gametes were constant at 44–46 Hz despite different distances from the sex pheromone source (within 150 μm from settled female gametes). A significant difference could be detected when compared to the control (53–54 Hz) ($P < 0.001$).

AF movements of male gametes during chemotaxis

In order to observe the relationship between swimming path curvature and AF waveform, male gametes (0.04–0.28 μm^{-1} of path curvature, n = 13) under the sex pheromone were analyzed (Plate 21a–d). I compared these chemotactic male gametes against thigmotactic gametes without the sex pheromone (from -0.008 to 0.008 μm^{-1} of path curvature, n = 7). The waveforms in the base region (1.05–1.24) and the middle region (1.19–1.30) of AF showed almost symmetric, but the tip region sometimes became highly asymmetric during chemotaxis resulting in a decrease in R-bend curvature (Plate 21a). Although a significant difference of the AF to the control in the tip region (Plate 21a, $P < 0.05$) was observed, a correlation between the path curvature and the AF asymmetric index could not be detected (Plate 21b).

The average value of the AF deflection angle of the chemotactic male gametes was 51.0° ± 23.6° and that of the thigmotactic-swimming male gametes without the sex pheromone was -22.9° ± 4.5° (Plate 21c). There was a significant difference between them ($P < 0.001$). However, there is no correlation between the deflection angle of the AF and the circular path curvature (0.04–0.28 μm^{-1}) (Plate 21d). The maximum amplitude of AF was almost the same in chemotactic (5.4 ± 0.2 μm, n=7) and thigmotactic (5.2 ± 0.6 μm, n=7) swimming gametes.

PF movements of male gametes during chemotaxis

PF unilateral beating of male gametes was occasionally observed when they were close (less than

100 μm) to the pheromone source (settled female gametes). When PF showed strong unilateral beating, the swimming-path curvature of male gametes suddenly increased, namely the swimming direction of male gametes strongly changed. Beat frequency of the PF increased when male gametes were closer to the pheromone source. Several beats of the PF were also detected when they were further away from the pheromone source (Plate 22). However, the exact timing of PF beating was still not known. Plates 23, 24 show two cases of PF beating of male gametes around settled female gametes, 1) PF bent for a while (Plate 23) and 2) PF repeated beating (Plate 24). Maximum and minimum values of the PF deflection angles became 151.3° and 12.0° (0.06–0.20 μm^{-1} of path curvatures, n = 4). The forward stroke of the PF took a longer time (8–16 ms) than the recovery stroke (5–8 ms). It also became clear that the AF waveform was not affected by the PF waveform in chemotactic male gametes.

Discussion

Brown algal swarmers (heterokont algae, stramenopiles) including gametes and zoospores have morphologically and functionally heterogeneous flagella. This is quite different from the cases of the green alga, *Chlamydomonas*, and the sperm of marine invertebrates. In this study, swimming velocities of *E. siliculosus* male and female gametes were about 200–240 μm s^{-1} in the free-swimming case and 130–150 μm s^{-1} in thigmotactic-swimming one. This value was similar to the previous observation using 16 mm film (Geller and Müller 1981). Although the number, length and beat frequency of flagella are diverse, swimming speeds of gametes or sperm in aquatic organisms are not so variable. Some of these values are 174 μm s^{-1} in *Chlamydomonas reinhardtii* P. A. Dangeard (Goodenough 1983), 165 μm s^{-1} in sea urchin (Wood et al. 2005), 276 μm s^{-1} in ascidians (Yoshida et al. 2002), and 375 μm s^{-1} in starfish (Shiba et al. 2006).

Thigmotactic-swimming gametes of *E. siliculosus* did not show helical rotations of their cell body and they displayed only two-dimensional waveforms of the AF. While, free-swimming gametes frequently showed helical rotations of their cell body and they displayed two- and three-dimensional waveforms of the AF. It was mathematically shown by Chwang and Wu (1971) and Keller and Rubinow (1976) that three-dimensional (helical) flagellar movement induces rotation

of the cell. Helical rotations of *Ectocarpus* gametes would be induced by a combination of several complex AF waveforms as the suggestions of Geller and Müller (1981). Although there is no significant difference in beat frequency of the AF between free- and thigmotactic-swimming gametes, swimming velocities between them were different. AF amplitude also did not seem to be effective to the gamete swimming speed. An increase in swimming speed in free-swimming gametes may be caused by helical rotation of the gamete cell body. While, Ishijima (2012) examined the movement characteristics of the sperm and flagella from a lancelet and 35 species of fishes using high-speed video microscopy. He concluded that flagellar beat frequency was most effective to the swimming speed, neither the flagellar wavelength nor amplitude.

After Müller (1967) and Müller et al. (1971) first discovered the brown algal pheromone 'ectocarpene' in *E. siliculosus*, many other sex pheromones in brown algae were identified (Maier and Müller 1986; Maier 1993). As a result of these studies, detailed observations of the behavior of male and female gametes during the fertilization process of *E. siliculosus* were carried out. *Ectocarpus* male and female gametes are morphologically isomorphic. Female gametes settle down on the substratum quicker than male gametes. When settled, the female gametes begin to secret the sex pheromone. However, the locomotion and flagellar waveforms of male and female gametes were observed to be almost same after adding them into the chamber.

During chemotaxis in the presence of sex pheromone, the AF deflection angle of male gametes significantly changed from the control with decreasing beat frequency of the AF. Geller and Müller (1981) showed a correlation between the average deflection angle of the AF and the radius of the track. In addition to their results, it was clarified that the deflection angle of the AF was significantly changed when male gametes altered their swimming pattern from highly linear paths to small or medium circular paths. However, the deflection angle did not significantly change when the gametes switched from medium to small circular paths. Therefore, it was suggested that changing the swimming paths of male gametes from a highly linear path to a circular path was affected by the AF itself. While, alternating the trajectory from a medium circular to a small circular path was attributed to the PF.

Geller and Müller (1981) and Maier and Calenberg (1994) showed that the PF performed

fast and unilateral beats, when the cell sensed decreasing concentration of pheromone. Unilateral beats of the PF were usually observed for reorientation of male gametes towards the sex pheromone source (settled female gametes). In this study, it became clear that, regardless of unilateral beating of the PF, the waveform of the AF remained stable (Plate 23c, 24c). It was suggested that the AF and PF would move independently in the presence of sex pheromone.

Matsunaga et al. (2010) showed the rapid lateral beats of the PF during phototactic-orientation of gametes in the brown alga, *Scytosiphon lomentaria*. Those studies reveal that the forward stroke of PF took a longer time (6–8 ms) than the recovery stroke (2–4 ms). When the gametes show phototactic turning, AF undulation ceased. Therefore, AF motion during phototactic turning of gametes is clearly different from the case of the chemotactic one, although unilateral beat patterns of the PF seem to be similar.

In the conclusion of this part, it was revealed that the AF plays a role in changing gamete locomotion from free- to thigmotactic-swimming and also from straight to circular swimming. Moreover, the AF changes the flagellar asymmetry and deflection angle during these steps but it does not change these properties in the presence of the sex pheromone. The PF shows irregular changes in the deflection angle and large bending are dependent on the concentration gradient of the sex pheromone. The exact timing and mechanism of large unilateral beats in the PF during chemotaxis remain unclear. In the ascidian, Yoshida and Yoshida (2011) report that sperm attractants appear to induce Ca^{2+} entry from extracellular spaces into sperm cells. This increases the intracellular Ca^{2+} concentration which mediates the beating patterns of sperm flagella. This increase in Ca^{2+} concentration results in the observed chemotactic turn. Maier and Calenberg (1994) report on the effects of calcium on flagellar movements of *E. siliculosus* male gametes during chemotaxis. They surveyed several calcium antagonists and channel blockers including Lanthanum, Ruthenium Red, Verapamil, Nifedipine, and Trifluoperazine, and showed that: 1) the asymmetric bending of the AF of male gametes will be strongly inhibited by La^{3+}, 2) Nifedipine might interact with Ca^{2+} channels which are involved in the action of PF, and 3) Trifluoperazine might bind to and activate the pheromone receptors in *Ectocarpus* via hydrophobic interactions. Recently, Fu et al. (2014) conducted a proteomics analysis of flagella of the brown alga, *Colpomenia bullosa* (Saunders)

Yamada suggested that 8% of the 495 flagellar proteins were related to proteins with calcium-binding function. Further investigation on the roles of calcium in flagellar bending using a high-speed camera will clarify the characteristic beat patterns of the heterogeneous AF and PF of brown algal gametes during chemotaxis.

Part 2. 2 Chemotaxis in the anisogamous brown alga *Mutimo cylindricus*

Introduction

Brown algae in the heterokonta are one of eukaryote groups that have evolved complex multicellularity and almost all members live in marine habitats (Clayton 1989; van den Hoek 1995; Cock et al. 2010). Life cycle of brown algae usually shows the alternation of diplohaplontic generations, gametophyte and sporophyte, and sexual reproduction includes isogamy, anisogamy and oogamy (Wynne and Loiseaux 1976; Silberfeld et al. 2010). In brown algae, the release and fusion of gametes is easy to manipulate in the laboratory; therefore, they are suitable for comparative studies on fertilization. The gametes of isogamous and anisogamous brown algae have a long anterior flagellum (AF) and a shorter posterior flagellum (PF). In addition, the sperm of oogamous species have PF that varies in length, i.e. no PF (e.g. *Dictyota*), short PF (e.g. *Sargassum*), or long PF (e.g. *Laminaria* or *Saccharina*) (Kawai 1992a) (Plate 12). The chemotactic swimming patterns and flagellar waveforms of male gametes have been studied in isogamous brown alga *Ectocarpus siliculosus* (Müller 1978; Geller and Müller 1981; Maier and Calenberg 1994; Kinoshita et al. 2016c) and in the sperm of the oogamous *Laminaria digitata* and *Fucus spiralis* Linnaeus, which has a long PF (Maier and Müller 1986, 1990).

Müller (1974) observed chemotactic male gametes in the anisogamous species, *Cutleria multifida* (Turner) Greville, and found that immediately after female gametes come to rest on the substratum, male gametes gather around them, where one of these gametes fuses with a female gamete. The male-attracting substance secreted by female gametes in *C. multifida* was identified as "multifidene" (Jaenicke et al. 1974; Boland et al. 1989) (Plate 13). The female gametes of anisogamous brown algae have a large cell body and the ability to swim using their AF and PF (Yamanouchi 1912; Fritsch 1945; La Claire II and West 1978, 1979; Kitayama et al. 1992). However, the swimming properties of the small male and large female gametes remain unclear.

In this part, comparative analysis of the swimming patterns of male and female gametes of the anisogamous brown alga *Mutimo cylindricus* (Okamura) Kawai and Kitayama was conducted using a high-speed camera. The chemotactic locomotion of male gametes was also quantitatively

analyzed and compared with that in isogamy (Kinoshita et al. 2016c).

Materials and Methods

The gametophytes of *M. cylindricus* were collected at Toba, Mie Prefecture, Japan (March 2015), and sent immediately to Muroran Marine Station, Hokkaido University. Male and female gametophytes were separately kept in autoclaved seawater and incubated at 15°C under a 14 h light:10 h dark, with 20–40 μmol photons m^{-2} s^{-1} using LED lamps (PF20-S9WT8-D, NKsystem, Osaka, Japan). From the next day, male and female gametes were continuously released for 4 days. Numerous gametes were released within 15 min after the light source was provided, and these gametes were used to analyze their locomotion. Moreover, the trichothallic meristems of male and female gametophytes were isolated using a stereomicroscope and cultured in half-strength PES medium (Provasoli 1968) for 3 months using the same culture conditions employed to establish the culture strains. Gametes were also obtained from these culture strains by changing the culture medium (Nagasato et al. 1998).

The flagellar length ratio (PF/AF) was determined in *Analipus japonicus* (Harvey) M.J.Wynne, *Colpomenia bullosa*, *Ectocarpus siliculosus*, and *Scytosiphon lomentaria* based on the images of swimming gametes obtained using a high-speed camera. *A. japonicus*, *C. bullosa*, and *S. lomentaria* were collected at Muroran, Hokkaido, Japan, between March and April 2015. *E. siliculosus* was the same strain as that described by Kinoshita et al. (2016c).

For immunofluorescent microscopy, 50 μl of freshly liberated male and female gametes were separately placed on a cover slip, to which was added the same volume of a fixative containing 3% paraformaldehyde, 0.1% glutaraldehyde, 2% NaCl, and PHEM buffer (PIPES 60 mM, HEPES 25 mM, EGTA 10 mM, $MgCl_2$ 2 mM, pH 7.5). After fixation at room temperature for 30 min, the samples were washed three times with PBS and incubated with PBS containing $NaBH_4$ (1 mg ml^{-1}) for 20 min. The samples were washed three times with PBS and incubated with a blocking solution (2.5% skim milk, 5% normal goat serum, 0.05% NaN_3 in PBS) for 30 min at 37°C. Next, they were incubated with anti-α-tubulin antibody (diluted to 1:200 with PBS, DM1A, Sigma-Aldrich, St Louis, MO, USA) for 1 h at 37°C. After washing with PBS, the samples were incubated with

rhodamine-conjugated goat anti-mouse IgG (diluted 1:50 with PBS, Sigma-Aldrich) for 1 h at 37°C. They were then washed three times with PBS and mounted in Mowiol 4-88 mounting medium (Osborn and Weber 1982) containing 0.2% *p*-phenylenediamine. An epifluorescence microscope (BX50-FLI, Olympus, Tokyo, Japan) and a digital camera (AxioCam MRm and Axio-Vision systems, Carl Zeiss, Oberkochen, Germany) were used to obtain the images of AF and PF.

Locomotion of male and female gametes was recorded and analyzed according to Kinoshita et al. (2016c). The swimming velocity, swimming path curvature, flagellar curvature, and deflection angle of gametes were analyzed using Bohboh software (Bohboh Soft, Tokyo, Japan). The swimming path curvature was calculated from the inverse of the radius of the track (swimming path). All values were expressed as absolute values. The asymmetric index was calculated from the flagellar curvature along the whole length of AF. The deflection angle was measured at a point located 8 μm from the tip of AF and 1 μm from the tip of PF. In observations of chemotactic male gametes, male and female gametes were mixed and the reaction of male gametes against sex pheromone from settled female gametes was examined.

Results

Morphology and swimming patterns of female and male gametes

The cell body of female gametes (length = 12.1 ± 1.0 μm; diameter = 6.7 ± 0.8 μm; mean ± SD, n = 28) was significantly larger than that of male gametes (length = 5.3 ± 0.4 μm; diameter = 2.7 ± 0.2 μm; n=28) ($P<0.0001$) (Plate 25a–c). The volume of female gametes was estimated at 10-times larger than that of the male gametes. AF and PF were two-times longer in female gametes (AF = 24.8 ± 2.3 μm; PF = 13.1 ± 1.5 μm) than in male gametes (AF = 12.3 ± 0.7 μm; PF = 5.4 ± 0.4 μm). The ratio of AF relative to PF (PF/AF) was almost the same in female (0.5, n = 20) and male (0.4, n = 25) gametes. The PF/AF ratio was similar to that of 0.45 found in many brown algal gametes from isogamous species, i.e., 0.5 in *A. japonicus* (n = 3) and *C. bullosa* (n = 3) and 0.4 in *E. siliculosus* (n = 5) and *S. lomentaria* (n = 4).

The free-swimming male and female gametes of *M. cylindricus* exhibited highly linear and spiral swimming paths with rotation of the cell body (Plate 26a, b). The swimming velocity of male

gametes (179.2 ± 40.5 μm s^{-1}) was significantly faster than that of female gametes (133.6 ± 31.5 μm s^{-1}) (Plate 26c) (Table 2).

Flagellar waveforms in female and male gametes

The beat frequency of AF did not significantly differ in female (39.9 ± 4.1 Hz) and male (38.4 ± 3.2 Hz; Plate 26 d–f) gametes. The amplitude of AF was higher in female gametes (2.4 ± 0.3 μm, n = 8) than male gametes (2.0 ± 0.1 μm, n = 8). Straight-swimming female and male gametes were used to analyze the flagellar waveforms (asymmetric index and average value of the deflection angle). The asymmetric index of AF was almost one in both female (1.07 ± 0.08) and male (1.03 ± 0.02) gametes, and thus the flagellar waveform was symmetric (Plate 27a). The average value of the deflection angle was slightly larger in female (17.9 ± 8.1°) than in male (10.7 ± 7.7°) gametes, but the difference was not significant (P = 0.08) (Plate 27b). In contrast to AF, PF occasionally exhibited small beats (Plate 27c–e). The average value of the deflection angle in PF was the same in female (21.6 ± 13.1°) and male (21.5 ± 11.8°) gametes. Thus, these results demonstrated that the waveforms of AF and PF were almost the same in female and male gametes, whereas the swimming velocity significantly differed between them.

Chemotactic locomotion of male gametes

Over half of the male gametes rapidly exhibited thigmotaxis in response to the sex pheromone from settled female gametes. Male gametes were quantitatively analyzed while swimming around settled female gametes (within 150 μm). The swimming velocity was 92.5 ± 25.2 μm s^{-1}, which was significantly less than that for male gametes in the absence of the sex pheromone (control). The AF amplitude was the same in male gametes with or without the sex pheromone. However, the beat frequency was significantly lower in chemotactic gametes (32.5 ± 3.6 Hz), and thus, the difference in the swimming velocity may have been related to the beat frequency of chemotactic gametes. Thigmotactic male gametes did not exhibit rotation of their cell body, and most had a swimming path that described a clockwise circle (focused on the cover slip). The swimming path curvature ranged between 0 and 0.16 μm^{-1} (Plate 28a, b). Some male gametes had small circular paths,

whereas others had linear swimming paths. Even if they lacked small circular paths, they still reacted to the sex pheromone, and there was a change from a free swimming pattern to a thigmotactic swimming pattern.

When swimming female and male gametes were mixed, some male gametes chased female gametes, where these male gametes then attached the tip of their AF to the female cell body. Female gametes might release the sex pheromone during swimming.

The flagellar waveforms were compared in chemotactic male gametes (swimming path curvature = 0.014–0.156 μm^{-1}) and the control (Plate 28c). The asymmetric index for AF was almost the same in chemotactic male gametes (1.10 ± 0.08) and the control, where both had symmetric waveforms. The average values of the deflection angle for AF and PF in chemotactic male gametes were 35.1 ± 19.3° and 44.1 ± 21.8°, respectively, and these values were significantly higher than those in the control. The swimming path curvature increased, and unilateral beating of PF was observed (Plate 28d, e). The unilateral beats of PF occurred independently of the AF waveform (Plate 28e).

Discussion

The PF/AF length ratio in usual zoospores and gametes may be conserved in brown algae, except for the sperm of oogamous groups. Motomura (1993) examined the elongation of AF and PF in the zoospores of *Saccharina angustata* (Kjellman) C.E.Lane, C.Mayes, Druehl and G.W.Saunders using unilocular sporangia, which showed that AF elongated slightly faster than PF until the length reached 5 μm. Next, AF and PF continued to elongate, but the PF/AF ratio remained at approximately 0.4. Therefore, this ratio is maintained from the early stage of zoidogenesis in brown algae.

The swimming velocity of male and female gametes was different in the anisogamous species *M. cylindricus*. By contrast, the swimming velocity of male and female gametes was nearly the same in the isogamous *E. siliculosus*, i.e. 205.2 ± 49.5 μm s^{-1} and 191.0 ± 48.4 μm s^{-1}, respectively (Kinoshita et al. 2016c). Swimming organisms with a small body size such as algal gametes have low Reynolds numbers. Thus, their movement is regulated by viscous forces, and

inertial forces can be ignored (Purcell 1977; Bray 1992). The viscous force depends on the size of organisms and is related to the linear dimension (L), velocity (v), and viscosity (η) of the liquid. The viscous force can be calculated according to the following equation: vLη. The mean length of female gametes was 12.1 μm and that of male gametes was 5.3 μm. The swimming velocity was 133.6 μm s^{-1} in female gametes and 179.2 μm s^{-1} in male gametes. Thus, the ratio of the viscous force for females and males can be calculated as: (133.6 × 12.1):(179.2 × 5.3) = 1:0.5 because the viscosity of seawater remains constant for both gametes. Therefore, theoretically, this suggests that the viscous force was much larger for female gametes than male gametes. This calculation indicates that the difference in the swimming velocities of female and male gametes may be due to difference in their cell sizes.

In the conclusion of this part, chemotactic male gametes of the anisogamous brown alga *M. cylindricus* exhibited the following behaviors: 1) free-swimming male gametes rapidly exhibited thigmotaxis in the presence of the sex pheromone, 2) the beat frequency of AF decreased, 3) the swimming velocity decreased, 4) the deflection angle of AF increased, 5) unilateral PF beats occurred due to the sex pheromone gradient, and 6) the radius of the swimming track decreased in male gametes. Thus, the behavior exhibited by the chemotactic male gametes of the anisogamous *M. cylindricus* was similar to that of the isogamous *E. siliculosus*.

Part 2. 3 Chemotaxis in the oogamous brown algae *Saccharina japonica* and *Fucus distichus*

Introduction

Sperm chemotaxis in response to sex pheromones (or the chemical attractant) released from eggs is a crucial factor during species-specific recognition and the fusion of both reproductive cells during initial stage of fertilization. Sex pheromones have been identified in mammals, marine invertebrate and vertebrate animals (Kaupp 2010; Yoshida and Yoshida 2011; Yoshida 2014), land plants (Higashiyama and Takeuchi 2015), and seaweeds and diatoms (Maier and Müller 1986; Frenkel et al. 2014). Chemotactic mechanism and pheromone receptors of sperm have also been elucidated in several organisms. For instance, in marine animals, such as sea urchins, ascidians, and starfish, uniflagellate sperm sense the sex pheromone gradient, change their flagellar waveform, and finally modify their swimming direction toward the egg (Kaupp et al. 2003; Böhmer et al. 2005; Shiba et al. 2008).

Brown algae belong to major linage of Heterokontophyta or stramenopiles, and their swarmers usually possess two heterogeneous flagella, a long, mastigonema-bearing anterior flagellum (AF) and a short, posterior flagellum (PF) (Plate 12). Müller et al. (1971) first identified the chemo-attractant "ectocarpene" from the isogamous brown alga *Ectocarpus siliculosus*, and revealed the sex pheromones released by female gametes of brown algae. Approximately 10 sex pheromones have been identified to date (Maier and Müller 1986; Boland 1995) (Plate 13). These brown algal pheromones are hydro-phyllic and volatile substances with unsaturated C_8 and C_{11} hydrocarbons. On the other hand, the sex pheromone receptor in sperm or male gametes of brown algae has been unidentified.

Detailed analyses of locomotion and the flagellar waveforms of male gametes in response to the sex pheromone released by female gametes have been conducted using the isogamous brown alga *E. siliculosus* (Müller 1978; Geller and Müller 1981; Maier and Calenberg 1994; Kinoshita et al. 2016c) and anisogamous brown alga *Mutimo cylindricus* (Müller 1974; Kinoshita et al. 2016d), where the responses of the both heterogeneous flagella, AF and PF were more complex than those of the uniflagellate sperm of animals. The waveform patterns of AF and PF in male gametes of

isogamous and anisogamous species were markedly different from one another.

Sexual reproduction of brown algal members of Laminariales and Fucales involves oogamy (Wynne and Loiseaux 1976; Silberfeld et al. 2010). Unlike swarmers (male gametes) of isogamous and anisogamous species of brown algae which have usually a long AF and a short PF (Kawai 1992a), the sperm of many species of oogamous brown algae have considerably longer PF than AF (Manton and Clarke 1950; Henry and Cole 1982b; Motomura and Sakai 1984). As sex pheromones (lamoxirene and fucoserratene) released from egg and involved in fertilization with sperm have been identified (Müller and Jaenicke 1973; Müller et al. 1979; Maier 1995).

Locomotion of brown algal sperm have been reported for several oogamous species, including *Laminaria digitata* (Maier and Müller 1986, 1990), *Hormosira banksii* (Turner) Decaisne (Maier et al. 1992), and *Fucus spiralis* Linnaeus (Maier and Müller 1986). According to these reports, the swimming patterns of sperm during chemotaxis were different from male gametes of isogamous and anisogamous species. In chemotactic response, the male gametes of *E. siliculosus* (isogamous species) and *M. cylindricus* (anisogamous species) change their swimming locomotion from linear paths to small circular paths when approaching the female gametes. On the other hand, the sperm in *L. digitata*, *H. banksii*, and *F. spiralis* (oogamous species) continued swimming pattern of linear paths, but they frequently exhibit drastic three-dimensional U-turns in response to the sex pheromone around eggs. This U-turn response may be attributed to the specific waveforms of PF (Maier and Müller 1986, 1990; Maier et al. 1992).

In this study, quantitatively analysis of the sperm locomotion and the waveforms of AF and PF during chemotaxis using two oogamous species of brown algae, *Saccharina japonica* (Areschoug) C. E. Lane, C. Mayes, Druehl and G. W. Saunders and *Fucus distichus* Linnaeus was conducted. In particular, I focused on the waveform pattern of PF and compared to that of the isogamous and anisogamous species previously reported (Kinoshita et al. 2016c, d).

Materials and Methods

Algal materials and culture

Mature sporophytes of *Saccharina japonica* were collected at Muroran, Hokkaido, Japan (Oct, 2014).

Zoospores were isolated in test tubes containing Fe-free $ASP_{12}NTA$ (Provasoli 1968; Motomura and Sakai 1981, 1984), and finally, sterile vegetative male and female gametophyte strains were established using a mixture of antibiotics (Tatewaki et al. 1989; Kawai et al. 2005). To induce the maturation of male and female gametophytes, they were transferred to PES medium (Provasoli 1968), and they matured within 1–2 weeks. The culture conditions comprised cool white fluorescent lamps (30–40 μmol m^{-2} s^{-1}) at 15°C with a long day length (14 h light:10 h dark).

Sporophyte thalli of *Fucus distichus* were collected from Muroran, Hokkaido, Japan (May, 2015). The procedures employed for separately releasing the eggs and sperm were based on those stated by Wakana and Abe (1992) and Nagasato et al. (1999). Receptacles were rinsed with filtered sea water and wiped with gauze, before being maintained in Petri dishes and incubated under a cool, white fluorescent lamp (30–40 μmol m^{-2} s^{-1}) at 20°C. On the following day, the receptacles were incubated at 4°C in dark conditions for 1 h. Pre-cooled autoclaved seawater containing EDTA (0.5 mg mL^{-1}) was used to release the oogonia and antheridia, which were then filtered through 38-μm mesh. The antheridia passed through the mesh whereas the oogonia remained on it. Some eggs were contaminated with seawater containing antheridia, so, after checking by microscopy, only antheridia were transferred to 1.5-mL microtubes (sperm were not released in this condition). Next, 30 μL of autoclaved seawater was added to 10 μL of EDTA-seawater containing antheridia in an observation chamber (Kinoshita et al. 2016c), and sperm release was observed within 0.4–1.5 s. The oogonia in EDTA-seawater also released their eggs with the same procedure.

Recording and analysis

High-speed video recordings and sperm locomotion analyses were performed according to Kinoshita et al. (2016c) and Part 2. 1 in this thesis. Chemotactic swimming behaviors of sperm was observed under the sex pheromone from eggs. The asymmetric index was calculated based on the whole length of AF in *S. japonica* sperm. In contrast, it was calculated only for the oscillating part of PF (up to 12 μm from the base of PF). The deflection angle was measured at a point of 7 μm from the tip of AF and at 5 μm from the base of PF. For the *F. distichus* sperm, the asymmetric index was calculated based on the whole part of AF and PF, and the deflection angles were measured at a point

of 7 μm from the tip in both AF and PF.

Results

Saccharina japonica

At 6 days after transferring to PES medium from Fe-free $ASP_{12}NTA$, the mature female gametophytes started to release their eggs. The liberation of eggs occurred within 30 min of the start of the dark period. Culture medium containing mature female gametophytes with many eggs, which implied the presence of the sex pheromone "lamoxirene" from the eggs, induced the active release of sperm from the antheridia of mature male gametophytes. The newly liberated sperm exhibited a low beating frequency of AF (13–22 Hz, n = 3) for a short time (200–500 ms, n = 3).

Sperm liberation was also induced by increasing the temperature of the culture medium containing mature male gametophytes. However, much greater sperm release was observed after adding culture medium containing mature female gametophytes bearing many eggs. I used these two methods for sperm release (condition 1: without pheromone; condition 2: with pheromone) to examine the behavior of sperm flagella. Under conditions 1 and 2, some of the sperm swam in contact with the surface of the glass slide, but the numbers of sperm did not increase in the presence of the sex pheromone. Thus, a conspicuous thigmotactic response was not detected in *S. japonica* sperm. The swimming paths of the sperm did not differ under conditions 1 and 2. The swimming paths of the sperm in contact with the glass surface ranged from mainly circular to highly linear, whereas those of the free-swimming sperm were highly linear or spiral with helical rotations of the cell body (Plate 29a, b, d, e). When the sperm swam in the vicinity of freshly liberated eggs (condition 3: within 200 μm of the eggs), they described small circular paths close to the cover or slide glass (Plate 29c) or they had swimming paths with frequent spiral rotations (Plate 29f).

I quantitatively analyzed the swimming behavior of sperm close to the surfaces of the glass slides because it was difficult to analyze the three-dimensional movements of free-swimming sperm. The sperm swimming path curvatures did not differ significantly under conditions 1 and 2, whereas those under condition 3 were larger than those under conditions 1 and 2, thereby indicating that the swimming paths of sperm under condition 3 described smaller circles than those under conditions 1

and 2 (Plate 29g). In both swimming patterns, i.e., sperm in contact with the glass surface and free-swimming sperm, the swimming velocity under condition 3 (c: 105.4 ± 29.3 μm s^{-1}, f: 99.5 ± 19.7 μm s^{-1}) was slightly higher than that under condition 2 (b: 88.8 ± 23.2 μm s^{-1}, e: 100.0 ± 24.9 μm s^{-1}), and the swimming velocity under condition 2 was slightly higher than that under condition 1 (a: 74.7 ± 16.4 μm s^{-1}, d: 91.3 ± 22.7 μm s^{-1}) (Plate 29h) (Table 2). I analyzed the beating frequency of AF and PF based on the oscillating flagella without the sex pheromone (condition 1) and with the sex pheromone (condition 2 and 3), which showed that the beating frequency was higher without the sex pheromone than in the presence of the sex pheromone (Plate 29i), i.e., 54.4 ± 8.0 Hz without the pheromone and 40.2 ± 7.2 Hz with the pheromone in AF and 95.2 ± 11.8 Hz without the pheromone and 68.1 ± 17.5 Hz with the pheromone in PF. The beating frequency of AF and PF was lower in the presence of the sex pheromone, but the flagellar amplitude increased, especially for PF (not shown). The ratios of (I) almost motionless or minimal beating by PF (Plate 30a) relative to (II) medium to high beating by PF (Plate 30b) were (I) 68% and (II) 32% without the sex pheromone (n = 55) and (I) 10% and (II) 90% with the sex pheromone (n = 55). According to these results, the increased swimming velocity of chemotactic sperm may have been due to the increased amplitude of PF in the presence of the sex pheromone. I occasionally observed that abnormal sperm possessing only PF could swim forward. Thus, PF had sufficient propulsive force to move the cell forward and the sperm velocity was 41.6–92.3 μm s^{-1} (n = 7).

The AF and PF lengths of *S. japonica* sperm were 17.4 ± 0.9 μm and 34.0 ± 2.2 μm, respectively (n = 6). AF oscillated periodically throughout the whole length. In contrast, PF oscillated only in the section located 12–13 μm from the flagellar base. The asymmetric index indicating the flagellar asymmetry and the average deflection angle indicating the angle between the cell axis and the flagellum did not differ in AF and PF under conditions 1 and 2. Plate 30c, d shows an example of sperm swimming straight with a path curvature of 0.0057 μm^{-1}. The asymmetric indices and deflection angles of AF and PF remained fairly stable (Plate 30c, d).

Dramatic U-turns by *S. japonica* sperm could be observed during chemotaxis, as described previously (Maier and Müller 1990), wherein the sperm exhibited three-dimensional movements during U-turns. Plate 31 shows the two typical waveform patterns for AF and PF based on

quantitative data (n = 7). Plate 31d, h show high speed video images, where neither AF nor PF stopped beating, but the waveforms of PF exhibited characteristic changes during U-turns. In particular, the asymmetric index of PF increased suddenly during U-turns (Plate 31a, e) and the deflection angle increased to 150° (Plate 31b, f). A large bend in PF was observed at approximately 200 ms. The deflection angle of AF during U-turns was similar to that in the straight swimming sperm, and there was no correlation between beating by AF and PF. The path curvature (Plate 31c, g) was 0.4–0.7 μm^{-1} in U-turns and the change in the swimming direction reached 130–180° (n = 6).

Fucus distichus

In *F. distichus* sperm, the lengths of AF and PF were 8.7 ± 0.2 μm and 17.7 ± 1.0 μm, respectively (n = 6). I analyzed the swimming behavior of sperm without eggs (condition 1) and in the presence of eggs (within 200 μm) (condition 2). No differences in flagellar waveforms were detected under conditions 1 and 2, except during dramatic U-turns (Plate 32a, b), which occurred more frequently under condition 2 than under condition 1. The swimming velocity was 132.9 ± 19.3 $\mu m\ s^{-1}$ (n = 44) and it did not differ between conditions 1 and 2. Under conditions 1 and 2, some sperm were swimming on the upper glass surface, but the number of sperm did not increase in the presence of eggs (sex pheromone). Thus, similar to the *S. japonica* sperm, a thigmotactic response was not conspicuous. Under condition 1, the free-swimming sperm exhibited strong negative phototaxis.

Under conditions 1 (n = 7) and 2 (n = 7), the sperm swimming in a linear manner had similar flagellar waveforms. The asymmetric indices of AF and PF were stable at 1–1.1, and the average deflection angle was 0–25° (Plate 32c–e). The flagellar beat frequency was approximately 40 Hz for AF and approximately 100 Hz for PF. The AF and PF amplitudes were also the same under conditions 1 and 2.

I quantitatively analyzed the dramatic U-turns made by *F. distichus* sperm near eggs (n = 7). The U-turns made by sperm were mainly three-dimensional movements, similar to those made by the *S. japonica* sperm. Two typical flagellar waveform patterns are shown in Plate 33. The asymmetric index and deflection angle did not change in AF during U-turns (Plate 33a, b, d–f, h). In contrast, PF exhibited high unilateral bending, where the asymmetric index was > 6 and the

deflection angle temporarily exceeded 180°. The large bending in PF during U-turns continued for approximately 300–450 ms. The path curvatures (Plate 33c, g) were 0.5–0.7 μm^{-1} during U-turns and the swimming direction of the sperm changed rapidly to 150–240° (n = 7). The oscillation of PF rested in *F. distichus* sperm during U-turns in contrast to the *S. japonica* sperm.

Discussion

It is known that temperature and light conditions are crucial factors that affect the maturation of male and female gametophytes as well as egg release in *Saccharina latissima* (Linnaeus) C. E. Lane, C. Mayes, Druehl and G. W. Saunders (Luning and Dring 1972, 1975). The timing of egg maturation and release were similar to those described in previous studies (Luning 1981; Motomura and Sakai 1981). In the present study, female *S. japonica* gametophytes matured within 6 days after being transferred to PES medium, and the eggs were released within 30 min at the beginning of the dark period. At the same time, antheridial maturation was completed by the male gametophytes, but the release of sperm did not depend on the light cycle. The *S. japonica* sperm did not exhibit phototaxis, whereas the *F. distichus* sperm performed negative phototaxis (Fu et al. 2016).

Maier and Müller (1990) reported that PF in the sperm of *L. digitata* (Hudson) J.V. Lamouroux was generally motionless, and they suggested that PF does not generate a propulsive swimming force. In contrast, PF beats actively in the sperm of the fucaleans, *Fucus spiralis* (Maier and Müller 1986) and *Hormosira banksii* (Maier et al. 1992). In the present study, similar to *F. distichus*, it was confirmed that PF beats conspicuously in *S. japonica* sperm according to high speed video analysis. The abnormal sperm of *S. japonica* only possessed a PF but they could swim forward at a swimming velocity of 41.6–92.3 $\mu m\ s^{-1}$, although this value was slightly slower than the velocity of normal sperm (Plate 29h). The PF length was ca. 34 μm in *S. japonica* sperm. The oscillation of PF occurred only along half its length (12–13 μm from the basal part), whereas the remainder was motionless. Henry and Cole (1982b) observed that PF of laminarialean sperm possesses the conventional "9+2" flagellar axoneme, but the nine-doublet microtubules are gradually disordered along the length to become singlet microtubules, where the number decreases and they are thinner toward the tip of PF. The moving and motionless parts of PF may be attributable to this

morphological deficiency in the axoneme of laminarialean sperm.

Detailed observations of the swimming paths of chemotactic *L. digitata* and *F. spiralis* sperm were reported by Maier and Müller (1986, 1990). Similar to their studies, the sperm turning frequency was enhanced markedly in both *S. japonica* and *F. distichus* sperm by the presence of sex pheromone. It was more difficult to observe both AF and PF simultaneously in *S. japonica* sperm compared with *F. distichus* sperm during U-turns. This was due to differences in the behavior of sperm during U-turns by these species. The *F. distichus* sperm exhibited almost two-dimensional movements and the swimming path was highly linear, whereas the *S. japonica* sperm performed three-dimensional movements and the swimming path was spiral.

Compared with male gametes of the isogamous species *E. siliculosus* (ca. 130–200 μm s^{-1}, Kinoshita et al. 2016c and Part 2. 1 in this thesis) and the anisogamous species *M. cylindricus* (Okamura) Kawai and Kitayama (ca. 180 μm s^{-1}, Kinoshita et al. 2016d and Part 2. 2 in this thesis), the swimming velocity of sperm was much slower in oogamous species (ca. 70–130 μm s^{-1}) (Table 2). As mentioned above, in oogamous species, PF of the sperm generates a propulsive force to move the sperm body forward. In contrast, the gametes of isogamous species of brown algae have a short PF, which cannot produce a propulsive force. Therefore, assuming that the swimming velocity of brown algal gametes depends on the total propulsive force generated by AF and PF is an oversimplification.

In isogamy and anisogamy, male gametes initially changed their swimming patterns from free to thigmotactic swimming in the presence of the sex pheromone. On the other hand, sperm in oogamous species did not exhibit significant thigmotaxis in the presence of the sex pheromone. The process of sexual reproduction may cause the differences between the behaviors of male gametes and sperm. In isogamy and anisogamy, female gametes settle on the substratum, draw the flagella, and secrete the sex pheromone (Plate 34). In contrast, eggs in oogamous species like the Dictyotales, the Laminariales, and the Fucales, start secreting the sex pheromone just after being liberated from the oogonia. After the sperm fuse to these eggs, the zygotes settle on the substratum and begin further development.

Plate 35 shows the schematic diagram of chemotactic male gametes (sperm) of isogamous,

anisogamous and oogamous species of brown algae. According to the quantitative analyses of the flagellar waveforms, especially in *F. distichus*, the waveform of AF did not change in sperm during U-turns, whereas it changed dramatically in PF. Therefore, the chemotactic U-turns performed by *Saccharina* and *Fucus* sperm depended mainly on these characteristic PF waveforms. In the case of the isogamous *E. siliculosus* and anisogamous *M. cylindricus*, the conspicuous change in the swimming direction of male gametes during chemotaxis is attributed mainly to an increase in the deflection angle of AF and a large bend in PF (Geller and Müller 1981; Kinoshita et al. 2016c, d). A large unilateral bend occurs in PF of isogamous and anisogamous species when the male gametes sense a decrease in the sex pheromone concentration (Geller and Müller 1981; Maier and Calenberg 1994; Kinoshita et al. 2016c, d). These male gametes exhibit two-dimensional turns and the swimming directional changes by approximately 90°, which is smaller than that found in *Saccharina* and *Fucus* sperm (> 130°). I found that the time required for unilateral bending by PF during the chemotactic turns of male gametes was similar in *S. japonica* and *F. distichus* (ca. 200–450 ms), as well as in *E. siliculosus* and *M. cylindricus* (ca. 100–500 ms). The dramatic U-turns by oogamous *Saccharina* and *Fucus* sperm depend on their characteristically long PF (Maier and Müller 1990).

The PF waveforms of the sperm of oogamous brown algae, i.e., *H. banksii* (Maier et al. 1992), *L. digitata* (Maier and Müller 1990), *F. spiralis* (Maier and Müller 1986), and *S. japonica* and *F. distichus* in the present study, exhibit unilateral bending in response to decreases in the sex pheromone concentration gradient. In particular, characteristic U-turns due to dramatic large bends in the long PF of sperm are a common feature of oogamous brown algae when sperm move away from the sex pheromone source (eggs). However, as an exception, at least for now, characteristic U-turns had not been observed in *Cystoseira hakodatensis* (Plate 36) and *Dictyota dichotoma* (Plate 37). According to observations of *E. siliculosus* and *M. cylindricus*, the response of PF in male gametes to a decrease in the sex pheromone concentration is a fundamental regulatory component during chemotaxis in brown algae with isogamy, anisogamy and oogamy. In addition, it is known that the sperm of sea urchins and ascidians can sense a decrease in the sex pheromone gradient and change their swimming direction via highly asymmetric flagellar waveforms (Kaupp et al. 2003; Shiba et al. 2008; Guerrero et al. 2010; Yoshida and Yoshida 2011). Moreover, increases in the

intercellular and flagellar Ca^{2+} concentrations are temporarily induced by the transient influx of Ca^{2+} from the outer environment, which is closely related to changes in the flagellar waveforms of sperm during chemotaxis (Shiba et al. 2008; Guerrero et al. 2010). The Ca^{2+} is also related to flagellar quiescence, in which the oscillation of the sperm flagellum ceases and it remains in a largely bent state, as shown by experiments using sea urchin sperm (Brokaw 1979; Gibbons and Gibbons 1980; Kambara et al. 2011). Flagellar quiescence appears to be quite similar to the state of PF during U-turns in *Fucus* sperm. In brown algae, Maier and Calenberg (1994) reported that the flagellar waveforms of AF and PF in the chemotactic male gametes of *E. siliculosus* were affected by extracellular Ca^{2+} using Ca^{2+} channel inhibitors. Thus, similar to the behavior of animal sperm during chemotaxis, it can presume that the influx of Ca^{2+} into the cell body and flagella is regulated after sensing a sex pheromone gradient in brown algae. However, the flagellar responses to the sex pheromone are distinct in AF and PF, which might be regulated independently by differences in the rate of Ca^{2+} influx.

In the conclusion of this part, compared with the male gametes of the isogamous brown alga *E. siliculosus* and anisogamous brown alga *M. cylindricus*, it was found that the sperm of *S. japonica* and *F. distichus* had the following characteristics during chemotaxis: 1) the long PF generated a propulsive force, 2) the number of sperm swimming on the glass surface (thigmotaxis) was not enhanced dramatically by the presence of the sex pheromone, 3) the swimming velocity did not decrease during chemotaxis, and 4) the dramatic U-turns made by sperm were attributable to extreme bending of PF. Unilateral beating of PF was observed often when the sex pheromone gradient decreased, which may be a crucial factor when sperm (male gametes) approach eggs (settled female gamete) during fertilization in brown algae.

Chapter 3 Phototactic behaviors of male gametes in brown algae

Part 3. 1 Calcium control of the sign of phototaxis in brown algal gametes

Introduction

Anterior flagellum (AF) and posterior flagellum (PF) of swarmers in brown algae show different responses to physicochemical signals such as light stimuli (phototaxis) and sex pheromones (chemotaxis) (Geller and Müller 1981; Maier and Müller 1986, 1990; Maier and Calenberg 1994; Maier 1995; Kawai and Kreimer 2000; Matsunaga et al. 2010; Kinoshita et al. 2016b, c, d). The swarmers respond to a blue light stimulus by an oriented swimming towards (positive phototaxis) or away (negative phototaxis) from the source of the stimulus (Müller et al. 1987) (Table 1, Plate 4). It is thought that positive or negative phototaxis of unicellular swarmers may influence their increasing or decreasing dispersal distance from thalli in natural habitats. Moreover, such behavior is thought to be adaptive because it results in the colonizing of these swarmers to the new substratum or increased encountering rates of male and female gametes (Reed et al. 1988; Amsler et al. 1992; Fletcher and Callow 1992).

Several experiments have been conducted on the phototaxis of brown algal swarmers, although regulation in the sign of phototaxis, namely positive or negative, has remained unclear. In brown algal swarmers, a 41-kDa flavoprotein (Fujita et al. 2005) and a 167-kDa LOV/RGS protein (named "helmchrome") (Fu et al. 2014) were thought candidates blue light photoreceptors. However, the function of these proteins *in vivo* has not been clarified. Negative phototactic responses were shown in swarmers of *Scytosiphon lomentaria* (Matsunaga et al. 2010). Shortly after the onset of the unidirectional blue light stimulus (437.1 nm), a brief cessation of the AF undulation and rapid lateral beating of the PF, for turning directions, was observed. In contrast, positive phototactic responses were shown in male gametes of *Ectocarpus siliculosus* and zoospores of *Pseudochorda gracilis* H. Kawai and S. Nabata (Kawai et al 1990, 1991). From the experiments on *E. siliculosus*, it was revealed that light intensity (4×10^{-3}–3.6×10^{3} μmol photons $m^{-2}s^{-1}$) and wavelength (350–650 nm) did not affect the sign of phototaxis in male gametes of *E. siliculosus* and most of these gametes showed positive phototaxis. Moreover, Flores-Moya and his co-author (2002) showed that when the light

(white light) intensity is too low (<10 μmol photons $m^{-2}s^{-1}$) or too high (>190 μmol photons $m^{-2}s^{-1}$), phototaxis of swarmers in *S. lomentaria* was prevented. *Ochromonas danica* E. G. Pringsheim, which is the chrysophycean unicellular alga in the stramenopile, changes in the phototactic sign depend on light (white light) intensity (Häder et al. 1981). Furthermore, in the unicellular green algae *Chlamydomonas reinhardtii* P. A. Dangeard, the increase of light intensity (Feinleib and Curry 1971), photosynthetic activity (Takahashi and Watanabe 1993), reduction-oxidation poise (Wakabayashi et al. 2011), and extracellular Ca^{2+} concentration ($[Ca^{2+}]$) (Morel-Laurens 1987) affected the sign of phototaxis.

Several physicochemical factors would affect the sign of phototaxis in brown algal swarmers; in this study, focusing on the effect of extracellular $[Ca^{2+}]$ on the determination of the phototactic sign, the behaviors of male gametes were quantitatively analyzed.

Materials and Methods

Preparation of male gametes of Mutimo cylindricus

Preparation of male gametes of *Mutimo cylindricus* was the same as Part 2. 2. From day 2–4, following the exchange of the culture medium, numerous male gametes were released, after the onset of light, and they showed strong positive phototaxis. These were used for analyzing locomotion and flagellar movement.

Observation mediums

The basal medium used in this study consisted of 465 mM NaCl, 10 mM KCl, 25 mM $MgSO_4$, 25 mM $MgCl_2$, and 10 mM Tris-HCl at pH 7.8. Including 10 % of the carry-over of the culture medium (autoclaved sea water; estimated as 10 mM $[Ca^{2+}]$, 50 mM $[Mg^{2+}]$) and 90 % of the basal medium, the final $[Ca^{2+}]$ of the observation medium was calculated. To make the observation medium, for example $[Ca^{2+}]$ at about 10^{-1} M, 10^{-2} M (control condition), 10^{-3} M, 10^{-4} M, 10^{-5} M, and 10^{-6} M, the amount of $CaCl_2$, EDTA, and EGTA, computed by the program CALCON (Goldstein 1979), were added to the basal medium. $LaCl_3$ (Stock sol. 100 mM in H_2O; Wako, Pure Chemical Industries, Ltd., Osaka, Japan) was used in control condition.

Phototaxis assay

The phototactic behaviors of male gametes were quantified by recording and analysing their behaviors under continuous, unidirectional illumination using a blue LED (465 nm, 15 µmol photons m^{-2} s^{-1}). The wavelength of the light source selected was close to the maximum absorption wavelength (400–480 nm) of brown algal gametes (Kawai 1992b). The photon flux density was measured with an LI-190SB Quantum sensor (Meiwa Shoji Co., Tokyo, Japan). To examine the behavior of male gametes, they were incubated under each condition for about 1 min and observations were recorded within 5 min. Male gametes (9.2×10^3–9.2×10^4 cells/ml) were suspended in 96-well plates (visual observation) or observation chambers made of double-faced adhesive tape (90 µm depth) between a slide glass and a cover slip (microscopic observation).

Observations and recording

Images of swimming male gametes were recorded with a phase contrast microscope (BX51, Olympus, Tokyo, Japan) using a 10× or 40× objective (UPlan FLN, Olympus, Tokyo, Japan) connected to a high-speed CCD camera (HAS220, Ditect, Tokyo, Japan) at 200 fps (frames per s) and 1/1000 s shutter speed. To prevent the effect of blue light on phototaxis (Kawai et al. 1990), observations were conducted using an R-58 red cut-off glass filter (S-058, HOYA, Tokyo, Japan) in the dark room. The angle (θ) between the light and swimming direction was manually measured. Images of swimming trajectories and velocities were automatically output by Bohboh software (Bohboh Soft, Tokyo, Japan).

Results

General motility of positive and negative phototaxis in various conditions

Two hundred µl of experimental media ($[Ca^{2+}]$; 10^{-1} M, 10^{-2} M (control condition), 10^{-3} M, 10^{-4} M, 10^{-5} M, and 10^{-6} M) containing male gametes (9.2×10^3–9.2×10^4 cells/ml) of *M. cylindricus* were added to each of the 96 multi-well plates and provided unidirectional blue light stimulation (465 nm, 15 µmol photons m^{-2} s^{-1}). Images of all the conditions were captured 1 and 3 min after providing

blue light stimulation. In addition to these external [Ca^{2+}] observations, La^{3+} ([La^{3+}]; 10^{-5} M, 10^{-4} M, 3×10^{-4} M, 5×10^{-4} M) was added to the control medium. These experiments were repeated three times and the same results were obtained.

Under control and extracellular 10^{-2}–10^{-3} M [Ca^{2+}] conditions, male gametes swam toward the light source (Plate 38). In contrast, at 10^{-4}–10^{-6} M [Ca^{2+}], they swam away from the light source. From 1 to 3 min, the number of male gametes which had migrated to one side increased.

Next, swimming directions (θ) of male gametes were measured under all conditions. Male gametes with no light stimulus under 10^{-2} M [Ca^{2+}] showed random movements (Plate 39a). After the illumination of unidirectional blue light, they immediately exhibited positive phototaxis (Plate 39b). At 10^{-3} M [Ca^{2+}], about 10 % of the male gametes did not show phototaxis and possessed circular swimming paths near the slide or cover slip. When viewed from the glass cover slip, male gametes mostly showed counter-clock wise circles. The others showed conspicuous phototaxis. More than half of the male gametes swam toward the light source (positive phototaxis), and the rest of them swam away from the light source (negative phototaxis) (Plate 39c). At 10^{-4} –10^{-5} M [Ca^{2+}], about 30 % of the male gametes did not show phototaxis as mentioned above, but the rest of them swam away from the light source (negative phototaxis) (Plate 39d, e). At 10^{-6} M [Ca^{2+}], about 30 % of male gametes stopped swimming and about 30 % swam but did not show phototaxis but swam as mentioned above. The others showed phototaxis and swam away from the light source (negative phototaxis) (Plate 39f).

Negatively phototactic male gametes, at low extracellular [Ca^{2+}] (less than 5 min), were transferred back to the control condition (10^{-2} M [Ca^{2+}]). Although some of male gametes were disordered, most gametes recovered and swam toward the light source (positive phototaxis) (Plate 39g). At 10^{-1} M [Ca^{2+}], male gametes swam toward the light source (positive phototaxis), although some were disordered (Plate 39h). Further increases in extracellular [Ca^{2+}] (>10^{-1} M) inhibited not only phototaxis, but also flagellar beating. From these data, it was revealed that only decreases in extracellular [Ca^{2+}] induced changes in the phototactic sign (positive to negative), and this change was reversible.

The experiments using La^{3+} in control condition of 10^{-2} M [Ca^{2+}] showed the same tendencies

as the above experiments (Plate 40). Similar to the control condition, at 10^{-5} M [La^{3+}], male gametes swam towards the light source (positive phototaxis) (Plate 40a, b). At 10^{-4} M [La^{3+}], they swam away from the light source (negative phototaxis) (Plate 40a, c), at 3×10^{-4} M [La^{3+}], male gametes did not show phototaxis, and at 5×10^{-4} M [La^{3+}], the motility of male gametes was inhibited.

Swimming velocities and trajectories of male gametes with positive and negative phototaxis

Swimming velocities of more than 50 of the male gametes in each condition, which typically swam with positive or negative phototaxis, were analyzed. Depending on the extracellular [Ca^{2+}], compared to the control condition, significant changes in swimming velocities could be observed at 10^{-1} M [Ca^{2+}] (average value ± standard deviation, 182.1 ± 46.5 μm s^{-1}) and 10^{-3} M [Ca^{2+}] (123.7 ± 27.1 μm s^{-1}) (Plate 41). However, negatively phototactic male gametes, at 10^{-4}–10^{-5} M [Ca^{2+}], showed nearly the same velocity as positively phototactic male gametes under the control condition (138.6 ± 34.5 μm s^{-1}). Moreover, La^{3+} somewhat induced significant changes in velocities, however, swimming velocities of two La^{3+} conditions, positively (119.0 ± 26.4 μm s^{-1} at 10^{-5} M [La^{3+}]) and negatively (99.7 ± 21.5 μm s^{-1} at 10^{-4} M [La^{3+}]) phototactic gametes, did not show significant differences to each other (Plate 41). Thus, these results suggested that the changes in the phototactic sign did not conspicuously affect the swimming velocities of male gametes.

Swimming paths of phototactic male gametes under the control condition ([Ca^{2+}], 10^{-2} M) and 10^{-3} M [Ca^{2+}] showed smooth spirals (Plate 42a), while, at 10^{-4}–10^{-6} M [Ca^{2+}], they showed conspicuous spiral paths (Plate 42b). However, negatively phototactic male gametes, which were induced by La^{3+}, showed smooth spiral paths (Plate 42c). This suggested that strong spiral paths were not characteristic of negative phototaxis, although the reason why they showed such strong spirals was still unclear.

Flagellar waveforms and swimming orientations in positive and negative phototaxis

Phototactic-turning of *M. cylindricus* occurred in 3-dimensional movements, making it difficult to focus on the two flagella, AF and PF. In this experiment, images of 19 positively phototactic male gametes and 10 negatively phototactic ones were acquired and analyzed. While gametes were

turning towards or away from the light source, the beat frequency of AF decreased from c.a. 38 Hz (Kinoshita et al. 2016d) to 11 Hz–25 Hz (n=15) and large unilateral bends in PF could be observed. In both situations, the bending direction of PF was from the ventral side (the side of the flagellar basal bodies) to the dorsal side of the gametes (Plate 43). This was commonly observed in acquired video images. Until the swimming directional change had been finished, PF bend continued with helical rotations of the cell body. The helical rotations of their cell body were mostly clockwise, when viewed from the advancing direction, and a rotation lasted approximately a third to a fourth of a second. Although non-phototactic gametes showed two-dimensional AF waveforms, phototactic gametes showed three-dimensional AF waveforms.

The timing of the PF beat differed between gametes swimming towards and away from the light source. In the first situation, the PF bend occurred when the light was provided from dorsal side (opposite side of the stigma) (Plate 43a, b, e). In the second situation, the PF bend occurred when the light was provided from the ventral side (stigma side) (Plate 43c, d, f). Furthermore, the bending time of PF sometimes differed in these situations. In the first situation, most of gametes 16 out of 19 showed long bending time for PF (>70 ms). While, in the second situation, only 2 out of 10 gametes showed a long bending time for PF and the others showed a short bending time (<15 ms). The short bending time of PF was repeated several times until the swimming directional change of the male gametes was complete.

Discussion

Cilia and flagella are well-conserved structures in the eukaryotic cells. In several eukaryotes (*Chlamydomonas*, sea urchins, ascidians, mammals, *Paramecium*, and *Trypanosoma*), Ca^{2+} is the critical intracellular factor effecting changes in the motility of cilia and flagella in response to extracellular environments (Inaba 2015). In brown algal swarmers that have two unique, heterogeneous flagella, only one experiment was reported, in which the response of male gametes to the sex pheromone from female gametes (chemotaxis) was inhibited by Ca^{2+} channel inhibitors (Maier and Calenberg 1994). The present study showed the relationship between the phototactic response of male gametes and the extracellular [Ca^{2+}] in brown algae.

At low extracellular [Ca^{2+}], phototaxis was inhibited in some male gametes of *M. cylindricus* and they swam near the cover slip or glass slide. Their swimming paths formed counter-clockwise circles when viewed from the cover glass. The PF of these gametes bent to the left side of their body. These movements were similar to thigmotaxis, which was induced by the sex pheromone secreted from female gametes. However, thigmotaxis usually showed that gametes swam in clockwise-circles and PF bent to the right side of the cell body when viewed from the cover glass (Kinoshita et al. 2016d and Part 2. 2 in this thesis). Their locomotion, when near the slide or cover glass, was usually composed of two-dimensional movements of the AF waveforms. Moreover, in swarmers of the brown alga *S. lomentaria*, AF showed a plane waving without cell rotation just near the surface of the slide or cover slip, which was different from their free-swimming movements with the helical rotation of the cell body (Matsunaga et al. 2010). The AF waveform change from three- to two-dimensions might be due to some change in the physiological properties of AF. In sea urchin sperm, $MgATP^{2-}$ and cAMP concentrations are known to be related to the three-dimensional flagellar movements (Ishijima 2013). To clarify the regulation of AF waveforms, further physiological experiments on brown algae are necessary.

M. cylindricus male gametes swimming with a helical rotation of their cell body showed phototaxis similar to that of *S. lomentaria* (Matsunaga et al. 2010). The phototactic sign changed from positive to negative at low extracellular [Ca^{2+}] and this change was reversible. In both positive and negative phototaxis, light reception by an unknown photoreceptor is believed to occur via the reflection of blue light at the concaved eyespot region in the brown algae, and to focus at the paraflagellar body of PF (Müller et al. 1987; Kawai et al. 1990; Kawai et al. 1991; Kreimer et al. 1991; Kawai and Kreimer 2000; Matsunaga et al. 2010; Fu et al. 2014).

La^{3+} binds negative surface charges on the external surface of the cell and blocks Ca^{2+} channels (Lansman et al. 1986; Carafoli 1992; Prakriya and Lewis 2015). In this study, La^{3+} experiments under 10^{-2} M [Ca^{2+}] inhibited positive phototaxis (10^{-4} M), phototaxis (3×10^{-4} M) and swimming (5×10^{-4} M). Therefore, it can be estimated that a higher influx of Ca^{2+} is required in positive phototaxis than negative or no phototaxis in *M. cylindricus*. Moreover, the previous study showed that La^{3+} (at 10^{-5} M) inhibited the asymmetric waveform of AF in chemokinetic responses of

male gametes of *E. siliculosus* (Maier and Calenberg 1994). Not only previously mentioned published data but also the data from the present study, it was revealed that Ca^{2+} channels inhibited by La^{3+} affected both responses to the sex pheromone (chemotaxis) and light stimulus (phototaxis), while affecting flagellar motion. Nifedipine, a specific blocker of the L-type voltage-dependent Ca^{2+} channel, and flunarizine, a T-type and L-type voltage-dependent Ca^{2+} channel blocker, did not significantly affect the sign of phototaxis, although flagellar beating and phototaxis were affected only at high concentrations (nifedipine 10^{-3} M, flunarizine 5×10^{-4} M) (unpublished data). Thus, it is unclear that these channels are related to the phototaxis. However, Ca^{2+} channels that were blocked by nifedipine (at 5×10^{-5} M) were known to affect chemotaxis with reorientation by a PF unilateral bend (Maier and Calenberg 1994). The transcriptome analysis confirmed the expression of the voltage dependent ion and Ca^{2+} channel-related genes in male and female gametes of the brown alga *E. siliculosus*, which suggests that these may actually control the flagellar beat during phototaxis (Lipinska et al. 2013). Furthermore, voltage-dependent Ca^{2+} channel-related genes have been detected in the flagellar proteomics in swarmers of *Colpomenia bullosa* (Fu et al. 2014). Perhaps, some of these voltage-dependent Ca^{2+} channels, which were not affected by nifedipine and flunarizine, might be related to the phototaxis.

Positively and negatively swimming gametes at 10^{-2} M and 10^{-4}–10^{-5} M [Ca^{2+}] respectively, showed similar swimming velocities which means that the extracellular [Ca^{2+}] in these ranges did not largely affect the swimming ability or AF beating pattern of male gametes. In contrast, swimming velocity of male gametes decreased at 10^{-3} M [Ca^{2+}]. This may be because about half of the male gametes showed positive phototaxis, but the others showed negative phototaxis, and collision between them frequently occurred, causing a decrease in velocity. In cases where the Ca^{2+} channel blocker La^{3+} was used, positively and negatively phototactic gametes could be detected at 10^{-5}M and 10^{-4} M [La^{3+}], respectively, and they showed similar swimming velocities when compared to each other.

M. cylindricus male gametes, which turned toward (positive phototaxis) or away (negative phototaxis) from the light source, showed clockwise helical rotations of the cell body similar to *Chlamydomonas*. However, the frequency of rotation was slightly different between *M. cylindricus*

male gametes (ca. 3-4 Hz) and *Chlamydomonas* (ca. 2 Hz) (Foster and Smyth 1980), possibly due to the size of their cell bodies. The beat frequency of AF decreased and the unilateral bend of PF occurred in positive and negative phototaxis, similar to *S. lomentaria* (Matsunaga et al. 2010). The bending direction of PF was the same in positive and negative phototaxis in *M. cylindricus* male gametes, although the timing of the PF bend differed. The timing of the PF bend after light reception might have an effect on the sign of phototaxis (Plate 43).

In *Chlamydomonas*, the reception of light by photoreceptors (channel rhodopsin) induces inward ion currents at the eyespot region and depolarizes the membrane. Membrane depolarization produces a Ca^{2+} influx through voltage-dependent Ca^{2+} channels on the flagellar membrane (Harz and Hegmann 1991; Harz et al. 1992). This results in increases in the intraflagellar [Ca^{2+}] (Beck and Uhl 1994; Yoshimura et al. 1997). Two equal-length flagella of *Chlamydomonas* are biochemically different in sensitivity to Ca^{2+}, thus, Ca^{2+} influx induces a change of balance between the two flagella. As a result, directional changes in swimming occurs (Kamiya and Witman 1984). In brown algae, these regulation pathways on the flagellar movement remained unclear. Similar to *Chlamydomonas*, two heterogeneous flagella of brown algal swarmers might have different sensitivities to [Ca^{2+}]. Further physiological investigations of flagellar movement need to be conducted.

Many eukaryotic cells usually maintain cytoplasmic free [Ca^{2+}] levels between 10^{-8} and 10^{-7} M most of the time (Blinks et al. 1982). For example, intracellular [Ca^{2+}] of brown algal gametes are assumed to be between 10^{-8} and 10^{-7} M in normal conditions. In this case, if the cytoplasmic Ca^{2+} channel opens, Ca^{2+} influx will be induced in any conditions that were conducted in this study (10^{-2}–10^{-6} M). Two hypothesis can account for finding in this study; 1) low extracellular Ca^{2+} may cause a change in the phototactic sign, from positive to negative, during the cascade reactions from the photoreception to the flagellar waveform change, or 2) there might be a threshold in the intracellular [Ca^{2+}], which produces the unilateral bend of the PF for the phototactic turning, and an increment in the intracellular [Ca^{2+}] to the threshold value would regulate positive or negative phototaxis. With regard to the first hypothesis, some proteins that regulate the sign of phototaxis may be involved. Proteomic analysis of swarmers under different [Ca^{2+}] conditions may give us some clues for determining the regulating system of the phototactic sign. In terms of the second hypothesis, at high

extracellular conditions, intracellular [Ca^{2+}] would immediately reach the threshold value and initiate the PF bend under the control condition, while at lower extracellular [Ca^{2+}] conditions, intracellular [Ca^{2+}] would slowly reach the threshold value and consequently delay the PF bend. When its delay applied to the half-rotation of their cell body, their turn will be the opposite side to the ordinary way (Plate 44). In this case, visualization of intracellular and flagellar [Ca^{2+}] would give a clue to determine the regulatory system of PF bend.

Under culture conditions in this study, male and female gametes of *M. cylindricus* were released, and they accumulated toward the light less than 30 min after the light was provided. However, most gametes showed negative phototaxis 7 h later (unpublished data). The rates of parthenogenesis in male gametes (3%) are much lower than in female gametes (Kitayama et al. 1992). In the natural environment, positive phototaxis of male and female gametes should be used to increase encounters between both gametes and increase fertilization efficiency, like in green algae (Togashi and Bartelt 2011). However, planogamy was not observed in brown algae but their fusion occurs after the settlement of female gametes on the substratum (Maier 1995). Thus, why male gametes of *M. cylindricus* initially show a positive phototaxis remains a mystery and more experiments are necessary to investigate this reaction.

In the conclusion of this part, two points were emphasized. First, extracellular [Ca^{2+}] affects the sign of phototaxis. Secondly, Ca^{2+} channels that were inhibited by La^{3+} affect the sign of phototaxis. From the results, it was suggested that the sign of phototaxis in male gametes of *M. cylindricus* was affected by the extracellular Ca^{2+} influx through Ca^{2+} channels that were blocked by La^{3+}. Moreover, these channels were also involved in the response of male gametes to sex pheromones that are secreted from female gametes. Thus, the responses to two different physicochemical signals (light and sex pheromone) may be controlled by a similar regulation of flagella.

Part 3. 3 Effect of sex pheromone on the sign of phototaxis in brown algal male gametes

Introduction

Male and female gametes of anisogamous brown alga *Mutimo cylindricus* swim toward the light direction (positive phototaxis) several minutes after the light was provided. About 7 hours after that, they start to accumulate at the opposite side of the light direction (negative phototaxis). The behaviors of microorganisms, including brown algal swarmers, in the natural habitat, are the result of a delicate balance between positive and negative phototaxis (sign of phototaxis) (Häder 1988).

In brown algae, the process of fertilization starts from secreting sex pheromone by female gametes, followed by receiving it by male gametes. Then, the male gametes change the locomotion patterns and gather around the female gametes (Müller 1974; Kinoshita et al. 2016d). In the case of isogamous and anisogamous species, female gametes are firstly settled on the substratum where is usually opposite side to the light direction, and secret sex pheromone. Therefore, it is considered that swimming to the opposite direction to the light (negative phototaxis) will be appropriate for male gametes to increase efficiency to encounter the female gametes.

In this study, it became clear that the sign of phototaxis in male gametes were affected by sex pheromone from female gametes. This result is the first approach to show the close interaction between the signaling pathways of photoreception and chemoreception in male gametes of brown algae.

Materials and Methods

Using the same culture methods as Kinoshita et al. (2016d) and Part 2. 2 in this thesis, numerous male and female gametes of *M. cylindricus* were obtained. The basal medium in this study was autoclaved sea water (estimated as 10 mM [Ca^{2+}]) containing half-strength PES medium (Provasoli 1968). To make the observation medium, various concentrations (1.3×10^{-3} M, 1.3×10^{-4} M, 1.3×10^{-5} M, 1.3×10^{-6} M) of artificially synthesized ectocarpene (stock sol. 1.3×10^{-1} M in DMSO), a gift from Dr. T. Umezawa, Graduate school of Environmental Science, Hokkaido University, or 50 µl of female gametes containing medium kept in 15 min at dark condition to induce releasing sex

pheromone were mixed with 150 µl of culture medium containing male gametes. To examine the behavior of male gametes in these conditions, photos were obtained 1) one and three min and 2) 20-40 min after they were mixed. Male gametes (9.0×10^{3}–9.0×10^{4} cells/ml) in various conditions were suspended in 96-well plates (visual observation) (Plates 45, 49) or observation chambers made of double-faced adhesive tape (90 µm depth) between a slide glass and a cover slip (microscopic observation) (Plates 47, 48), and provided unidirectional blue LED (465 nm, 15 µmol photons m^{-2} s^{-1}). The photon flux density was measured with an LI-190SB Quantum sensor (Meiwa Shoji Co., Tokyo, Japan). The phototactic behaviors of male gametes were recorded and their swimming velocities and directions were quantified with the same methods as mentioned in Part 3. 1 in this thesis.

Results

Male gametes with artificially synthesized ectocarpene

The sex pheromone from female gametes of *M. cylindricus* mostly contain multifiden, with aucantene and ectocarpene (Jaenicke et al. 1974). In the previous work by Müller (1976), the male gametes showed chemotaxis to ectocarpene (gradient condition) in the concentration more than 3.1×10^{-5} M. In this study, artificially synthesized ectocarpene (stock concentration 1.3×10^{-1} M) was used.

When ectocarpene was completely mixed with culture medium containing male gametes (final concentration of ectocarpene; 1.3×10^{-3} M), male gametes did not show phototaxis (Plate 45). They became immotile and some of them took their flagella into their cell bodies (not shown). At the concentration of ectocarpene 1.3×10^{-4} M, more than 20 % of male gametes showed thigmotactic swimming (swimming just on the substratum and eliminating helical rotations of the cell) forming small circular paths without phototaxis (Plate 46a). The others mostly showed negative phototaxis (Plates 47a, 48f). The sign of phototaxis in male gametes changed, but in female gametes did not change in this condition. At 1.3×10^{-5} M, less than 10 % of male gametes showed thigmotaxis and the rest of them showed negative or positive phototaxis (Plates 46b, 47b, 48e). At 1.3×10^{-6} M, most of them showed only positive phototaxis (Plates 46c, 47c, 48d). These phenomena could be confirmed

in both dish assay and microscopic observations using the chamber made with cover slip and slide glass. These experiments were conducted more than three times and the same results were obtained, except in the condition at 1.3×10^{-4} M ectocarpene. In this condition, numbers of male gametes that showed positive phototaxis was sometimes increased, but in every experiments majority of them showed negative phototaxis. The swimming velocity of each condition was slightly different compared to the control condition (176.7 ± 42.0 μm/s). Swimming velocities of typically swimming (showing phototaxis) male gametes at 1.3×10^{-6} M, 1.3×10^{-5} M, 1.3×10^{-4} M were 182.1 ± 55.8, 207.0 ± 50.9, 154.3 ± 38.2 μm/s, respectively.

Male gametes with sex pheromone from settled female gametes

At the condition of which mixed with sex pheromone released from settled female gametes (containing female gametes), more than 30 % of male gametes showed thigmotaxis, and ones which swam nearby settled female gametes showed small circular swimming paths (Plate 46d), and the rest showed negative or positive phototaxis, similar to the case of ectocarpene 1.3×10^{-5} M (Plate 47d). These experiments were carried out more than three times and the same results were obtained. The swimming velocity of typically swimming (showing phototaxis) male gametes was 236.9 ± 60.1 μm/s. It was higher than the control condition and similar value to that of male gametes in 1.3×10^{-5} M concentration of ectocarpene.

In the culture dishes, more than 1 h after light was provided, when male and female gametophytes were incubated together, some gametes were accumulated in the light direction but the others accumulated in opposite side of the light direction. The gametes gathering at the opposite side of the light direction were mainly composed of male gametes, and female gametes were few.

Times after incubation of male gametes with ectocarpene or female gametes

After male gametes were mixed with ectocarpene or female gametes as mentioned above, they were incubated for 20-40 min at dark condition (Room temperature). After illuminating by blue light, in all conditions that incubated with ectocarpene, male gametes mostly showed positive phototaxis (Plate 49). These experiments were conduced more than three times but the time of recovering from

negative to positive phototaxis was not stable between 20 min to 40 min. On the contrary, the condition of which mixed with female gametes, male gametes showed negative or positive phototaxis even after 1h.

Discussion

It was estimated from the study by Müller (1976), the concentration of ectocarpene 10^{-6} M was below the threshold that male gametes could react, therefore male gametes might show only positive phototaxis. On the other hand, under the concentration higher than 1.3×10^{-5} M ectocarpene or culture medium containing female gametes, only a part of male gametes changed from positive to negative phototaxis. The change of phototactic sign (positive to negative) in male gametes by artificial and natural sex pheromones, may actually take advantage of increasing encountering rate of male and female gametes in the field (Plate 50). However, why only some part of male gametes showed negative phototaxis is mystery. They may have different sensitivity to the sex pheromone.

Boland (1995) reported that the ectocarpene is volatile and also inactivation process takes place with several minutes and controlled by temperature, not requiring any additional enzymatic activity. For that reason, ectocarpene which were mixed with culture medium containing male gametes may be volatilized or inactivated during 20–40 min, and male gametes started to show positive phototaxis. On the other hand, in the case of the medium containing male gametes that were mixed with female gametes, sex pheromone secreted by female gametes would not entirely be volatilized, because female gametes kept releasing sex pheromone in turns. Therefore, the negative phototaxis of *M. cylindricus* male gametes induced by sex pheromone was a reversible change. Moreover, it was assumed that the different perceiving systems of male gametes against light and sex pheromone might have a common part between photo- and chemosignaling pathways.

In my previous study, it became clear that the extracellular Ca^{2+} concentration change affect to the sign of phototaxis of male gametes in *M. cylindricus*. It indirectly suggested that the intracellular Ca^{2+} concentration had a crucial role in the control of phototactic sign. Therefore, change of phototactic sign by sex pheromone may be regulated by intracellular Ca^{2+} concentration change. However, change of phototactic sign by sex pheromone was not drastic as in the case of

Ca^{2+} concentration change. Even in higher concentration of ectocarpene, some male gametes still showed positive phototaxis. Therefore, it was presumed that, not like in the case of Ca^{2+}, each of male gametes may have different sensitivity to sex pheromone.

Chemotaxis to sex pheromone in sperm of animals is especially well studied and many part of signaling pathways become clear (Kaupp et al. 2008). Although much of the studies are accumulated about phototaxis in green flagellates, chemotaxis to sex pheromone remains mostly unclear (Govorunova and Sineshchekov 2003), while there is an interesting examination using the model green alga, *Chlamydomonas*. Gametes of the heterotrophic strain *Chlamydomonas reinhardtii* swim toward tryptone, which is used as the growth medium suppliment. This phenomena was only seen in gametes not in vegitative cells, therefore, the chemotaxis is thought not only for leading gametes to the food source but also to the attraction of gametes to the other sex (Govorunova and Sineshchekov 2003). Moreover, Govorunova and Sineshchekov (2003) showed that tryptone rapidly inhibit the photoreceptor currents, which initiated by rhodopsin-type receptors (Harz and Hegmann 1991), only in gametes not in vegetative cells. The tryptone-induced inhibition of photoreceptor current due to activate chemosensory systems in *C. reinhardtii* presumed that integration of the photo- and chemosensory signals already occurs at the initial steps of the signaling pathways. In brown algae, electrical process in the plasma membrane in photo- and chemosensory transduction had not been studied. However, this information provides a clue for finding the start where a common part between photo- and chemosignaling pathways in brown algal gametes.

In the conclusion of this part, some of male gametes in *M. cylindricus* were especially induced the change of phototactic sign (positive to negative) adding to chemotaxis by the reception of sex pheromone. It was assumed that the signals (light and sex pheromone) perceived by different sensory systems of male gametes might have a common part between photo- and chemosignaling pathways.

Concluding remarks and future perspectives

From the perspective of the eukaryote evolution, brown algae are distinct from other organisms including animals and land plants, and are an intriguing model when considering the mechanisms of phototaxis and chemotaxis. In this thesis, firstly, the flagellar basal apparatus of the brown alga was re-investigated using electron tomography and the precise position of two flagellar basal bodies, bands, and flagellar rootlets was determined. Moreover, a new numbering system of the flagellar axoneme was presented.

Secondly, it was quantitatively revealed that the responses of AF and PF of male gametes to sex pheromone was different. This suggested that they would have the distinct regulating systems. Unilateral bending of PF when sensing a decrease in the concentration of sex pheromone was a common response in male gametes (sperm) in isogamy, anisogamy and oogamy of brown algae. The response of PF during chemotaxis was similar to that of sperm of marine invertebrates, which are phylogenetically distant to brown algae. They may be using similar signaling pathways to change their flagellar waveforms. The comparative analysis of proteins, which control the flagellar waveforms between brown algae and marine invertebrates, will be attractive in the field of evolution and adaptation in the aquatic environment.

Thirdly, it was shown that PF bending also had an important role in phototactic turning. Moreover, intracellular Ca^{2+} had a crucial role for regulating the timing of PF bending and was controlling the sign of phototaxis in brown algae. It is now widely known that a transient increase in intracellular Ca^{2+} concentration induced by chemo-attractants cause changes in flagellar asymmetry, resulting in the re-orientation of the swimming sperm (Kaupp et al. 2008; Shiba et al. 2008; Yoshida and Yoshida 2011; Mizuno et al. 2012). Therefore, visualization of intracellular Ca^{2+} during phototaxis using brown algae will be interesting work and should be studied in near future.

Finally, recepting the sex pheromone was also revealed to be a factor for changing the sign of phototaxis, and it would be controlled by intracellular Ca^{2+}. From all these results, I presumed that the signals (light and sex pheromone) perceived by different sensory systems of male

gametes might have a common part between photo- and chemosignaling pathways.

For future studies, the following questions should be answered about the phototactic responses of brown algal swarmers: 1) what kind of protein is working as a photoreceptor and where does it exist? 2) What kind of signaling pathway participates in the flagellar waveform change after photoreception? 3) What kinds of proteins in the flagellar axoneme are related to the changes in flagellar waveforms? 4) What is the benefit of exhibiting a positive or negative phototaxis in their living field? All these questions should be taken into account in studies on the chemotactic response in male gametes. Especially, distinct proteins and regulating systems of AF and PF should be examined, and the common proteins relating to phototaxis and chemotaxis should be clarified. Moreover, about these proteins, comparative analysis with other organism that phylogenetically close to brown algae (ex. Plate 51) or distinct to brown algae (ex. Plate 52) has to be conducted.

References

Adl SM, Simpson AG, Lane CE, Lukeš J, Bass D, Bowser SS, Brown MW, Burki F, Dunthorn M, Hampl V, Heiss A, Hoppenrath M, Lara E, Gal LL, Lynn DH, McManus H, Mitchell EA, Mozley-Stanridge SE, Parfrey LW, Pawlowski J, Rueckert S, Shadwick RS, Schoch CL, Smirnov A and Spiegel FW (2012) The revised classification of eukaryotes. *J. Eukaryot. Microbiol.* **59**:429–493.

Afzelius BA (1959) Electron microscopy of the sperm tail. Results obtained with a new fixative. *J. Biophys. Biochem. Cytol.* **5**:269–278.

Amsler CD, Neushul M (1989) Chemotactic effects of nutrients on spores of the kelps *Macrocytis pyrifera* and *Pterygophora california*. *Mar. Biol.* **102**:557–564.

Amsler CD, Neushul M (1990) Nutrient stimulation of spore settlement in the kelps *Pterygophora californica* and *Macrocystis pyrifera*. *Mar. Biol.* **107**:297–304.

Amsler CD, Reed DC, Neushul M (1992) The microclimate inhabited by macroalgal propagules. *Br. Phycol. J.* **27**:253–270.

Andersen RA (2004) Biology and systematics of heterokont and haptophyte algae. *American J. Bot.* **91**:1508–1522.

Baba SA, Mogami Y (1985) An approach to digital image analysis of bending shapes of eukaryotic flagella and cilia. *Cell Motility* **5**:475–489.

Beck C, Uhl R (1994) On the localization of voltage-sensitive calcium channels in the flagella of *Chlamydomonas reinhardtii*. *Biophys. J.* **125**:1119–1125.

Böhmer M, Van Q, Weyand I, Hagen V, Beyermann M, Matsumoto M, Hoshi M, Hildebrand E, Kaupp UB (2005) Ca^{2+} spikes in the flagellum control chemotactic behavior of sperm. *EMBO* **24**:2741–2752.

Blinks JR, Wier WG, Hess P, Prendergast FG (1982) Measurement of Ca^{2+} concentrations of living cells. *Prog. Biophys. Mol. Biol.* **40**:1–114.

Boland W (1995) The chemistry of gamete attraction: Chemical structures, biosynthesis, and (a)biotic degradation of algal pheromones. *Proc. Natl. Acad. Sci. USA* **92**:37–43.

Boland W, Konig WA, Müller DG (1989) Separation of enantomeric algal pheromones and related

hydrocarbons by gas-liquid chromatography on modified cyclodextrins as chiral stationary phases. Biosynthetic relevance of racemic by-products. *Helvetica Chimica. Acta.* **72**:1288–1292.

Bouck GB (1969) Extracellular microtubules: the origin, structure, and attachment of flagellar hairs in *Fucus* and *Ascophyllum antherozoids*. *J. Cell Biol.* **40**:446–460.

Bray D (1992) Cell swimming. In: Bray D (ed) Cell movements. Garland, New York, pp 3–16.

Brokaw CJ (1979) Calcium-induced asymmetrical beating of Triton-demembranated sea urchin sperm flagella. *J. Cell Biol.* **82**:401–411.

Brokaw CL, Kamiya R (1987) Bending patterns of *Chlamydomonas* flagella: IV. Mutants with defects in inner and outer dynein arms indicate differences in dynein arm function. *Cell Motil. Cytoskeleton* **8**:68–75.

Bui KH, Sakakibara H, Movassagh T, Oiwa K, Ishikawa T (2009) Asymmetry of inner dynein arms and inter-doublet links in *Chlamydomonas* flagella. *J. Cell Biol.* **186**:437–446.

Carafoli E (1992) The Ca^{2+} Pump of the Plasma Membrane. *J. Bol. Chem.* **267**:2115–2118.

Cardullo RA, Herrick SB, Peterson MJ, Dangott LJ (1994) Speract receptors are localized on sea urchin flagella using a fluorescent peptide analog. *Dev. Biol.* **162**:600–607.

Cheignon M (1964) Ultrastructure du gamète mâle d'*Ascophyllum nodosum*. *C. R. Acad. Sci. Paris* **258**:676–678.

Chwang AT, Wu TY (1971) A note on the helical movement of micro-organisms. Proceedings of the Royal Society of London. *Series B, Biol. Sci.* **178:**327–346.

Clayton MN (1989). Brown algae and chromophyte phylogeny. In: Green JC, Leadbeater BSC, Diver WL (eds) The Chromophyte Algae: problems and perspectives. The Systematics Association Special, **38**. Clarendon Press, Oxford, UK, pp 230–253.

Cock JM, Sterck L, Rouze P, Scornet D, Allen AE, Amoutzias G, Anthouard V, Artiguenave F, Aury JM, Badger JH, et al. (2010) The *Ectocarpus* genome and the independent evolution of multicellularity in brown algae. *Nature* **465**:617–621.

Coleman AW (1988) The autofluorescent flagellum: a new phylogenetic enigma. *J Phycol* **24**:118–120.

Dring MJ (1988) Photocontrol of development in algae. Annu. Rev. Plant Physiol. *Plant Mol. Biol.*

39:199–207.

Dring MJ, Lüning K (1975) A photoperiodic response mediated by blue light in the brown alga *Scytosiphon lomentaria*. *Planta* **125**:25–32.

Feinleib MEH, Curry GM (1971) The relationship between stimulus intensity and oriented phototactic response (topotaxis) in *Chlamydomonas. Physiol. Plant* **25**:346–352.

Fletcher RL, Callow ME (1992) The settlement, attachment and establishment of marine algal spores. *Br. Phycol. J.* **27**:303–329.

Flores-Moya A, Posudin YI, Fernández JA, Figueroa FL, Kawai H (2002) Photomovement of the swarmers of the brown algae *Scytosiphon lomentaria* and *Petalonia fascia*: effect of photon irradiance, spectral composition and UV dose. *J. Photochem. Photobiol. B* **66**:134–140.

Foster KW, Smyth RD (1980) Light antennas in phototactic algae. *Microbiol. Rev.* **44**:572–630.

Frenkel J, Vyverman W, Pohnert G (2014) Pheromone signaling during sexual reproduction in algae. *Plant J.* **79**:632–644.

Fritsch FE (1945) The structure & reproduction of the algae. Vol. II. Foreword, Phaeophyceae, Rhodophyceae, Myxophyceae. Cambridge University Press, Cambridge.

Fu G, Nagasato C, Ito T, Müller DG, Motomura T (2013) Ultrastructural analysis of flagellar development in plurilocular sporangia of *Ectocarpus siliculosus* (Phaeophyceae). *Protoplasma* **250**:261–272.

Fu G, Nagasato C, Oka S, Cock JM, Motomura T (2014) Proteomics analysis of heterogeneous flagella in brown algae (Stramenopiles). *Protist* **165**:662–675.

Fu G, Nagasato C, Yamagishi T, Kawai H, Okuda K, Takao Y, Horiguchi T, Motomura T (2016) Ubiquitous distribution of helmchrome in phototactic swarmers of the stramenopiles. *Protoplasma* **253**:929–941.

Fujita S, Iseki M, Yoshikawa S, Makino Y, Watanabe M, Motomura T, Kawai H, Murakami A (2005) Identification and characterization of a fluorescent flagellar protein from the brown alga *Scytosiphon lomentaria* (Scytosiphonales, Phaeophyceae): A flavoprotein homologous to Old Yellow Enzyme. *Eur. J. Phycol.* **40**:159–167.

Geller A, Müller DG (1981) Analysis of the flagellar beat pattern of male *Ectocarpus siliculosus*

gametes (Phaeophyta) in relation to chemotactic stimulation by female cells. *J. Exp. Biol.* **92**:53–66.

Gibbons IR (1981) Cilia and flagella of eukaryotes. *J. Cell Biol.* **91** (suppl) :107s–124s.

Gibbons BH, Gibbons IR (1973) The effect of partial extraction of dynein arms on the movement of reactivated sea-urchin sperm. *J. Cell Sci.* **13**:337–357.

Gibbons BH, Gibbons IR (1980) Calcium-induced quiescence in reactivated sea urchin sperm. *J Cell Biol.* **84**:13–27.

Glantz ST, Carpenter EJ, Melkonian M, Gardner KH, Boyden ES, Wong GK, Chow BY (2016) Functional and topological diversity of LOV domain photoreceptors. *Proc. Natl. Acad. Sci.* **113**: E1442–E1451, doi: 10.1073/pnas.1509428113.

Goldstein DA (1979) Calculation of the concentrations of free cations and cation-ligand complexes in solutions containing multiple divalent cations and ligands. *Biophys. J.* **26**:235–242.

Goodenough UW (1983) Motile detergent-extracted cells of *Tetrahymena* and *Chlamydomonas*. *J. Cell Biol.* **96:**1610–1621.

Govorunova EG, Sineshchekov OA (2003) Integration of photo- and chemosensory signaling pathways in *Chlamydomonas*. *Planta* **216**:535–540.

Guerrero A, Nishigaki T, Carneiro J, Tatsu Y, Wood CD, Darszon A (2010) Tuning sperm chemotaxis by calcium burst timing. *Develop. Biol.* **344**:52–65.

Häder D-P (1988) Ecological consequences of photomovement in microorganisms. *J. Photochem. Photobiol. B* **1**:385–414.

Häder D-P, Colombetti G, Lenci F, Quaglia M (1981) Phototaxis in the flagellates, *Euglena gracilis* and *Ochromonas danica*. *Arch. Microbiol.* **130**:78–82.

Harz H, Hagemann P (1991) Rhodopsin-regulated calcium currents in *Chlamydomonas*. *Nature* **351**:489–491.

Harz H, Nonnengässer C, Hegemann P (1992) The photoreceptor current of the green alga *Chlamydomonas*. *Phil. Trans. R. Soc. Lond. B* **338**:39–52.

Henry EC, Cole KM (1982a) Ultrastructure of swarmers in the Laminariales (Phaeophyceae). I. Zoospores. *J. Phycol.* **18**:550–569.

Henry EC, Cole KM (1982b) Ultrastructure of swarmers in the Laminariales (Phaeophyceae). II. Sperm. *J. Phycol.* **18**:570–579.

Higashiyama T, Takeuchi H (2015) The mechanism and key molecules involved in pollen tube guidance. *Annu. Rev. Plant Biol.* **66**:393–413.

Holwill MEJ, Sleigh MA (1967) Propulsion by hispid flagella. *J. Exp. Biol.* **47**:267–276.

Hoops HJ, Witman GB (1983) Outer doublet heterogeneity reveals structural polarity related to beat direction in *Chlamydomonas* flagella. *J. Cell Biol.* **97**:902–908.

Inaba K (2003) Molecular architecture of the sperm flagella: molecules for motility and signaling. *Zool. Sci.* **20**:1043–1056.

Inaba K (2011) Sperm flagella: comparative and phylogenetic perspectives of protein components. *Mol. Hum. Reprod.* **17**:524–538.

Inaba K (2015) Calcium sensors of ciliary outer arm dynein: functions and phylogenetic considerations for eukaryotic evolution. *Cilia* **4**:6.

Ishijima S (2012) Comparative analysis of movement characteristics of lancelet and fish spermatozoa having different morphologies. *Biol. Bull.* **222**:214–221.

Ishijima S (2013) Regulations of microtubule sliding by Ca^{2+} and cAMP and their roles in forming flagellar waveforms. *Cell Struct. Funct.* **38**:89–95.

Jaenicke L, M Müller DG, Moore RE (1974) Multifidene and aucantene, C11 hydrocarbons in the male-attracting essential oil from the gynogametes of *Cutleria multifida* (Phaeophyta). *J. American Chem. Soc.* **96**:3324–3325.

Jahn TL, Landman MD, Fonseca JR (1964) The mechanism of locomotion of flagellates. II. Function of the mastigonemes of *Ochromonas*. *J. Protozool.* **11**:291–296.

Kambara Y, Shiba K, Yoshida M, Sato C, Kitajima K, Shingyoji C (2011) Mechanism regulating Ca^{2+}-dependent mechanosensory behaviour in sea urchin spermatozoa. *Cell Struct. Funct.* **36**:69–82.

Kamiya R, Witman GB (1984) Submicromolar levels of calcium control the balance of beating between the two flagella in demembranated models of *Chlamydomonas. J. Cell Biol.* **98**:97–107.

Katsaros C, Maier I, Melkonian M (1993) Immunolocalization of centrin in the flagellar apparatus of

male gametes of *Ectocarpus siliculosus* (Phaeophyceae) and other brown algal motile cells. *J. Phycol*. **29**:787–797.

Kaupp UB (2010) Olfactory signallyng in vertebrates and insects: differences and commonalities. *Nature Rev.* **11**:188–200.

Kaupp UB, Kashikar ND, Weyand I (2008) Mechanisms of sperm chemotaxis. *Annu. Rev. Physiol.* **70**:93–117.

Kaupp UB, Solzin J, Hildebrand E, Brown JE, Helbig A, Hagen V, Beyermann M, Pampaloni F, Weyand I (2003) The signal flow and motor response controling chemotaxis of sea urchin sperm. *Nat. Cell Biol.* **5**:109–117.

Kawai H (1988) A flavin-like autofluorescent substance in the posterior flagellum of golden and brown algae. *J. Phycol.* **24**:114–117.

Kawai H (1992a) A summary of the morphology of chloroplasts and flagellated cells in the Phaeophyceae. *Korean J. Phycol.* **7**:33–43.

Kawai H (1992b) Green flagellar autofluorencence in brown algal swarmers and their phototactic responses. *Bot. Mag. Tokyo* **105**:171–184.

Kawai H, Kreimer G (2000) Sensory mechanisms: light perception and taxis in algae. In: Leadbeater B, Green J (eds) The Flagellates: Unity, Diversity and Evolution. Taylor and Francis, London, pp 124–146.

Kawai H, Kubota M, Kondo T, Watanabe M (1991) Action spectra for phototaxis in zoospores of the brown alga *Pseudochorda gracilis*. *Protoplasma* **161**:17–22.

Kawai H, Motomura T, Okuda K (2005) Isolation and purification techniques for macroalgae. In: Andersen AA (ed) Algal culturing techniques. Elsevier Academic Press, London, pp 133–143.

Kawai H, Müller DG, Fölster E, Häder D-P (1990) Phototactic responses in the gametes of the brown alga, *Ectocarpus siliculosus*. *Planta* **182**:292–297.

Keller JB, Rubinow SI (1976) Swimming of flagellated microorganisms. *Biophys. J.* **16:**151–170.

Kinoshita N, Nagasato C, Motomura T (2016b) Chemotactic movement in sperm of the oogamous brown algae, *Saccharina japonica* and *Fucus distichus*. *Protoplasma* DOI 10.1007/s00709-016-0974-y.

Kinoshita N, Shiba K, Inaba K, Fu G, Nagasato C, Motomura T (2016c) Flagellar Waveforms of

gametes in the brown alga, *Ectocarpus siliculosus*. *Eur. J. Phycol.* **51**:139–148.

Kinoshita N, Tanaka A, Nagasato C, Motomura T (2016d) Chemotaxis in the anisogamous brown alga *Mutimo cylindricus*. *Phycologia* **55**:359–364.

Kitayama T, Kawai H, Yoshida T (1992) Dominance of female gametophytes in field populations of *Cutleria cylindrica* (Cutleriales, Phaeophyceae) in the Tsugaru Strait, Japan. *Phycologia* **31**:449–461.

Kochert G (1978) Sexual pheromones in algae and fungi. *Annu. Rev. Plant Physiol.* **29**:461–486.

Kreimer G (1994) Cell biology of phototaxis in flagellate algae. *Int. Rev. Cytol.* **148**:229–310.

Kreimer G, Kawai H, Müller DG, Melkonian M (1991) Reflective properties of the stigma in male gametes of *Ectocarpus siliculosus* (Phaeophyceae) studied by confocal laser scanning microscopy. *J. Phycol.* **27**:268–276.

Kremer J, Mastronarde DN (1996) Computer visualization of three-dimensional image data using IMOD. *J. Struct. Biol.* **116**:71–76.

La Claire II JW, West JA (1978) Light-and electron-microscopic studies of growth and reproduction in *Cutleria* (Phaeophyta). I. Gametogenesis in the female plant of *C. hancockii*. *Protoplasma* **97**:93–110.

La Claire II JW, West JA (1979) Light-and electron-microscopic studies of growth and reproduction in *Cutleria* (Phaeophyta). II. Gametogenesis in the male plant of *C. hancockii*. *Protoplasma* **101**:247–267.

Lansman JB, Hess P, Tsien RW (1986) Blockade of current through single calcium channels by Cd^{2+}, Mg^{2+}, and Ca^{2+}. Voltage and concentration dependence of calcium entry into the pore. *J. Gen. Physiol.* **88**:321–347.

Lindemann CB (2004) Testing the geometric clutch hypothesis. *Biol. Cell.* **96**:681–690.

Lipinska AP, Damme EJV, Clerck OD (2016) Molecular evolution of candidate male reproductive genes in the brown algal model *Ectocarpus. BMC Evol. Biol.* **16**:5.

Lipinska AP, D'hondt S, Damme EJV, Clerck OD (2013) Uncovering the genetic basis for early isogamete differentiation: a case study of *Ectocarpus siliculosus. BMC Genomics* **14**:909.

Lüning K (1981) Egg release in gametophytes of *Laminaria saccharina*: induction by darkness and inhibition by blue light and UV. *Br. Phycol. J.* **16**:379–393.

Lüning K, Dring MJ (1972) Reproduction induced by blue light in female gametophytes of *Laminaria saccharina*. *Planta* **104**:252–256.

Lüning K, Dring MJ (1975) Reproduction, growth and photosynthesis of gametophytes of *Laminaria saccharina* grown in blue and red light. *Mar. Biol.* **29**:195–200.

Luthringer R, Cormier A, Ahmed S, Peters AF, Cock JM, Coelho SM (2014) Sexual dimorphism in the brown algae. *Perspect. Phycol.* **1**:11–25.

Maier I (1993) Gamete orientation and induction of gametogenesis by pheromone in algae and plants. *Plant Cell Environ.* **16**:891–907.

Maier I (1995) Brown algal pheromones. In Round FE, Chapman DJ (eds) Progress in Phycological Research 11. Biopress, Bristol, pp 51–102.

Maier I (1997a) The fine structure of the male gamete of *Ectocarpus siliculosus* (Ectocarpales, Phaeophyceae). I. General structure of the cell. *Eur. J. Phycol.* **32**:241–253.

Maier I (1997b) The fine structure of the male gamete of *Ectocarpus siliculosus* (Ectocarpales, Phaeophyceae). II. The flagellar apparatus. *Eur. J. Phycol.* **32**:255–266.

Maier I, Calenberg M (1994) Effect of extracellular Ca^{2+} and Ca^{2+} antagonists on the movement and chemoorientation of male gametes of *Ectocarpus siliculosus* (Phaeophyceae). *Bot. Acta.* **107**:451–460.

Maier I, Müller DG (1982) Antheridium fine structure and spermatozoid release in *Laminaria digitata*. *Phycologia* **21**:1–8.

Maier I, Müller DG (1986) Sexual pheromones in algae. *Biol. Bull.* **170**:145–175.

Maier I, Müller DG (1990) Chemotaxis in *Laminaria digitata* (Phaeophyceae) I. Analysis of spermatozoid movement. *J. Exp. Bot.* **41**:869–876.

Maier I, Schmid CE (1995) An immunofluorescence study on lectin binding sites in gametes of *Ectocarpus siliculosus* (Ectocarpales, Phaeophyceae). *Phycol. Res.* **43**:33–42.

Maier I, Wenden A, Clayton MN (1992) The movement of *Hormosira banksii* (Fucales, Phaeophyta) spermatozoids in response to sexual pheromone. *J. Exp. Bot.* **43**:1651–1657.

Manton I (1956) Plant cilia and associated organelles. In: Rudnick D (ed) Cellular Mechanisms in Differentiation. Growth Princeton University Press, Princeton, pp 61–71.

Manton I (1957) Observations with the electron microscope on the internal structure of the zoospore of brown alga. *J. Exp. Bot.* **8**:294–303.

Manton I (1959) Observations on the internal structure of the spermatozoid of *Dictyota*. *J. Exp. Bot.* **10**:448–461.

Manton I (1964) A contribution towards understanding of 'the primitive fucoid'. *New Phytol.* **63**:244–254.

Manton I, Clarke B (1950) Electron microscope observation on the spermatozoids of *Fucus*. *Nature* **166**:973–974.

Manton I, Clarke B (1951) Electron microscope observations on the zoospores of *Pylaiella* and *Laminaria*. *J. Exp. Bot*. **2**:242–243.

Manton I, Clarke B (1956) Observations with the electron microscope on the internal structure of the spermatozoids of *Fucus*. *J. Exp. Bot.* **7**:416–432.

Mastronarde DN (1997) Dual-axis tomography: an approach with alignment methods that preserve resolution. *J. Struct. Biol.* **120**:343–352.

Matsunaga S, Uchida H, Iseki M, Watanabe M, Murakami A (2010) Flagellar motions in phototactic steering in a brown algal swarmer. *Photochem. Photobiol.* **86**:374–381.

Melkonian M (1984) Flagellar apparatus ultrastructure in relation to green algal classification. In: Irvin DEG, John DM (eds) Systematics of the green algae. Academic Press, London Orlando, pp 73–120.

Miller RL (1975) Chemotaxis of the spermatozoa of *Ciona intestinalis*. *Nature*, **254:**244–245.

Miller RL (1977) Chemotactic behavior of the sperm of chitons (Mollusca: Polyplacophora). *J. Exp. Zoo.* **202:**203–211.

Miller RL, Brokaw C J (1970) Chemotactic turning behaviour of *Tubularia* spermatozoa. *J. Exp. Biol.* **52:**699–706.

Mitchell DR (2000) *Chlamydomonas* flagella. *J. Phycol.* **36:**261–273.

Mizuno K, Shiba K, Okai M, Takahashi Y, Shitaka Y, Oiwa K, Tanokura M, Inaba K (2012) Calaxin drives sperm chemotaxis by Ca^{2+}-mediated direct modulation of a dynein motor. *Proc. Natl. Acad. Sci. USA* **109**:20497–20502.

Moestrup Ø (2000) The flagellate cytoskeleton. Introduction of a general terminology for microtubular flagellar roots in protists. In: Leadbeater BSC, Green JC (eds) The flagellates. Unit, diversity and evolution. Taylor and Francis, New York, pp 69–94.

Morel-Laurens N (1987) Calcium control of phototactic orientation in *Chlamydomorias reinhardtii*: sign and strength of response. *Photochem. Photobiol.* **45**:119–128.

Motomura T (1989) Ultrastructural study of sperm in *Laminaria angustata* (Laminariales, Phaeophyta), especially on the flagellar apparatus. *Jpn. J. Phycol.* **37**:105–116.

Motomura T (1993) Ultrastructural and immuneofluorescence studies of zoosporogenesis in *Laminaria angustata*. *Scientific Papers of the Institute of Algological Research, Faculty of Science, Hokkaido University* **9**:1–32.

Motomura T, Sakai Y (1981) Effects of chelated iron in culture media on oogenesis in *Laminaria angustata*. *Bull. Jap. Soc. Sci. Fish.* **27**:1535–1540.

Motomura T, Sakai Y (1984) Ultrastructural studies of gametogenesis in *Laminaria angustata* (Laminariales, Phaeophyta) regulated by iron concentration in the medium. *Phycologia* **23**:331–343.

Müller DG (1967) Ein leicht flüchtiges Gyno-Gamon der Braunalge *Ectocarpus siliculosus*. *Naturwissenschaften* **54:**496–497.

Müller DG (1974) Sexual reproduction and isolation of a sex attractant in *Cutleria multifida* (Smith) Grev. (Phaeophyta). *Biochemie und Physiologie der Pflanzen* **165**:212–215.

Müller DG (1976) Quantitative evaluation of sexual chemotaxis in two marine brown algae. *Z. Pflanzenphysiol. Bd.* **80**:120–130.

Müller DG (1977) Sexual reproduction in British *Ectocarpus siliculosus* (Phaeophyta). *Br. Phycol. J.* **12**:131–136.

Müller DG (1978) Locomotive responses of male gametes to the species-specific sex attractant in *Ectocarpus siliculosus* (Phaeophyta). *Arch. Protistenk.* **120**:371–377.

Müller DG (1979) Olefinic hydrocarbons in seawater: Signal molecules for sexual reproduction in brown algae. *Pure Appl. Chem.* **51**:1885–1891.

Müller DG, Falk H (1973) Flagellar structure of the gametes of *Ectocarpus siliculosus* (Phaeophyta)

as revealed by negative staining. *Arch. Microbiol.* **91**:313–322.

Müller DG, Gassmann G, Lüning K (1979) Isolation of a spermatozoid-releasing and -attracting substance from female gametophytes of *Laminaria digitata*. *Nature* **279**:430–431.

Müller DG, Jaenicke L (1973) Fucoserraten, the female sex attractant of *Fucus serratus* L. (phaeophyta). *FEBS Lett.* **30**:137–139.

Müller DG, Jaenickel L, Donike M, Akintobi, T (1971) Sex attractant in a brown alga: chemical structure. *Science* **171**:815–817.

Müller DG, Maier I, Müller H (1987) Flagellum autofluorescence and photoaccumulation in heterokont algae. *Photochem. Photobiol.* **46**:1003–1008.

Nagasato C, Motomura T (2002) Ultrastructural study on mitosis and cytokinesis in *Scytosiphon lomentaria* zygotes (Scytosiphonales, Phaeophyceae) by freeze-substitution. *Protoplasma* **219**:140–149.

Nagasato C, Motomura T (2004) Destruction of maternal centrioles during fertilization of the brown alga, *Scytosiphon lomentaria* (Scytosiphonales, Phaeophyceae). *Cell Motil. Cytoskel*. **59**:109–118.

Nagasato C, Motomura T, Ichimura T (1998) Selective disappearance of maternal centrioles after fertilization in the anisogamous brown alga *Cutleria cylindrica* (Cutleriales, Phaeophyceae): Paternal inheritance of centrioles is universal in the brown algae. *Phycol. Res.* **46**:191–198.

Nagasato C, Motomura T, Ichimura T (1999) Influence of centriole behavior on the first spindle formation in zygotes of the brown alga *Fucus distichus* (Fucales, Phaeophyceae). *Develop. Biol*. **208**:200–209.

Nishigaki T, Chiba K, Hoshi M (2000) A 130-kDa membrane protein of sperm flagella is the receptor for asterosaps, sperm-activating peptides of starfish *Asterias amurensis*. *Dev. Biol.* **219**:154–162.

Nozaki H, Yamada TK, Takahashi F, Matsuzaki R, Nakada T (2014) New “missing link” genus of the colonial volvocine green algae gives insights into the evolution of oogamy. *BMC Evol. Biol.* **14**:37.

Nultsch W, Häder D-P (1988) Photomovement in motile microorganisms. II. *Photochem. Photobiol.*

47:837–869.

Osborn M, Weber K (1982) Immunofluorescence and immunocytochemical procedures with affinity purified antibodies: tubulin-containing structures. In: Wilson L (ed) Methods in cell biology. Academic Press, New York, pp 97–132.

O' Kelly CJ (1989) The evolutionary origin of the brown algae: information from studies of motile cell structure. In: Green JC, Leadbeater BSC, Diver WL (eds) The Chromophyte Algae: Problems and Perspectives, Systematics Association Special, 38. Clarendon Press, Oxford, pp 256–278.

O'Kelly CJ, Floyd GL (1984) The absolute configuration of the flagellar apparatus in zoospores from two species of Laminariales (Phaeophyceae). *Protoplasma* **123**:18–25.

Pearson GA, Serrão EA, Dring MJ, Schmid R (2004) Blue- and green-light signals for gamete release in the brown alga, *Silvetia compressa*. *Oecologia.* **138**:193–201.

Prakriya M, Lewis RS (2015) Store-operated calcium channels. *Physiol. Rev.* **95**:1383–1436.

Provasoli L (1968) Media and prospects for the cultivation of marine algae. In: Watanabe A and Hattori A (eds) Cultures and collections of algae. Japanese Society of Plant Physiology, Hakone, pp 63–75.

Purcell EM (1977) Life at low Reynolds number. *American J. Physics* **45**:3–11.

Reed DC, Laur DR, Ebeling AW (1988) Variation in algal dispersal and recruitment: the importance of episodic events. *Ecol. Monogr.* **58**:321–335.

Reynolds ES (1963) The use of lead citrate at high pH as an electron-opaque stain in electron microscopy. *J. Cell Biol.* **17**:208–212.

Sale WS (1986) The axonemal axis and Ca^{2+}-induced asymmetry of active microtubule sliding in sea urchin sperm tails. *J. Cell Biol*. **102:**2042–2052.

Salisbury JL, Baron AT, Sanders MA (1988) The centrin-based cytoskeleton of *Chlamydomonas reinhardtii*: distribution in interphase and mitotic cells. *J. Cell Biol*. **107**:635–641.

Salisbury JL, Baron A, Surek B, Melkonian M (1984) Striated flagellar rootlets: isolation and partial characterization of a calcium-modulated contractile organelle. *J. Cell Biol.* **99**:962–970.

Schmid CE (1993) Cell-cell-recognition during fertilization in *Ectocarpus siliculosus*

(Phaeophyceae). *Hydrobiologia* **261**:437–443.

Schmid CE, Schroer N, Müller DG (1994) Female gamete membrane glycoproteins potentially involved in gamete recognition in *Ectocarpus siliculosus* (Phaeophyceae). *Plant. Sci.* **102**:61–67.

Shiba K, Baba SA, Inoue T, Yoshida M (2008) Ca^{2+} bursts occur around a local minimal concentration of attractant and trigger sperm chemotactic response. *Proc. Natl. Acad. Sci. USA* **105**:19312–19317.

Shiba K, Tagata T, Ohmuro J, Mogami Y, Matsumoto M, Hoshi M, Baba SA (2006) Peptide-induced hyperactivation-like vigorous flagellar movement in starfish sperm. *Zygote* **14**:23–32.

Silberfeld T, Leigh JW, Verbruggen H, Cruaud C, de Reviers B, Rousseau F (2010) A multi-locus time-calibrated phylogeny of the brown algae (Heterokonta, Ochrophyta, Phaeophyceae): Investigating the evolutionary nature of the "brown algal crown radiation". *Mol. Phylogenet. Evol.* **56**:659–674.

Singh S, Lowe DG, Thorpe DS, Rodriguez H, Kuang W-J, Dangott LJ, Chinkers M, Goeddel DV, Garbers DL (1988) Membrane guanylate cyclase is a cell-surface receptor with homology to protein kinases. *Nature* **334**:708–712.

Takahashi F (2016) Blue-light-regulated transcription factor, Aureochrome, in photosynthetic stramenopiles. *J. Plant Res.* **129**:189–197.

Takahashi T, Watanabe M (1993) Photosynthesis modulates the sign of phototaxis of wild-type *Chlamydomonas reinhardtii*. Effects of red background illumination and 3-(3',4'-dichlorophenyl)-1,1-dimethylurea. *FEBS Lett.* **336**:516–520.

Tatewaki M, Wang XY, Wakana I (1989) A simple method of red seaweed axenic culture by spore-washing. *Jpn J. Phycol.* **37**:150–152.

Togashi T, Bartelt JL (2011) Evolution of anisogamy and related phenomena in marine green algae. In: Togashi T, Cox PA (eds) The evolution of anisogamy: a fundamental phenomenon underlying sexual selection. Cambridge University Press, Cambridge, pp 194–242.

Ueki C, Nagasato C, Motomura T, Saga N (2008) Reexamination of the pit plugs and the

characteristic membranous structures in *Porphyra yezoensis* (Bangiales, Rhodophyta). *Phycologia* **47**:5–11.

Wakabayashi K, Misawa Y, Mochiji S, Kamiya R (2011) Reduction–oxidation poise regulates the sign of phototaxis in *Chlamydomonas reinhardtii*. *Proc. Natl. Acad. Sci. USA* **108**:11280–11284.

Wakana I, Abe M (1992) Artificial insemination 'regulated by EDTA' in the monoecious brown alga *Fucus evanescens*. *Plant Cell physiol.* **33**:569–575.

Wood CD, Nishigaki T, Furuta T, Baba SA, Darszon A (2005) Real-time analysis of the role of Ca^{2+} in flagellar movement and motility in single sea urchin sperm. *J. Cell Biol.* **169**:725–731.

Wooly D (2010) Flagellar oscillation: a commentary on proposed mechanisms. *Biol. Rev.* **85**:453–470.

Wynne MJ, Loiseaux S (1976) Recent advances in life history studies of the Phaeophyta. *Phycologia* **15**:435–452.

Yamagishi T, Motomura T, Nagasato C, Kato A, Kawai H (2007) A tubular mastigoneme-related protein Ocm1 isolated from the flagellum of a chromophyte alga *Ochromonas danica*. *J. Phycol.* **43**:519–527.

Yamagishi T, Motomura T, Nagasato C, Kato A, Kawai H (2009) Novel proteins comprising the stramenopile tripartite mastigoneme in *Ochromonas danica* (Chrysophyceae). *J. Phycol.* **45**:1100–1105.

Yamanouchi S (1912) The life history of *Cutleria*. Contr Hull Bot Lab163. *Bot. Gaz*. **54**:441–502.

Yoshida M (2014) Sperm chemotaxis: The first authentication events between conspecific before fertileization. In: Sawada H, Inoue N, Iwano M (eds) Sexual reproducetion in animals and plants. Springer Open, Tokyo, pp 3–11.

Yoshida M, Murata M, Inaba K, Morisawa M (2002) A chemoattractant for ascidian spermatozoa is a sulfated steroid. *Proc. Natl. Acad. Sci. USA* **99:**14831–14836.

Yoshida M, Yoshida K (2011) Sperm chemotaxis and regulation of flagellar movement by Ca^{2+}. *Mol. Hum. Reprod.* **17**:457–465.

Yoshimura K, Shingyoji C, Takahashi K (1997) Conversion of beating mode in *Chlamydomonas* flagella induced by electric stimulation. *Cell Motil. Cytoskeleton* **36**:236–245.

Legends of plates

Plate 1 Vegetative and reproductive cells of several brown algal species which was used in this study. Male and female gametophytes (a), released gametes (arrows) from gametophytes (b) and plurilocular of male gametophytes (c) of *Ectocarpus siliculosus*. Released gametes (arrows) from gametophytes (d), plurilocular of male (e) and female (f) gametophytes of *Mutimo cylindricus*. Sporophytes (g), antheridia (h) and an egg (i) of *Fucus distichus*. Sporophytes (j), antheridia (k) and eggs (i) of *Saccharina japonica*.

Plate 2 Vegetative and reproductive cells of oogamous brown algal species which was used in this study. Gametophytes (a), eggs (b) and antheridia (c) of *Cystoseira hakodatensis*. Gametophytes (d), egg and sperm (e) of *Sargassum thunbergii*. Sporophytes (f), egg and sperm (g) of *Dictyota dichotoma*.

Plate 3 Life cycles of *Ectocarpus siliculosus* (top), *Mutimo cylindricus* (down left) and *Saccharina japonica* (down right). A Life cycle of *Ectocarpus* is isomorphic alternation of generations. While, life cycles of *Mutimo* and *Saccharina* are heteromorphic alternation of generations. Sexual reproductions are isogamous in *Ectocarpus*, anisogamous in *Mutimo* and oogamous in *Saccharina*.

Plate 4 Schematic illustration of the swarmers response to the light and chemical signals. UV, V, B, G, Y, O, R, IR represent ultra violet, violet, blue, green, yellow, orange, red, infrared light, respectively.

Plate 5 Several images of flagella of male gametes. (a) Negative staining image of male gametes in *Ectocarpus siliculosus*. (b) SEM image of basal part of flagella in *Scytosiphon lomentaria*. (c) TEM image of a axonema (9+2) in *Colpomenia bullosa*.

Plate 6 A schematic representation of the flagellar apparatus from the dorsal side of male gamete of *Ectocarpus siliculosus*. Transverse images of flagellar axonemes are from the distal

to the proximal parts of the anterior flagellar (AF) and posterior flagellar (PF), respectively, with a new numbering system for the nine doublet MTs of the flagellar axoneme. AB, anterior flagellar basal body; BR, bypassing rootlet; DB, deltoid band; MAR, major anterior rootlet, mar, minor anterior rootlet; mpr, minor posterior rootlet; PB, posterior flagellar basal body; pfb, posterior fibrous band; SB striated strap-shaped band.

Plate 7 Modeling images of bands and microtubular rootles near the basal bodies. The upper figure indicates positions of three tomogram slices (1–3). In the below figures, fibrous structures connecting AB and MAR, SB and DB are represeted in bright orange, blue and dark blue, and green and pink objects, respectively. Tubular structures in below pictures indicate mar (orange) and mpr (bright pink).

Plate 8 Longitudinal and transverse sections of AB and PB. Two serial tomograms (0.627 nm-thick tomogram slices) (a–h, i–k), viewed from the dorsal side of male gametes. Arrowheads and double arrowheads in d, e indicate the connection of mar to AB and PB, and MAR to AB, respectively. Arrowhead in g shows electron dense material at the center of the basal plate. (i–k) Three tomogram slices (0.784 nm-thick) viewed from the distal side of AB. Arrows show the connection between AB and each of microtubular rootlets (mar, MAR and BR). Arrowheads indicate BR and MAR. Ch, chloroplast; G, Golgi body.

Plate 9 Four tomogram slices (0.627 nm-thick) of PB viewed from the dorsal side of the male gamete. Arrowhead in c indicates electron dense material at the center of the basal plate.

Plate 10 Longitudinal sections of AB and PB. (a–d) Four tomogram slices (0.627 nm-thick) showing SB. (e–h) Four tomogram slices (0.784 nm-thick) showing DB and pfb. (i–k) Three tomogram slices (1.25 nm-thick) showing the connection between PB and chloroplast (arrows). Ch, chloroplast; G, Golgi body; N, nucleus.

Plate 11 Transverse sections of AB and PB with a conventional transmission electron microscope observation. The new numbering system for outer doublets of MTs is adopted. (a–d) Serial cross-sections of AB. (e, f) Two serial sections of AB and PB. (e) Section showing the position of BR, MAR and DB. Inset is the enlarged image. (f) Section showing the position of BR, MAR, mar and SB and mar. Inset is the enlarged image. (g, h) Two serial sections of PB. An arrow in inset shows connection between chloroplast and PB. (i) Section showing position of electron-dense material and crystallized material in paraflagellar body of PF.

Plate 12 Schematic morphology of reproductive cells in all mating types of brown algae. (a) The male and female gamete in isogamous species. (b) The male and female gamete in anisogamous species. (c) The several types of perm and egg in oogamous species.

Plate 13 Structures of selected sex pheromones in brown algae. Corresponding genus to the selected sex pheromone: ectocarpene (*Ectocarpus, Adenocystis, Sphacelaria*); hormosirene (*Hormosira, Durvillea, Xiphophora, Scytosiphon, Colpomenia*); dictyotene (*Dictyota*); desmarestene (*Desmarestia, Cladostephus*); lamoxirene (*Laminaria, Alaria, Undaria, Macrocystis, Nereocystis*); multifidene (*Cutleria, Chorda, Zonaria*); fucoseratene (*fucus*).

Plate 14 Schematic diagram of fertilization process in isogamous species. Firstly, female gametes settle on substratum and secret sex pheromone. Secondly, male gametes gather around female gametes by sensing sex pheromone. Finally, one of male gametes fuses with a female gamete.

Plate 15 Mating process of isogamous species. Light microscopic images (a) of *Ectocarpus siliculosus*, SEM images (b) and TEM images (c) of *Scytosiphon lomentaria* during fertilization.

Plate 16 Definitions of the terms for analysis of swimming trajectories and flagellar waveforms. Definition of the swimming path curvature (Γ) and the flagellar curvature (γ) (top). Blue dots

and lines show the center of cell body and zigzag trajectory of the cell body. Definition of the deflection angle (θ) (down).

Plate 17 The trajectories of free- and thigmotactic-swimming male gametes in *Ectocarpus siliculosus*. The swimming trajectories of free-swimming male gametes (a) and thigmotactic-swimming male gametes (b) are obtained by image processing during a period of 2s. Frequency of the swimming path curvatures (Γ) (absolute value) of thigmotactic-swimming male gametes (n = 115) (c).

Plate 18 The anterior flagellar (AF) waveforms of free- and thigmotactic-swimming male gametes. (a) A typical flagellar waveform of free-swimming gametes (symmetrical waveform of the AF) recorded at 1.6-ms intervals. (b) A typical flagellar waveform of thigmotactic-swimming male gametes recorded at 1.6-ms intervals. (c) Trace of AF waveforms in free-swimming male gametes (left) and thigmotactic-male gametes (right). Twenty frames were chosen every 1.6 ms and traces of the AF were merged. Black bars show 5 μm reference line and grey dots indicate the anterior end of the cell body. (d) Flagellar asymmetric indices of free- and thigmotactic- swimming male gametes. I. Basal region of the AF; II. Middle region; III. Tip region; IV. Whole region. Free- vs. thigmotactic-swimming male gametes, *P < 0.001. (e) Average value of the deflection angle at 8 μm from the tip of the AF. I. Free-swimming male gametes; II. Thigmotactic-male gametes. Free- vs. thigmotactic-swimming male gametes, *P<0.001.

Plate 19 The posterior flagellar (PF) waveforms of free- and thigmotactic-swimming male gametes. (a) Trace of the PF waveforms in free- (left) and thigmotactic-swimming male gametes (right). Twenty forms were chosen every 1.6 ms and traces of the PF were merged. Black bars show 5 μm reference line and gray dots indicate the anterior end of the cell body. (b) The deflection angle at 1 μm from the tip of PF is plotted against time.

Plate 20 The trajectories of chemotactic male gametes. The swimming trajectories of chemotactic gametes are obtained by image processing during the period of 2s. (a) Free-swimming male gametes on the upper region from settled female gametes. (b) Thigmotactic-swimming male gametes near settled female gametes. (c) Frequency of the swimming path curvatures (n = 115).

Plate 21 The AF beat patterns of chemotactic male gametes. (a) The AF asymmetric indices of chemotactic male gametes. I. Base region; II. Middle region; III. Tip region; IV. Whole region. Control vs. Chemotactic gametes, **P < 0.05. (b) Asymmetric indices of tip region in the AF plotted against path curvatures. (c) Average value of deflection angle at 8 μm from the tip of AF. I. Control; II. Chemotactic gametes. Control vs. chemotactic gametes, *P < 0.001. (d) Average value of deflection angles at 8 μm from the tip of AF plotted against path curvatures.

Plate 22 A trajectory and PF bending pattern of a chemotactic male gamete (♂) near female gamete (♀). White squares show the timing of lateral PF beating of male gamete. Gray squares show the motionless PF. 1-7 show detailed images of male gametes at each square, respectively. Arrows indicate the position of the PF.

Plate 23 and 24 The typical flagellar waveform patterns of chemotactic male gametes. (a) Images were recorded at 1.6-ms intervals under the same conditions. (b) Trajectories of chemotactic male gametes. Arrows indicate the timing of unilateral beats of PF. Trace of AF and PF waveforms. Twenty forms were chosen every 1.6 ms and merged. Black bars show 5 μm reference line and grey dots indicate the anterior end of cell body. (c) Deflection angles at 8 μm from the tip of the AF and at 1 μm from the tip of the PF are plotted. Arrows indicate the timing of unilateral beats of PF in (a-b).

Plate 25 Morphological comparison of female and male gametes of *Mutimo cylindricus*. (a, b) Immunofluorescence images of microtubules in female (a) and male (b) gametes. (c) Cell body size and flagellar length. Values represent the mean ± S.D., n = 20–28. *$P < 0.0001$.

Plate 26 Locomotion of female and male gametes of *Mutimo cylindricus*. (a, b) Swimming trajectories of female (a) and male (b) gametes (free-swimming gametes, 1 s). (c) Swimming velocity. n = 120. (d, e) Flagellar waveforms of female (d) and male (e) gametes. (f) Beat frequency of AF. n = 45. *$P < 0.0001$, t-test.

Plate 27 Flagellar waveforms of female and male gametes of *Mutimo cylindricus*. (a) Asymmetric index for AF. (b) Average values of the deflection angles for AF and PF. Values represent the mean ± S.D., n = 8–17. **$P < 0.001$, t-test. (c, d) Deflection angles in female (c) and male (d) gametes. (e) Fifteen frames were chosen every 5 ms, and the traces of AF and PF were merged. Left; female gametes, right; male gametes.

Plate 28 Chemotactic male gametes of *Mutimo cylindricus*. (a) Swimming path curvatures of chemotactic male gametes. n = 120. (b) Swimming trajectories of chemotactic male gametes (2 s). The inset shows a magnified view (4 s). (c) Example showing the swimming trajectory and flagellar waveforms of chemotactic male gametes (arrows indicate the timing of beating by PF). (d, e) Swimming path curvature (d) and deflection angle (e) based on data shown in (c).

Plate 29 Swimming trajectories and quantitative analysis of *Saccharina japonica* sperm. Swimming paths of sperm in contact with the glass surface (a, b, c) and free-swimming sperm (d, e, f) (10 s recording). Condition 1: medium without the sex pheromone (a, d); condition 2: medium containing the sex pheromone secreted by released eggs (b, e); and condition 3: near to freshly liberated eggs (c, f). (g) Path curvatures in a (n = 125), b (n = 125), c (n = 129). (h) Swimming velocities in a (n = 125), b (n = 125), c (n = 129), d (n = 141), e (n = 97), and f (n = 150). (i) Beating frequency of AF and PF without pheromone (n = 50) and with pheromone (n = 55). *$P < 0.0001$, **$P < 0.05$, t-test.

Plate 30 Analysis of the flagellar waveforms in *Saccharina japonica* sperm. (a, b) Motionless PF

(a) and vigorously beating PF (b). (c, d) Asymmetric indices (c) and deflection angles (d) of AF and PF with the sex pheromone (condition 2).

Plate 31 Analysis of the flagellar waveforms and locomotion of *S. japonica* sperm during chemotactic U-turns. Asymmetric indices (a, e), deflection angles (b, f), and path curvatures (c, g) of chemotactic sperm (d, h). Asterisks indicate the positions of the eggs, arrowheads indicate the positions of U-turns, and arrows indicate the direction of sperm swimming.

Plate 32 Analysis of locomotion and the flagellar waveforms in *Fucus distichus* sperm. (a) Condition 1: sperm swimming without eggs; and (b) condition 2: sperm swimming near an egg (10 s recording, arrows indicate the positions of U-turns). (c) Sperm under condition 1. (d, e) Asymmetric indices and deflection angles of AF and PF of sperm under condition 1.

Plate 33 Analysis of locomotion and the flagellar waveforms of *Fucus distichus* sperm during chemotactic U-turns. (a, e) Asymmetric indices, (b, f) deflection angles, and (c, g) path curvatures in the chemotactic sperm (d, h). Asterisks indicate the positions of eggs, arrowheads indicate the positions of U-turns, and arrows indicate the direction of sperm swimming.

Plate 34 Schematic diagram of chemotactic male gametes (sperm) in isogamous, anisogamous and oogamous species. Thigmotactic swimming by sex pheromone can not be detected in oogamous speceies, unlike isogamous and anisogamous species.

Plate 35 Schematic diagram of chemotactic male gametes (sperm) of isogamous, anisogamous and oogamous species of brown algae. Gray lines indicate swimming trajectories and black lines indicate the timming of PF bend. Drastic turning by PF bend is only seen in oogamous species.

Plate 36 Swimming trajectories and flagellar waveforms of *Cystoseira hakodatensis.* (a, b) The

swimming trajectories of free-swimming sperm (a) and chemotactic male gametes (b) are obtained by image processing during a period of 2s. (c) One of the flagellar waveform of chemotactic sperm recorded at 5-ms intervals.

Plate 37 Swimming trajectories and flagellar waveforms of *Dictyota dichotoma.* (a, b) The swimming trajectories of free-swimming sperm (a) and chemotactic male gametes (b) are obtained by image processing during a period of 2s. (c) One of the flagellar waveform of chemotactic sperm recorded at 5-ms intervals.

Plate 38 Dish phototaxis assay of *Mutimo cylindricus* male gametes. Cell suspensions with various extracellular [Ca^{2+}], 10^{-2} M, 10^{-3} M, 10^{-4} M, 10^{-5} M, and 10^{-6} M, were photographed 1 and 3 min after providing unidirectional blue light stimulation on the upper side.

Plate 39 Swimming direction of the male gametes of *Mutimo cylindricus.* The angle (θ) between the light direction and the cell swimming direction was measured several seconds after the unilateral light was turned on. The percentage of the cells moving in a particular direction relative to the light direction (0°) is shown in histogram (12 bins of 30°, n=50 cells per each condition). Various [Ca^{2+}] were used in 10^{-2} M in dark conditions (a), 10^{-2} M (b), 10^{-3} M (c), 10^{-4} M (d), 10^{-5} M (e), 10^{-6} M (f), 10^{-4} M restored to 10^{-2} M (g), and 10^{-1} M (h) with unidirectional blue light.

Plate 40 Dish phototaxis assay and swimming direction of the male gametes of *Mutimo cylindricus.* (a) Cell suspensions in various [La^{3+}], 10^{-5} M, 10^{-4} M, and 3×10^{-4} M in 10^{-2} M [Ca^{2+}] control conditions, were photographed 1 and 3 min after providing unidirectional blue light stimulation on the upper side. (b, c) The angle (θ) between the light and cell swimming direction was measured several seconds after the unilateral light was turned on. The percentage of the cells moving in a particular direction relative to the light direction (0°) is shown in histogram (12 bins of 30°, n=50 cells per each condition), 10^{-5} M (b), 10^{-4} M (c) [La^{3+}] with

unidirectional blue light.

Plate 41 Swimming velocities of the male gametes of *Mutimo cylindricus* in various conditions of [Ca^{2+}] and [La^{3+}] (n>50 cells per each conditions). The bars indicate the minimum and maximum velocity measured for each condition. The boxes contain 25% to 75% of the data points and bold lines represent the median velocity. Circles represent the outliers. Asterisks indicate significant differences from the control condition (a grey square) ($P<0.001$, t-test).

Plate 42 Swimming trajectories of the male gametes of *Mutimo cylindricus* under various conditions. Tracings of gametes were carried out for 2s. Positively phototactic male gametes in the control condition ([Ca^{2+}], 10^{-2} M) (a), negatively phototactic male gametes that were induced by 10^{-4} M [Ca^{2+}] (b), negatively phototactic male gametes that were induced by 10^{-4} M [La^{3+}] in 10^{-2} M [Ca^{2+}] control conditions (c). Grey and black dots show the start and end position respectively.

Plate 43 Posterior flagellar waveforms and eyespot positions of male gametes of *Mutimo cylindricus* during phototactic turn. Unidirectional light was provided from the left side of pictures. The turning toward the light source (a, b). The turning away from the light source (c, d). Arrowheads indicate stigma. Schematic diagram represent positively phototactic (e) and negatively (f) phototactic turning of the cell.

Plate 44 A diagram illustrating some of the swimming patterns of the male gametes of *Mutimo cylindricus* based on hypothesis 2. Refer to the text in Part 3. 1.

Plate 45 Dish phototaxis assay of *Mutimo cylindricus* male gametes. One min after cell suspensions was mixed with various concentrations of ectocarpene (1.3×10^{-3} M, 1.3×10^{-4} M, 1.3×10^{-5} M, 1.3×10^{-6} M) or female gametes, were photographed 1 and 3 min after providing unidirectional blue light stimulation from the upper side.

Plate 46 Swimming trajectories of the male gametes of *Mutimo cylindricus* under various conditions focusing on the cover slip. Tracings of gametes were carried out for 2s. Thigmotactic male gametes forming small circular paths induced by 10^{-4} M ectocarpene (a). Freely swimming male gametes and a few of thigmotactic male gametes at 10^{-5} M (b), 10^{-6} M (c) ectocarpene. Thigmotactic male gametes forming small circular paths induced sex pheromone secreted from female gametes. Asterisk indicates the position of female gametes.

Plate 47 Swimming trajectories of the male gametes of *Mutimo cylindricus* under various conditions focusing on between cover and slid glass. Tracings of gametes were carried out for 2s. Negatively phototactic male gametes that were induced by 1.3×10^{-4} M ectocarpene (a). Negatively and positively phototactic male gametes that were induced by 1.3×10^{-5} M ectocarpene (b). Positively phototactic male gametes at 1.3×10^{-6} M ectocarpene (c). Negatively and positively phototactic male gametes that were induced by sex pheromone secreted form female gametes (d). Thick lines in (d) represent the swimming trajectories of female gametes. Grey and black dots show the start and end position respectively.

Plate 48 Swimming directions of the male gametes of *Mutimo cylindricus.* The angle (θ) between the light direction and the cell swimming direction was measured several seconds after the unilateral light was turned on. The percentage of the cells moving in a particular direction relative to the light direction (0°) is shown in histogram (12 bins of 30°, n=40 cells per each condition). Various ectocarpene concentrations were used. (a) Control condition at dark. (b) control condition, (c) female gametes containing medium, (d) 1.3×10^{-6} M ectocarpene (e) 1.3×10^{-5} M ectocarpene and (f) 1.3×10^{-4} M ectocarpene with unidirectional blue light.

Plate 49 Dish phototaxis assays of *Mutimo cylindricus* male gametes. Forty min after cell suspensions was mixed with various concentrations of ectocarpene (1.3×10^{-3} M, 1.3×10^{-4} M, 1.3×10^{-5} M, 1.3×10^{-6} M) or female gametes containing medium were photographed 1 and 3 min

after providing unidirectional blue light stimulation on the upper side.

Plate 50 Schematic hypothetical representation of sex pheromone effect on the sign of phototaxis in male gametes of brown algae. When male gametes sense the sex pheromone, many of them started to show negative phototaxis to get closer to settled female gametes.

Plate 51 Flagellar waveforms of other stramenopile organisms. (a) *Schizocladia ischiensis*, (b) *Pythium porphyrae*. They show similar flagellar waveforms to brown algal swarmers. Especially, from the observations of *Pythium porphyrae*, drastic turn by PF bend was observed.

Plate 52 Flagellar waveforms of green algal gametes, *Monostroma angicava*. Female gametes (a), male gametes (b) and planogamy (male and female gametes) (c). They show completely different flagellar waveforms to brown algal swarmers.

Table 1 Distributions of autofluorescence and stigma in various species of brown algae

Species	Type of swarmers	Flagellum autofluorescence	Stigma	Phototaxis	Reference
Isogamous species					
Sphacelaria rigidula	male gametes	+	+	positive	Müller et al. (1987)
Adenocystis utricularis	female gametes	+	+	nagative	Müller et al. (1987)
Geminocarpus geminatus	zoospores	+	+	positive	Müller et al. (1987)
Giffordia mitchellae	male gametes	+	+	positive	Müller et al. (1987)
Leathesia difformis	zoospores	+	+	+	Fu et al. (2016), Kawai (1988)
Melanosiphon intestinalis	zoospores	+	+	+	Fu et al. (2016), Kawai (1988)
Sphaerotrichia divaricata	female gametes	+	+	positive	Müller et al. (1987)
Ectocarpus siliculosus	male gametes	+	+	positive	Müller et al. (1987)
Analipus japonicus	zoospores	+	+	+	Fu et al. (2016), Kawai (1988)
Colpomenia bullosa	zoospores	+	+	+	Fu et al. (2016)
Scytosiphon lomentaria	gametes	+	+	negative	Kawai (1988), Matsunaga et al. (2010)
Anisogamous species					
Mutimo cylindricus	female gametes	+	+	+	Fu et al. (2016)
Oogamous species					
Desmarestia ligulata	zoospores	+	+	+	Fu et al. (2016), Kawai (1988)
	sperm	-	-	-	Fu et al. (2016), Kawai (1988)
Desmarestia munda	sperm	-	-	-	Müller et al. (1987)
Perithalia caudata	sperm	+	-	-	Müller et al. (1987)
Halosiphon tomentosus	zoospores	+	+	negative	Müller et al. (1987)
	sperm	-	-	-	Müller et al. (1987)
Agarum clathratum	zoospores	-	-	-	Fu et al. (2016), Kawai (1988)
Alaria nana	sperm	-	-	-	Müller et al. (1987)
Alaria crassifolia	zoospores	-	-	-	Fu et al. (2016), Kawai (1988)
Chorda filum	zoospores	+	+	negative	Müller et al. (1987)
	sperm	-	-	-	Müller et al. (1987)
Laminaria digitata	sperm	-	-	-	Müller et al. (1987)
Macrocystis pyrifera	zoospores	-	-	-	Müller et al. (1987)
	sperm	-	-	-	Müller et al. (1987)
Saccharina angustata	zoospores	-	-	-	Fu et al. (2016), Kawai (1988)
Saccharina japonica	zoospores	-	-	-	Fu et al. (2016), Kawai (1988)
	sperm	-	-	-	Fu et al. (2016), Kawai (1988)
Saccorhiza dermatodea	sperm	-	-	-	Müller et al. (1987)
Saccorhiza polyschides	sperm	-	-	-	Müller et al. (1987)
Hormosira banksii	sperm	+	+	negative	Müller et al. (1987), Maier et al. (1992)
Fucus disticus	sperm	+	+	negative	Kawai (1988), Kinoshita et al. (2016b)
Fucus serratus	sperm	+	+	pos/nega	Müller et al. (1987)

+=present, -=absent.

Table 2 Swimming velocities and beat frequencies of flagella in brown algal male gametes

Species	Swimming velocity	Swimming velocity (chemo)	Beat frequency AF	Beat frequency PF	Beat frequency (chemo) AF	Beat frequency (chemo) PF	Reference
Isogamous species							
Ectocarpus siliculosus	*205.2 ± 49.5 μm s^{-1} **131.5 ± 24.1 μm s^{-1}	**78.1 ± 14.3 μm s^{-1}	*54.2 ± 3.0 Hz **53.6 ± 1.9 Hz	n. a.	**45.1 ± 3.5 Hz	n. a.	Kinoshita et al. (2016d)
	*116 - 351 μm s^{-1} **110 μm s^{-1}	**84 μm s^{-1}	**30 - 50 Hz	n. a.	**30 - 50 Hz	n. a.	Geller and Müller (1981)
Anisogamous species							
Mutimo cylindricus	*179.2 ± 40.5 μm s^{-1}	**92.9 ± 25.2 μm s^{-1}	*38.4 ± 3.2 Hz	n. a.	**32.5 ± 3.6 Hz	n. a.	Kinoshita et al. (2016c)
Oogamous species							
Fucus distichus	93.7 ± 32.1 μm s^{-1}	79.4 ± 27.7 μm s^{-1}	41.6 ± 3.0 Hz	ca. 100 Hz	31.9 ± 3.3 Hz	59.9 ± 9.0 Hz	Kinoshita et al. (2016b)
Hormosira banksii	*194 ± 35 μm s^{-1} ***96 ± 14 μm s^{-1}	70 - 80 μm s^{-1}	n. i.	n. a.	n. i.	n. a.	Maier et al. (1992)
Laminaria digitata	30 - 60 μm s^{-1}	ca. 55 μm s^{-1}	ca. 30 Hz	n. i.	n. i.	n. i.	Maier and Müller (1990)
Saccharina japonica	74.7 ± 16.4 μm s^{-1}	88.8 ± 23.2 μm s^{-1}	54.4 ± 8.0 Hz	95.2 ± 11.8 Hz	40.2 ± 7.2 Hz	68.1 ± 17.5 Hz	Kinoshita et al. (2016b)

*Free-swimming male gametes, **Thigmotactic male gametes, ***Swimming male gametes in contact with the glass surface, n.a.=not applicable, n. i.=not investigated.

Plate 1

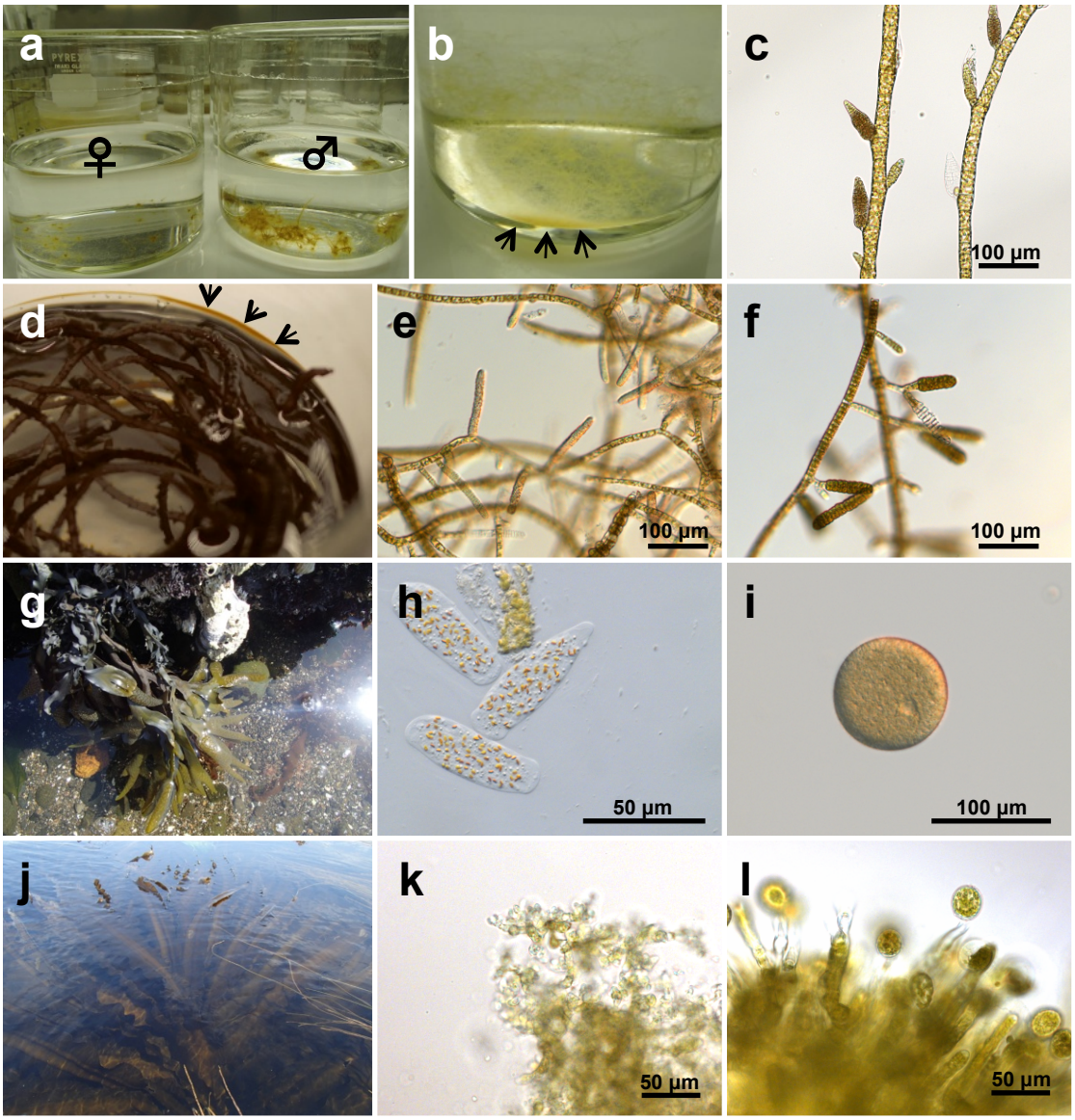

Plate 2

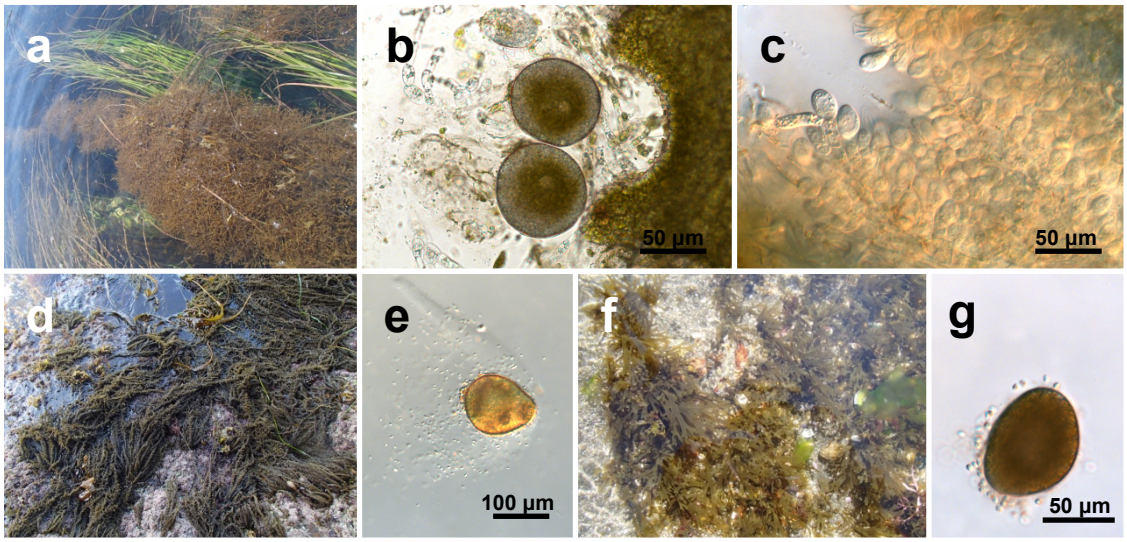

Plate 3

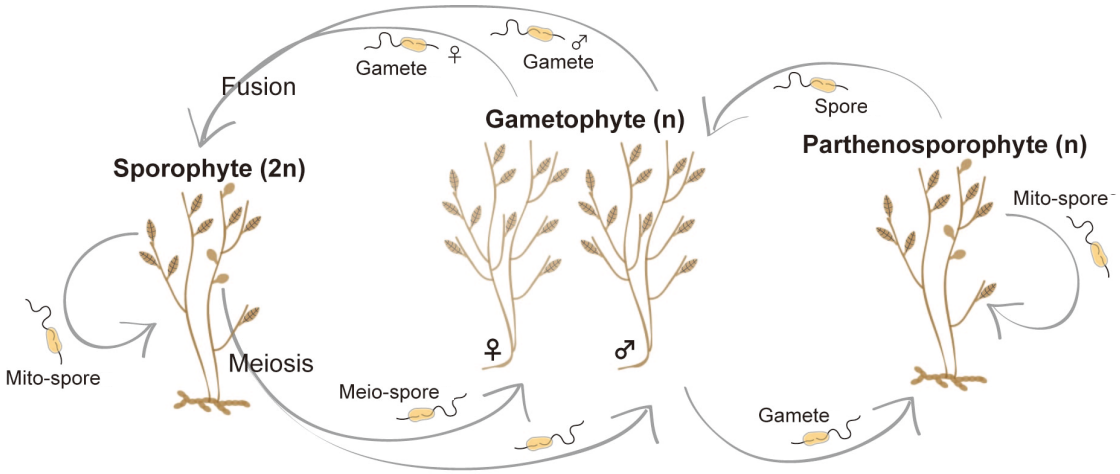
Gamete
Gamete
Fusion
Gametophyte (n)
Spore
Parthenosporophyte (n)
Sporophyte (2n)
Mito-spore
Mito-spore
Meiosis
Meio-spore
Gamete

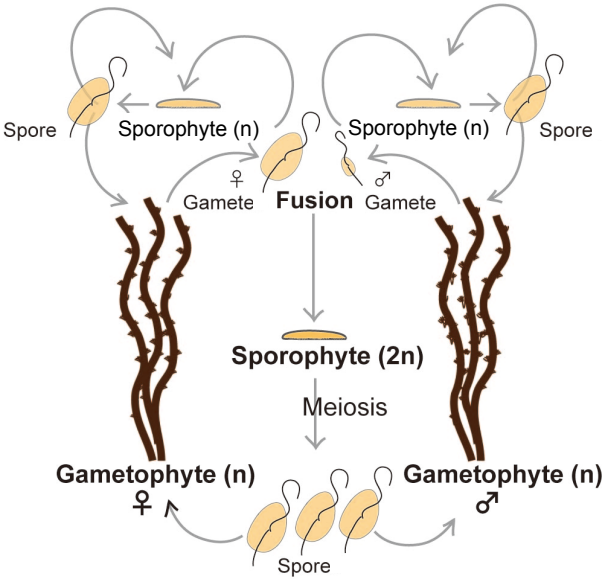
Spore
Sporophyte (n)
Sporophyte (n)
Spore
Gamete
Fusion
Gamete
Sporophyte (2n)
Meiosis
Gametophyte (n)
Gametophyte (n)
Spore

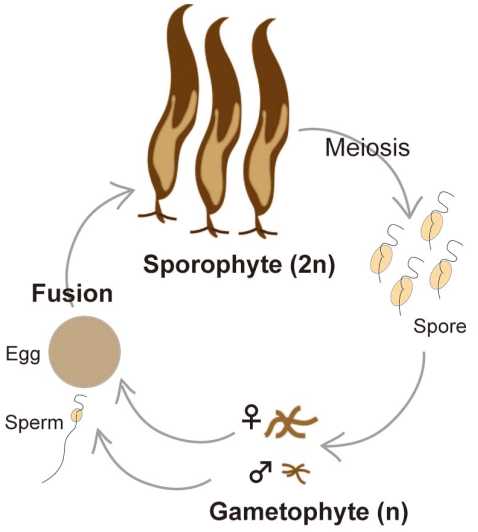
Meiosis
Sporophyte (2n)
Fusion
Spore
Egg
Sperm
Gametophyte (n)

Plate 4

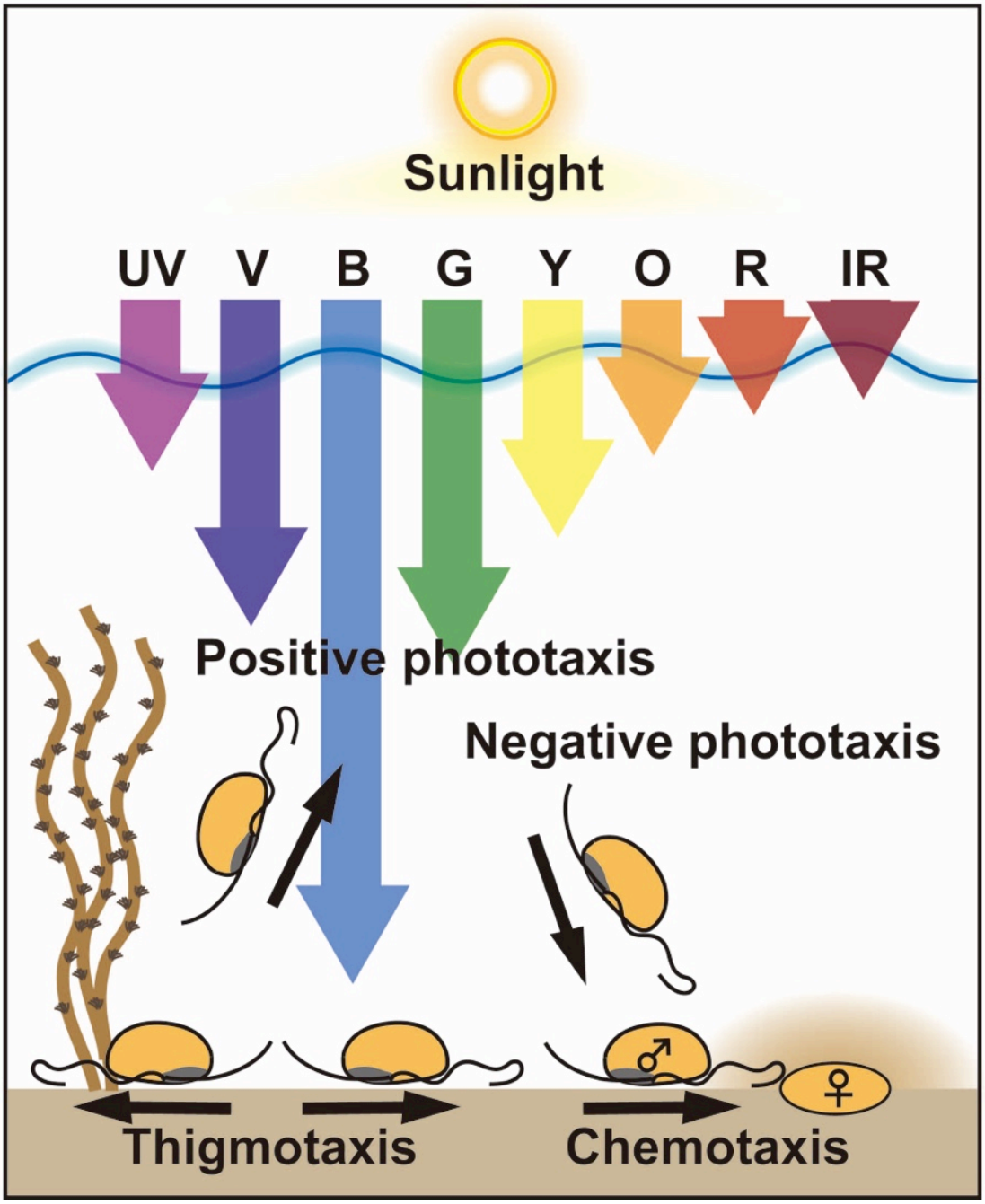
Sunlight
UV V B G Y O R IR
Positive phototaxis
Negative phototaxis
♂
♀
Thigmotaxis
Chemotaxis

Plate 5

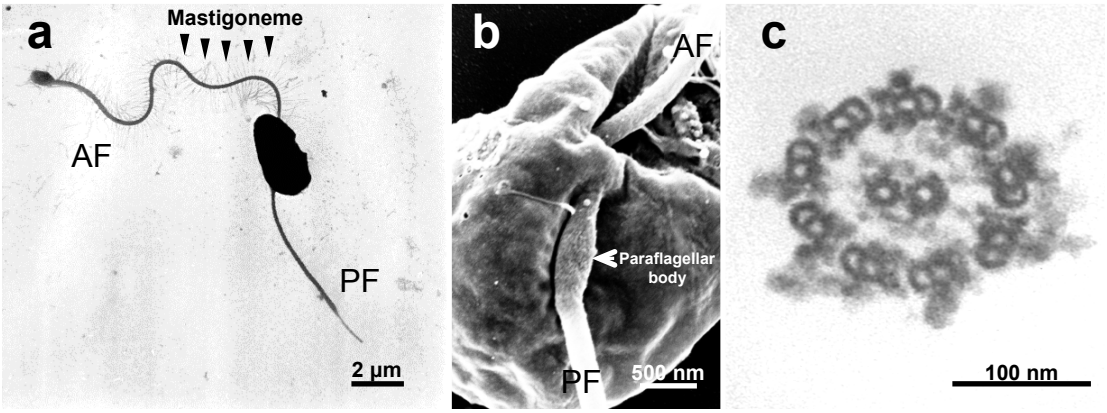
a
Mastigoneme
AF
PF
2 µm
b
AF
Paraflagellar body
PF
500 nm
c
100 nm

Plate 6

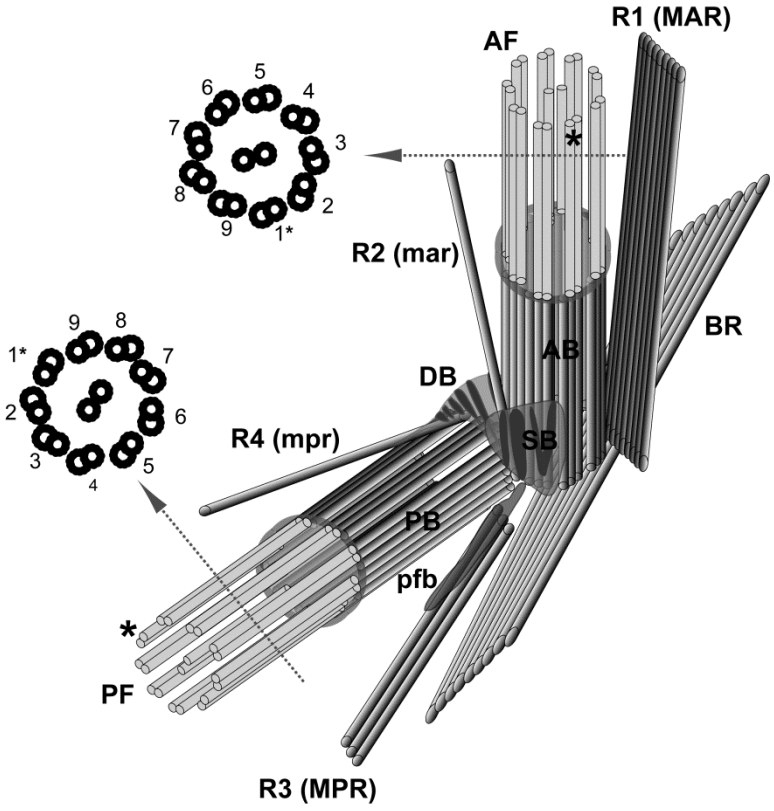
R1 (MAR)
AF
5
6
4
7
3
8
2
9
1*
*
R2 (mar)
BR
AB
9
8
1*
7
DB
2
6
R4 (mpr)
SB
3
5
4
PB
pfb
*
PF
R3 (MPR)

Plate 7

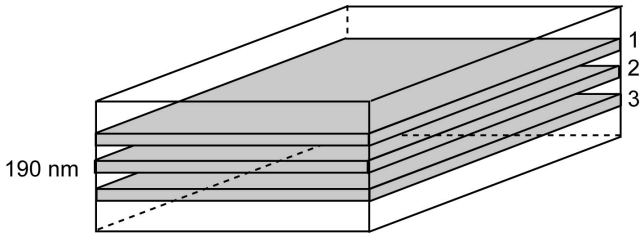

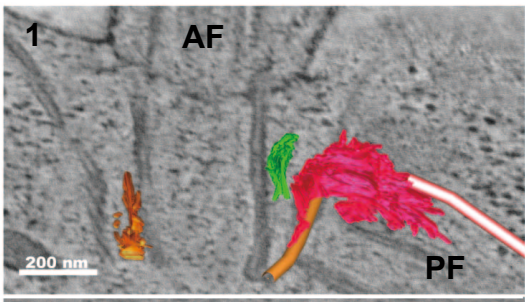

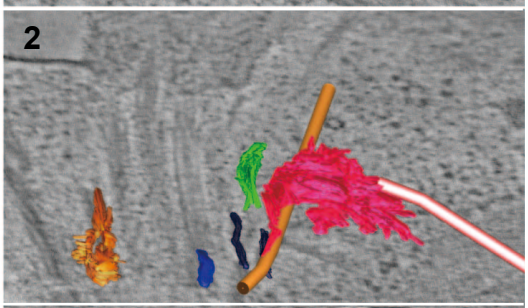

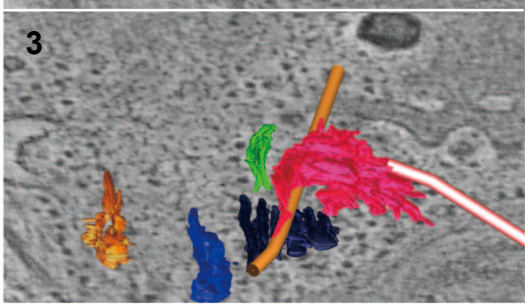

Plate 8

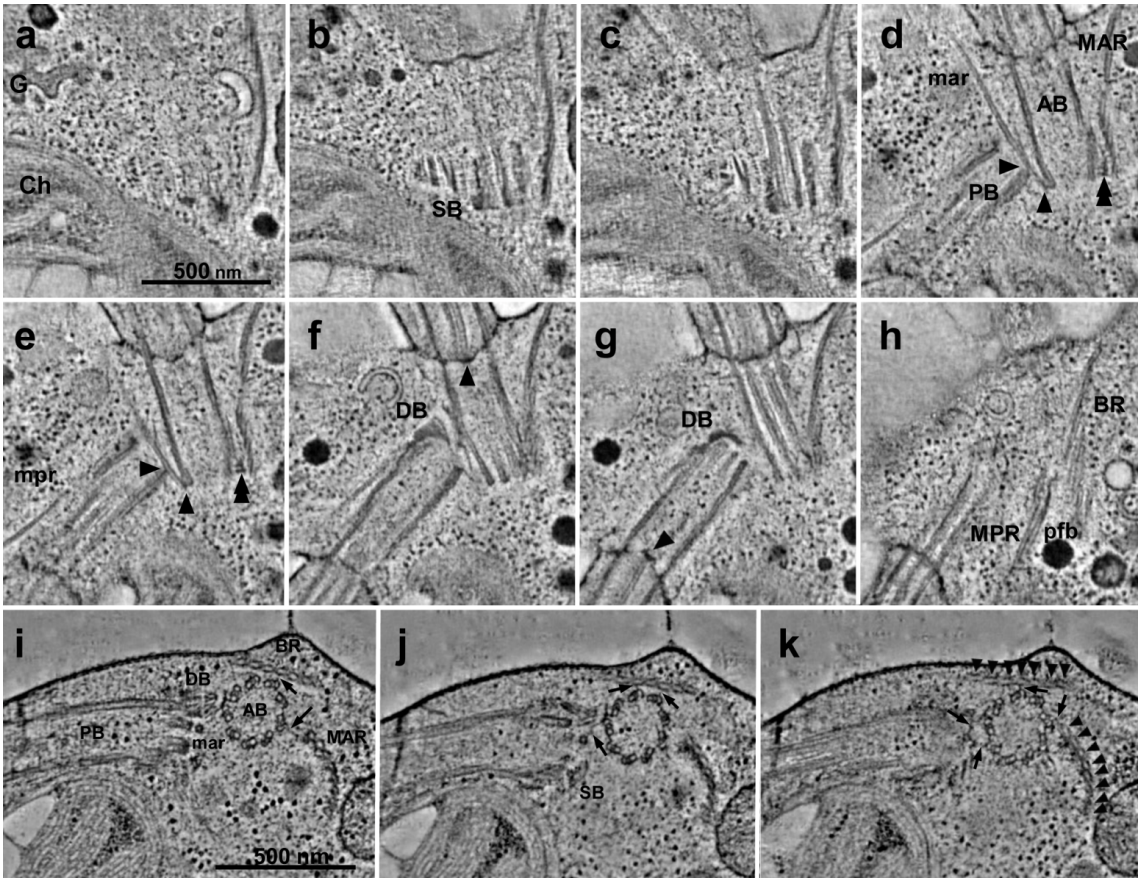
a
G
Ch
500 nm
b
SB
c
d
MAR
mar
AB
PB
e
mpr
f
DB
g
DB
h
BR
MPR
pfb
i
BR
DB
AB
PB
mar
MAR
500 nm
j
SB
k

Plate 9

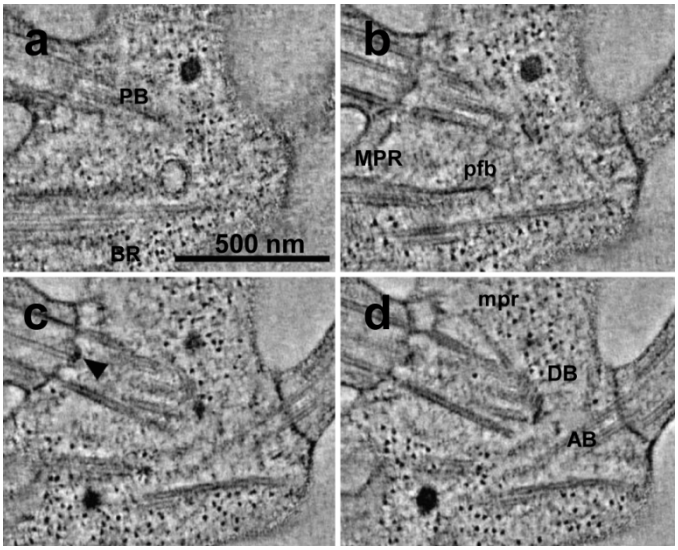

Plate 10

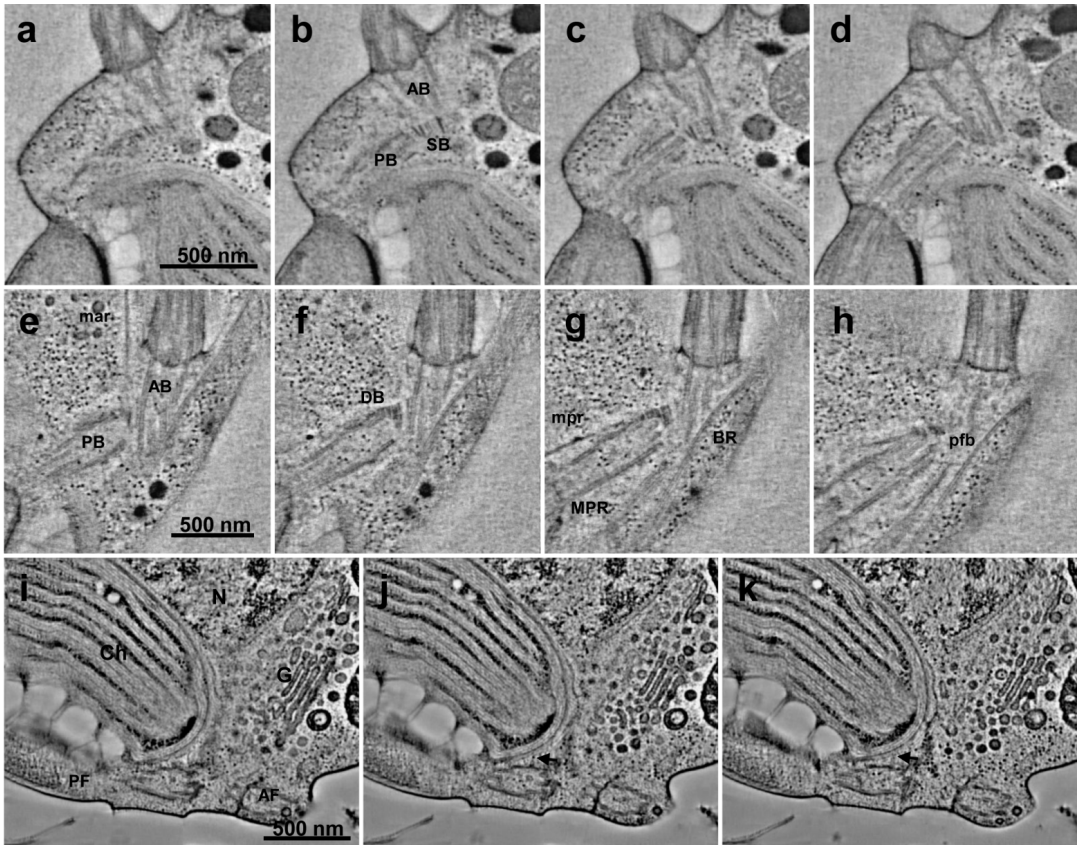
a
500 nm
b
AB
SB
PB
c
d
e
mar
AB
PB
500 nm
f
DB
g
mpr
BR
MPR
h
pfb
i
N
Ch
G
PF
AF
500 nm
j
k

Plate 11

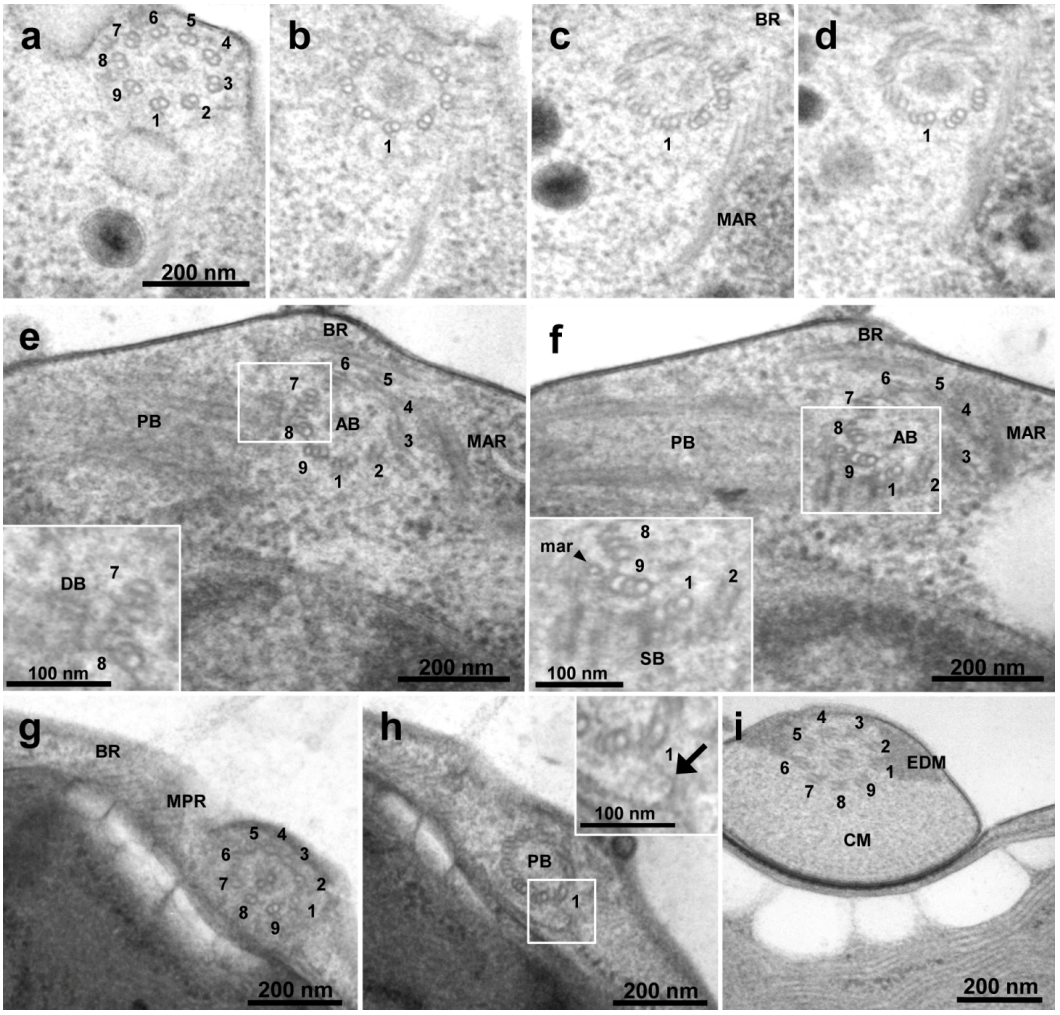

Plate 12

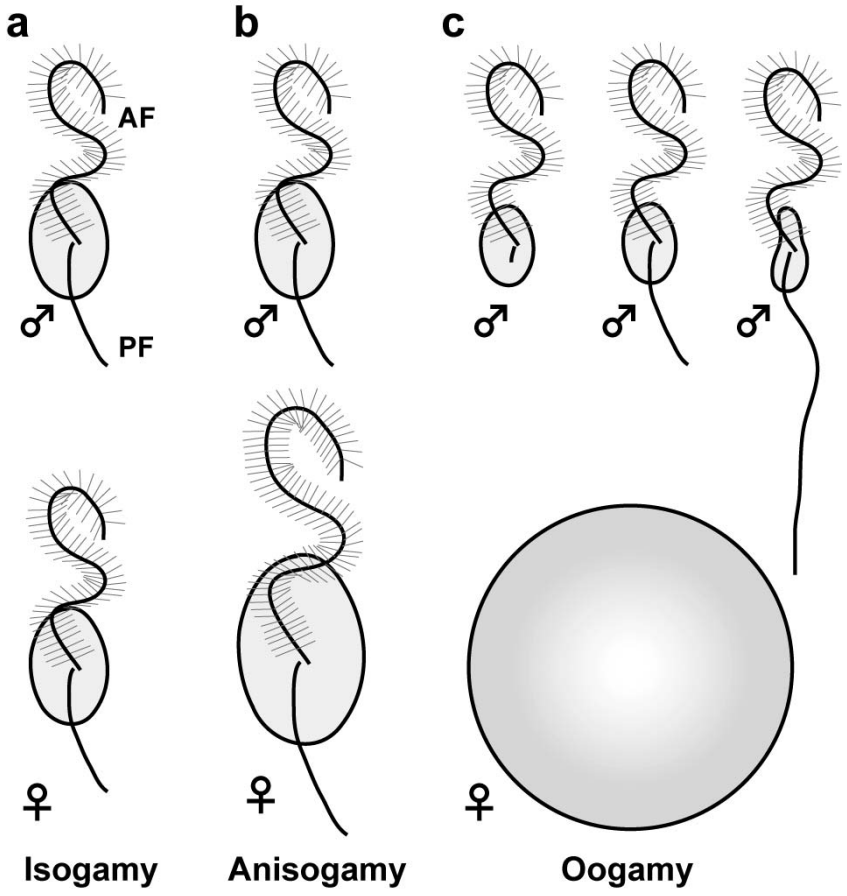

Plate 13

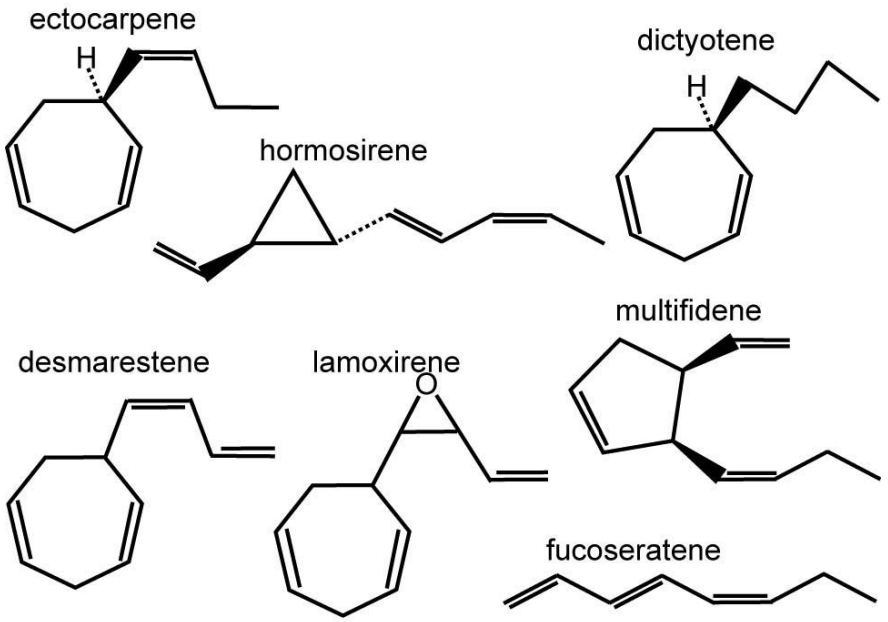
ectocarpene
H
hormosirene
dictyotene
H
desmarestene
lamoxirene
O
multifidene
fucoseratene

Plate 14

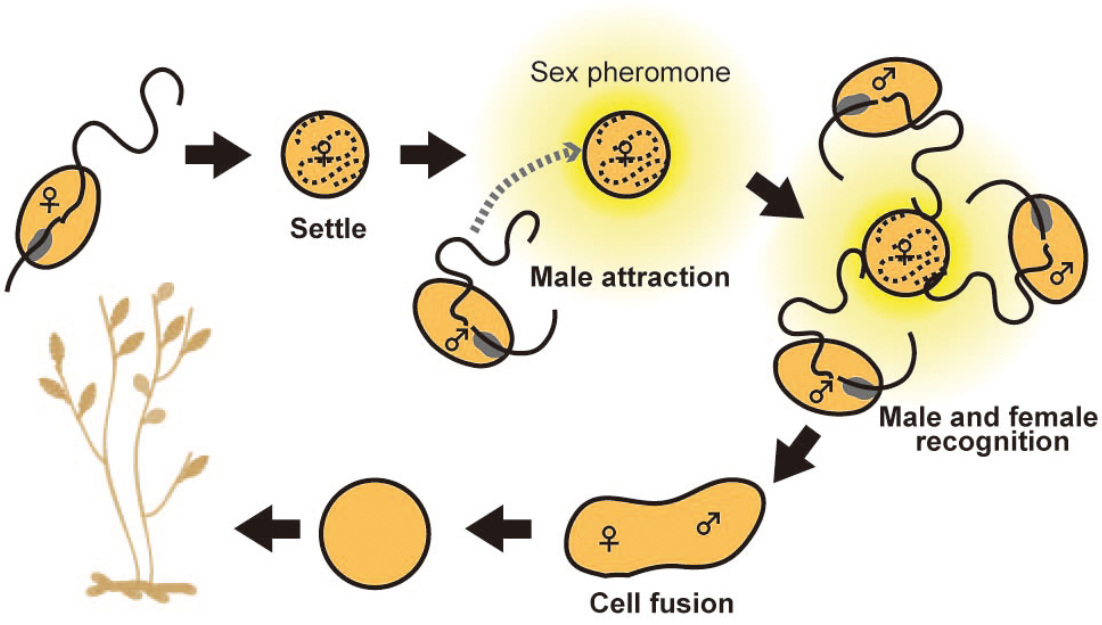
Sex pheromone
Settle
Male attraction
Male and female recognition
Cell fusion

Plate 15

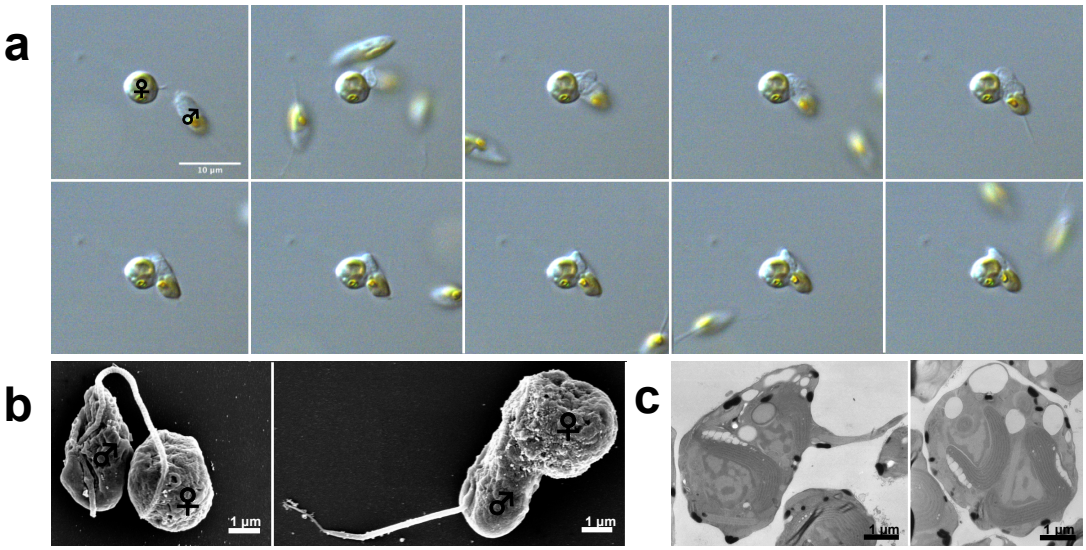

Plate 16

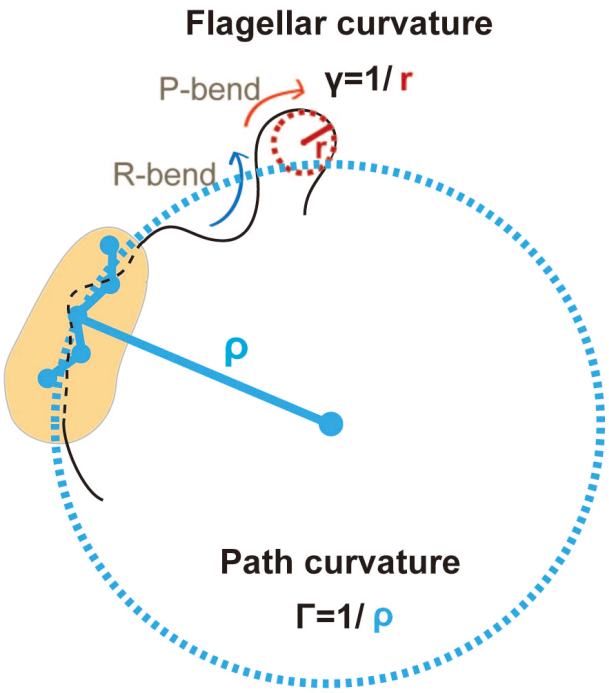
Flagellar curvature
P-bend
γ=1/ r
r
R-bend
ρ
Path curvature
Γ=1/ ρ

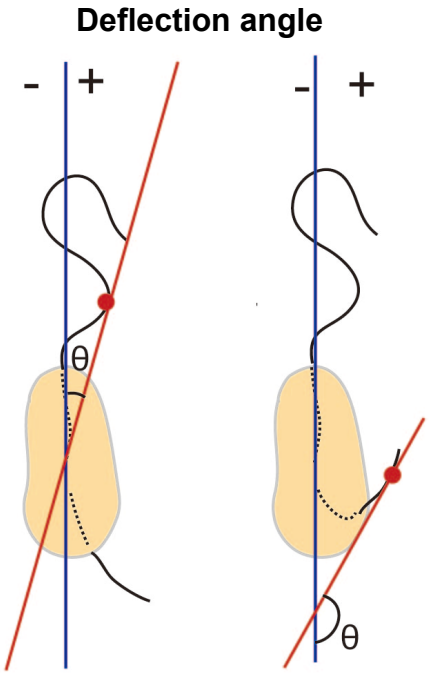
Deflection angle
-
+
θ
-
+
θ

Plate 17

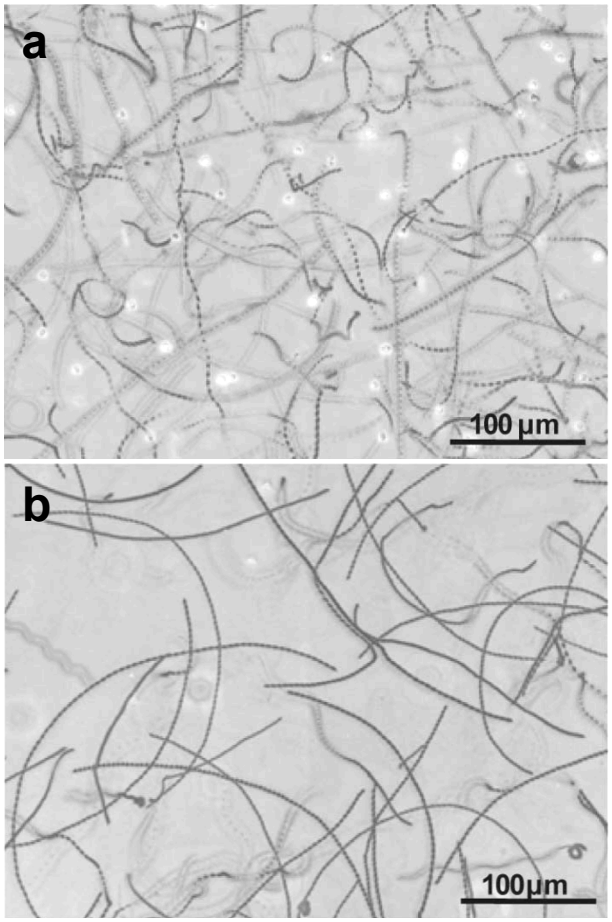
a
100 µm
b
100µm

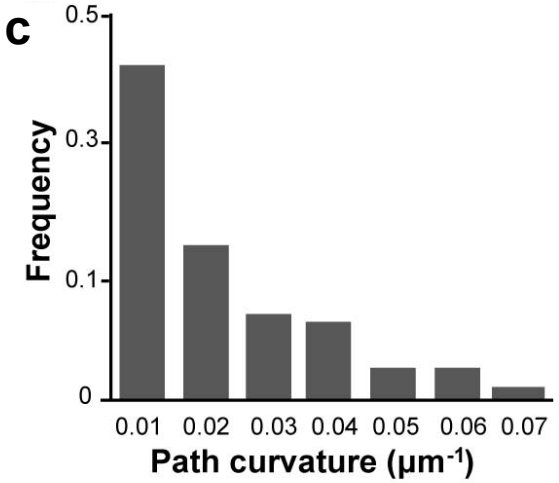
c
0.5
0.3
0.1
0
Frequency
0.01
0.02
0.03
0.04
0.05
0.06
0.07
Path curvature (µm-1)

Plate 18

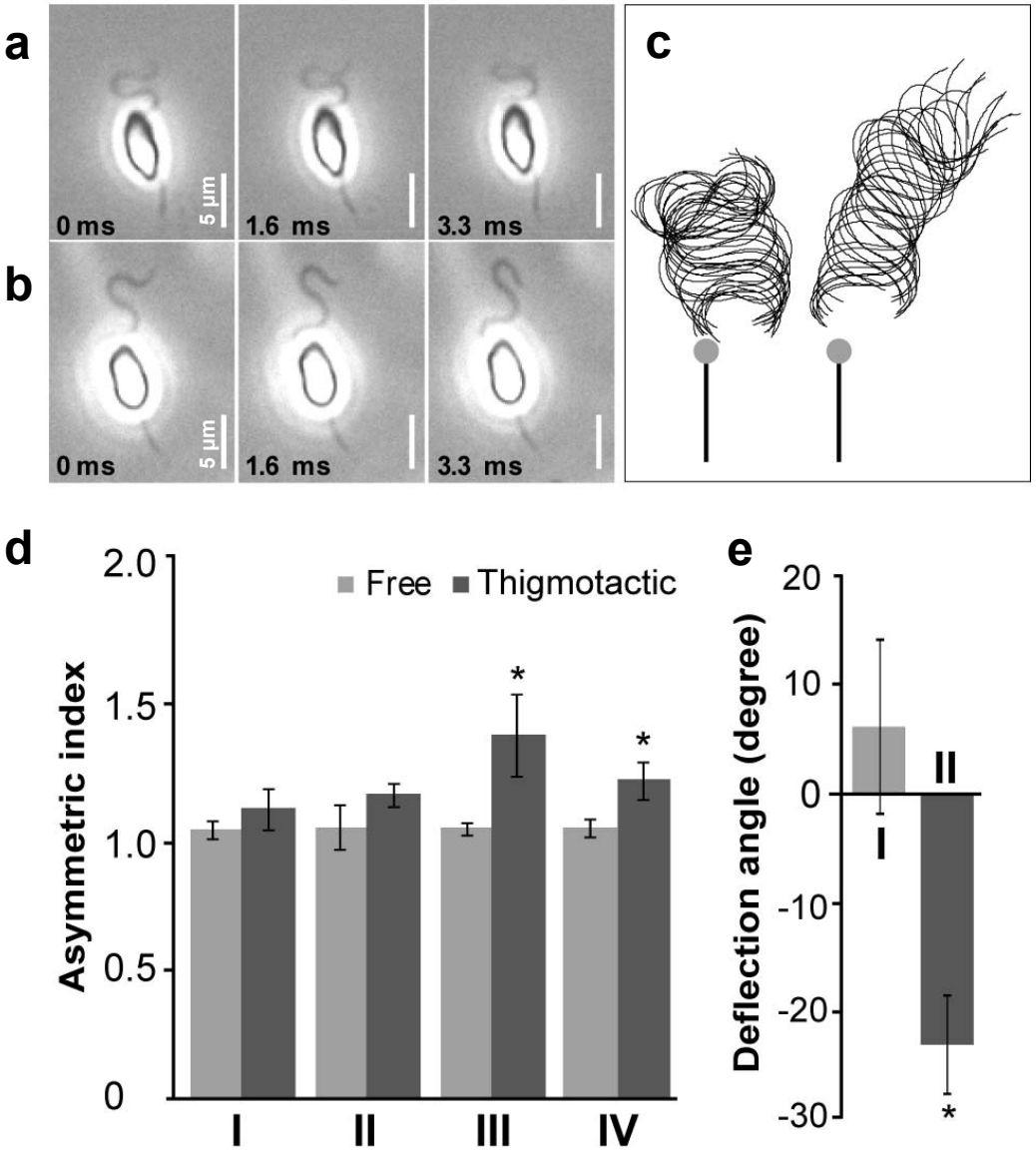
a
b
c
0 ms
5 µm
1.6 ms
3.3 ms
0 ms
5 µm
1.6 ms
3.3 ms
d
Free
Thigmotactic
Asymmetric index
2.0
1.5
1.0
0.5
0
I
II
III
IV
*
*
e
Deflection angle (degree)
20
10
0
-10
-20
-30
I
II
*

Plate 19

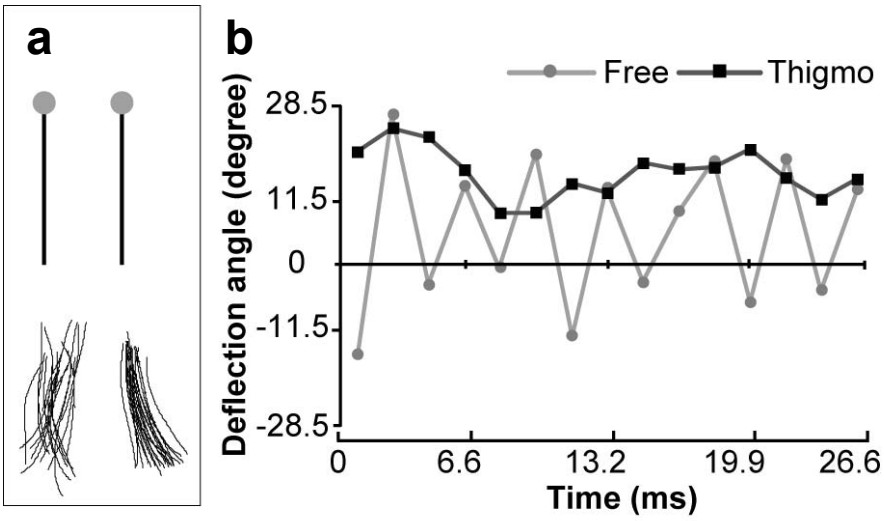
a
b
Free
Thigmo
Deflection angle (degree)
28.5
11.5
0
-11.5
-28.5
0
6.6
13.2
19.9
26.6
Time (ms)

Plate 20

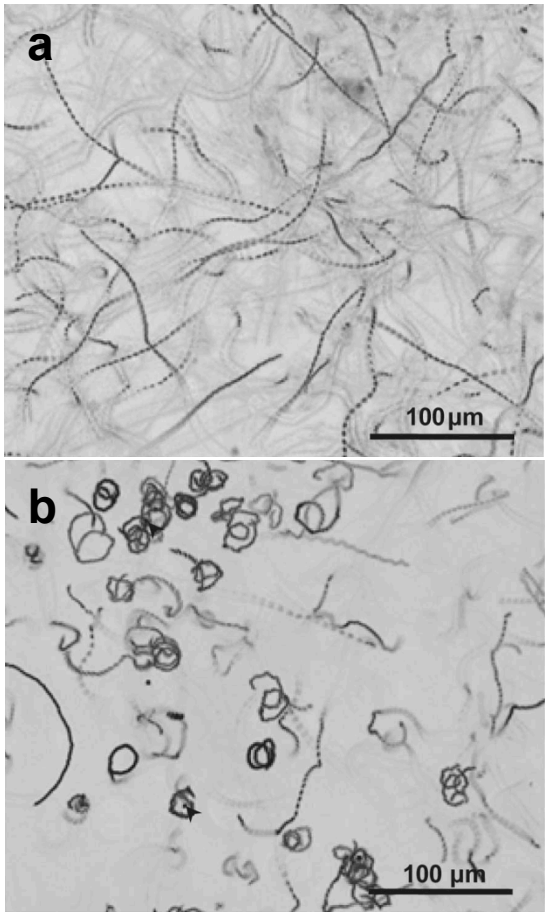
a
100 µm
b
100 µm

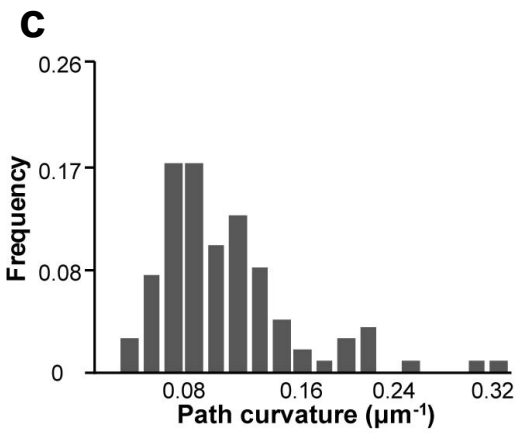
c
0.26
0.17
0.08
0
Frequency
0.08
0.16
0.24
0.32
Path curvature (µm-1)

Plate 21

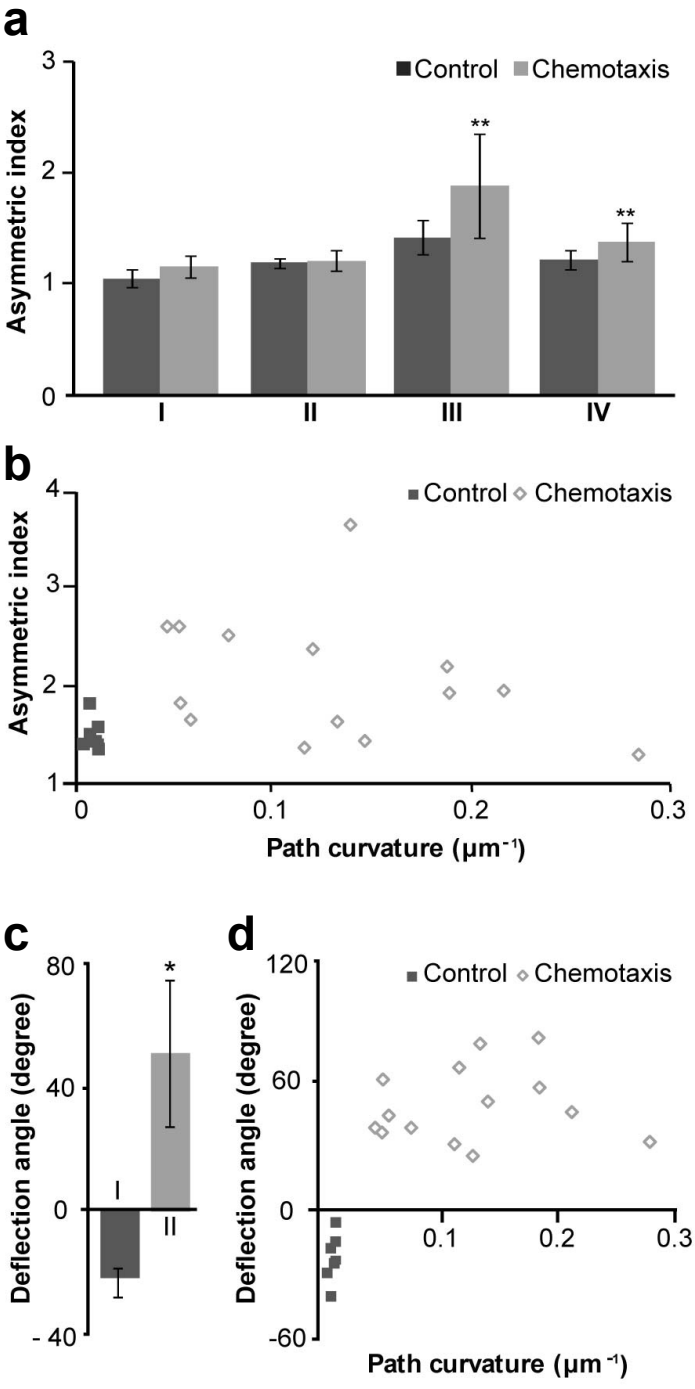
a
Control
Chemotaxis
Asymmetric index
3
2
1
0
**
**
I
II
III
IV
b
Control
Chemotaxis
Asymmetric index
4
3
2
1
0
0.1
0.2
0.3
Path curvature (μm⁻¹)
c
Deflection angle (degree)
80
40
0
- 40
*
I
II
d
Control
Chemotaxis
Deflection angle (degree)
120
60
0
-60
0.1
0.2
0.3
Path curvature (μm⁻¹)

Plate 22

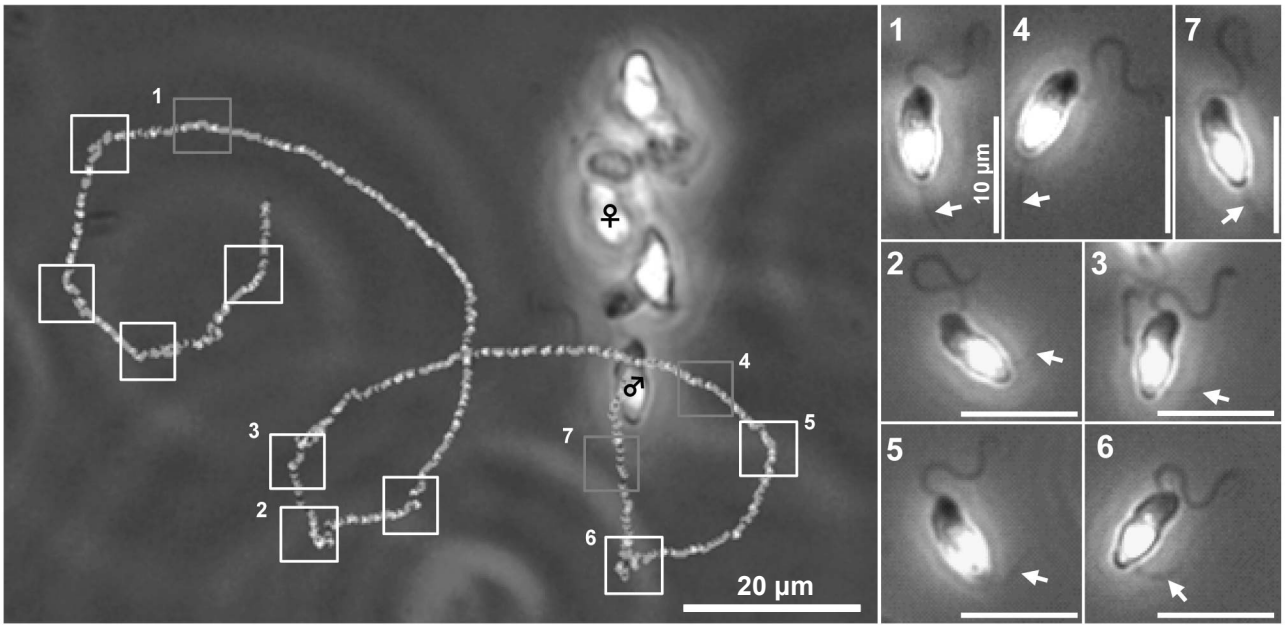

Plate 23

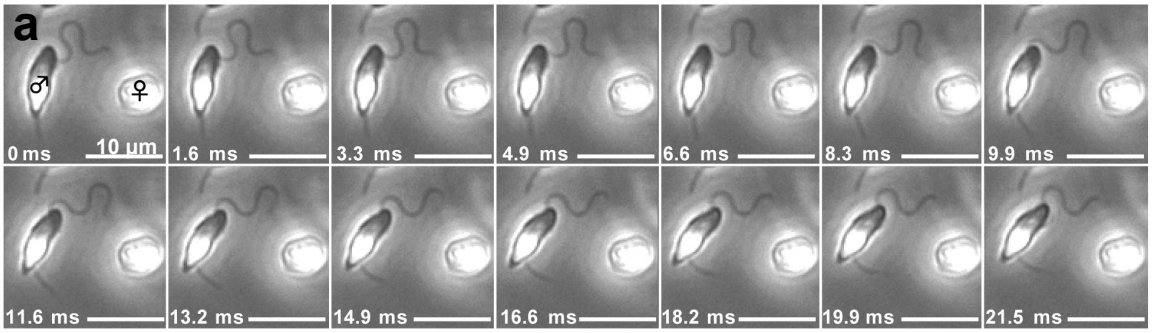
a
♂
♀
0 ms
10 μm
1.6 ms
3.3 ms
4.9 ms
6.6 ms
8.3 ms
9.9 ms
11.6 ms
13.2 ms
14.9 ms
16.6 ms
18.2 ms
19.9 ms
21.5 ms

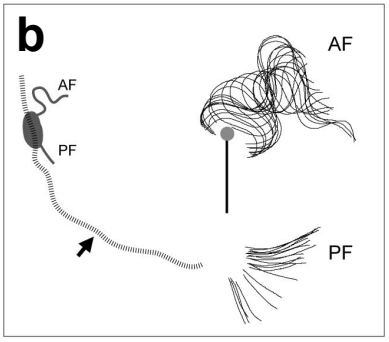
b
AF
PF
AF
PF

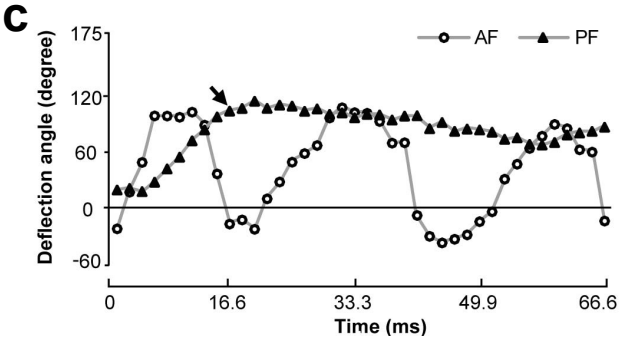
c
AF
PF
Deflection angle (degree)
175
120
60
0
-60
0
16.6
33.3
49.9
66.6
Time (ms)

Plate 24

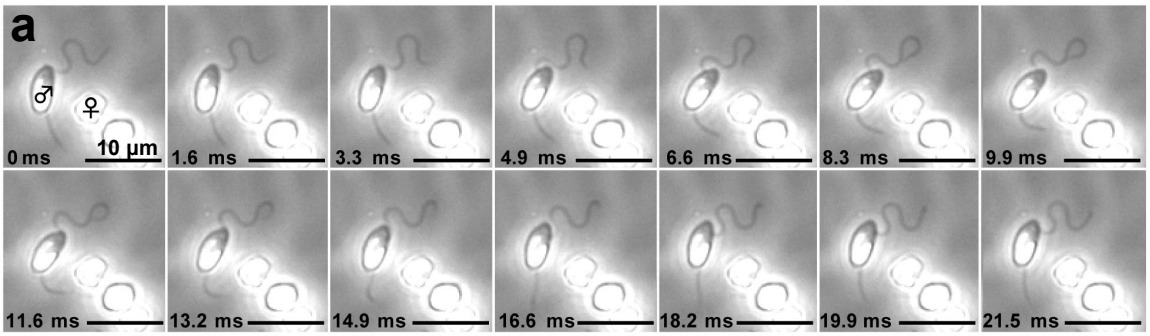
a
♂
♀
0 ms
10 µm
1.6 ms
3.3 ms
4.9 ms
6.6 ms
8.3 ms
9.9 ms
11.6 ms
13.2 ms
14.9 ms
16.6 ms
18.2 ms
19.9 ms
21.5 ms

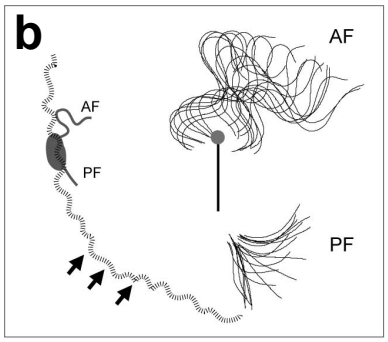
b
AF
AF
PF
PF

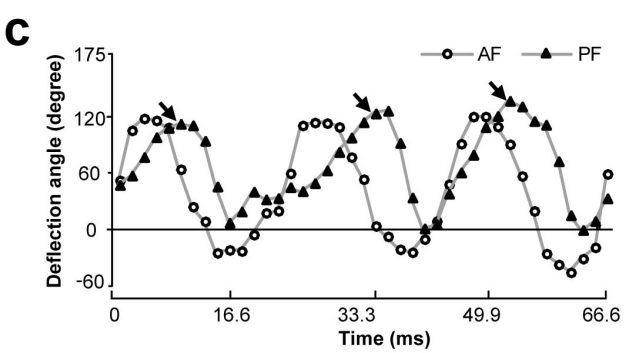
c
AF
PF
Deflection angle (degree)
175
120
60
0
-60
0
16.6
33.3
49.9
66.6
Time (ms)

Plate 25

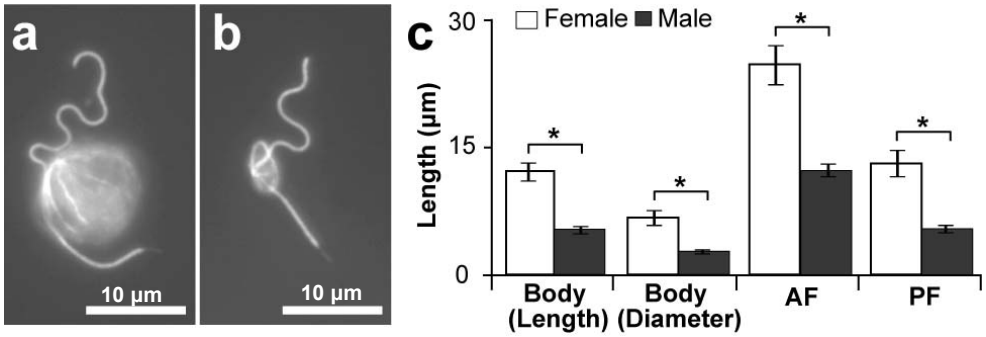
a
10 µm
b
10 µm
c
Female
Male
30
15
0
Length (µm)
*
*
*
*
Body (Length)
Body (Diameter)
AF
PF

Plate 26

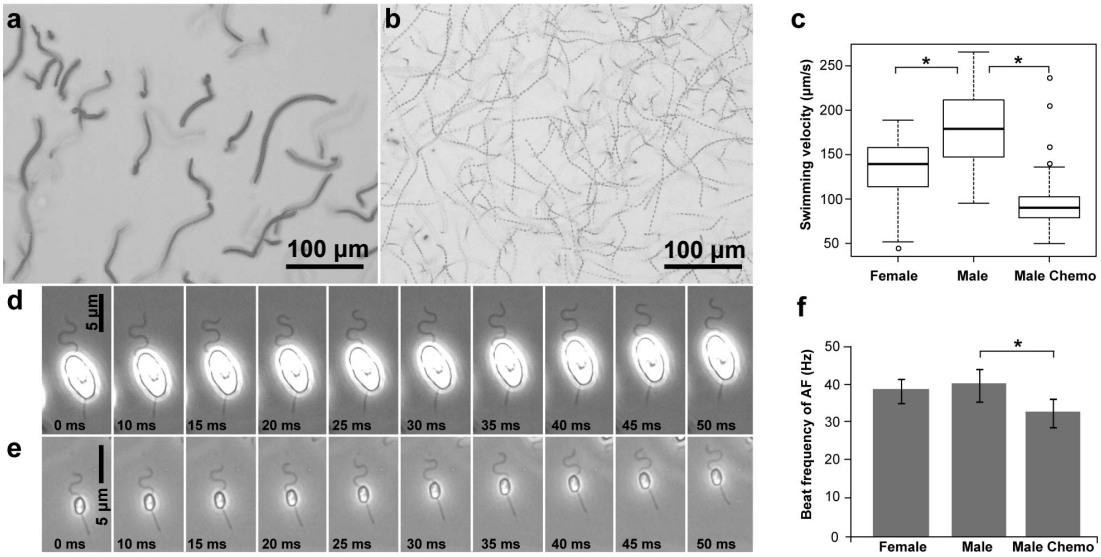
a
100 µm
b
100 µm
c
Swimming velocity (µm/s)
250
200
150
100
50
*
*
Female
Male
Male Chemo
d
5 µm
0 ms
10 ms
15 ms
20 ms
25 ms
30 ms
35 ms
40 ms
45 ms
50 ms
e
5 µm
0 ms
10 ms
15 ms
20 ms
25 ms
30 ms
35 ms
40 ms
45 ms
50 ms
f
Beat frequency of AF (Hz)
50
40
30
20
10
0
*
Female
Male
Male Chemo

Plate 27

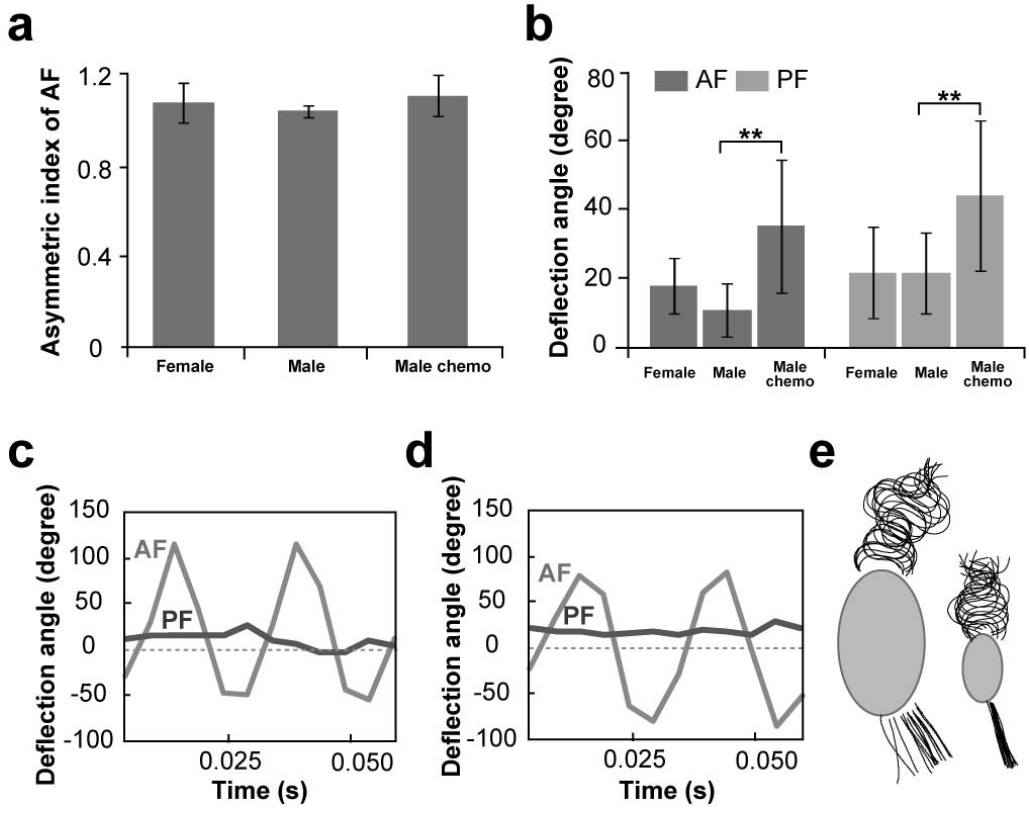
a
Asymmetric index of AF
1.2
0.8
0.4
0
Female
Male
Male chemo
b
Deflection angle (degree)
80
60
40
20
0
AF
PF
**
**
Female
Male
Male chemo
Female
Male
Male chemo
c
Deflection angle (degree)
150
100
50
0
-50
-100
AF
PF
0.025
0.050
Time (s)
d
Deflection angle (degree)
150
100
50
0
-50
-100
AF
PF
0.025
0.050
Time (s)
e

Plate 28

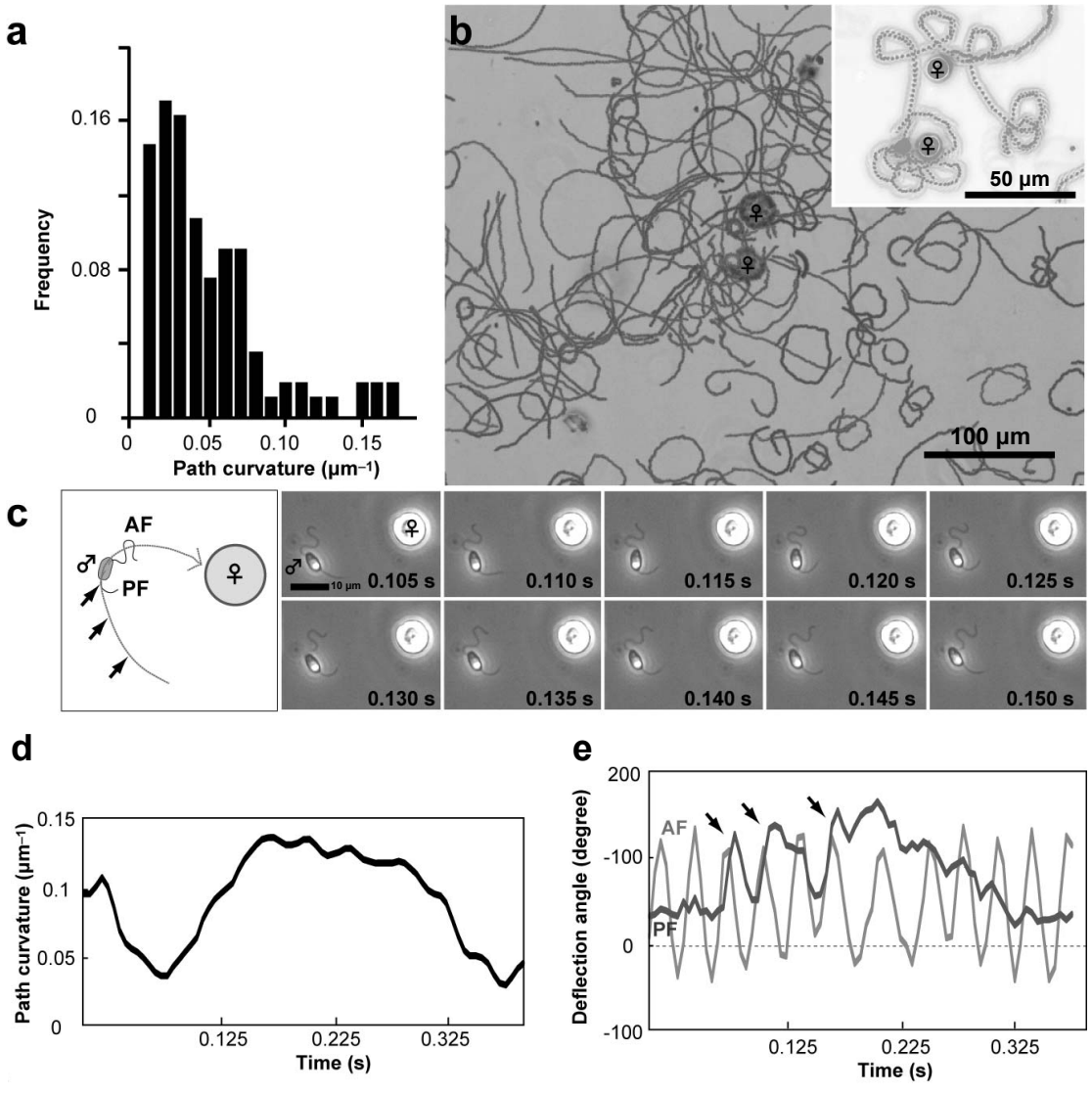
a
Frequency
0.16
0.08
0
0
0.05
0.10
0.15
Path curvature (μm⁻¹)
b
50 μm
100 μm
c
AF
PF
10 μm
0.105 s
0.110 s
0.115 s
0.120 s
0.125 s
0.130 s
0.135 s
0.140 s
0.145 s
0.150 s
d
Path curvature (μm⁻¹)
0.15
0.1
0.05
0
0.125
0.225
0.325
Time (s)
e
Deflection angle (degree)
200
-100
0
-100
AF
PF
0.125
0.225
0.325
Time (s)

Plate 29

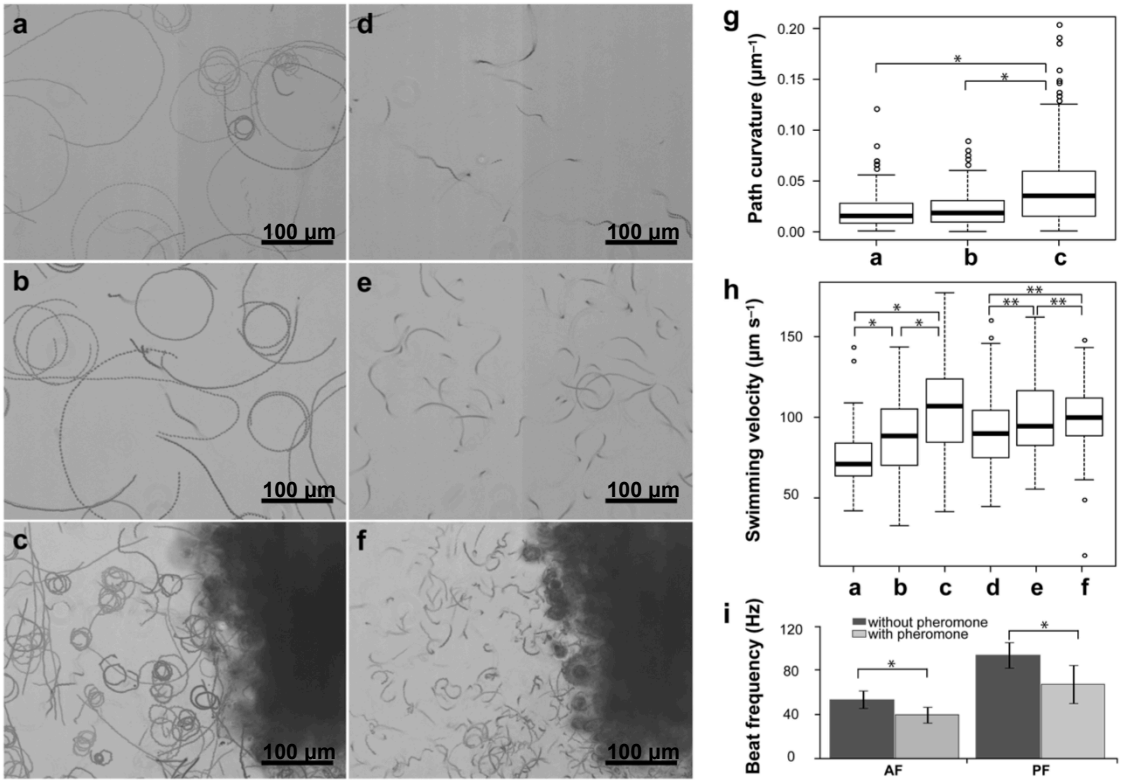
a
d
b
e
c
f
100 µm
g
Path curvature (µm⁻¹)
0.20
0.15
0.10
0.05
0.00
a
b
c
h
Swimming velocity (µm s⁻¹)
150
100
50
a
b
c
d
e
f
i
Beat frequency (Hz)
120
80
40
0
without pheromone
with pheromone
AF
PF

Plate 30

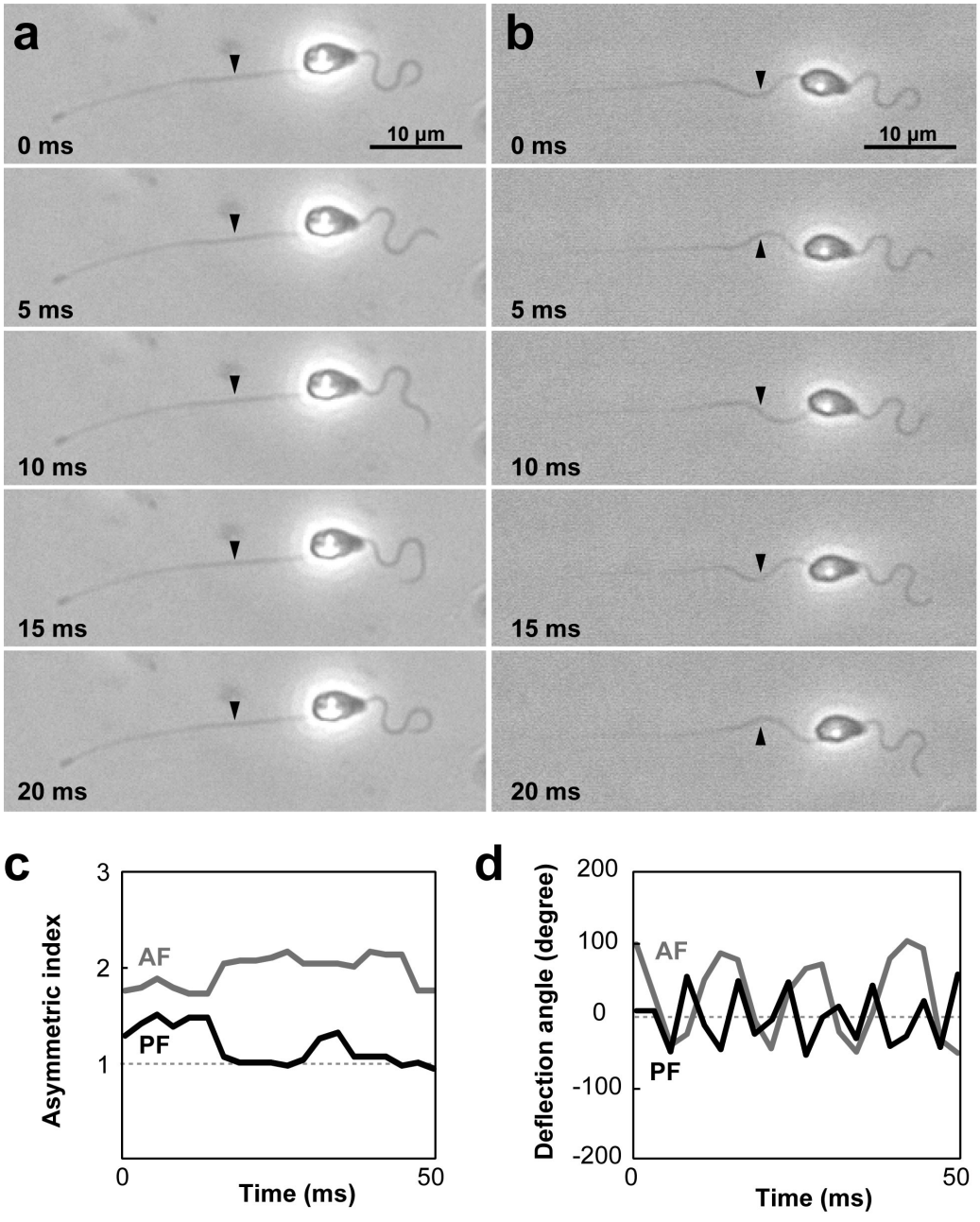
a
0 ms
10 μm
5 ms
10 ms
15 ms
20 ms
b
0 ms
10 μm
5 ms
10 ms
15 ms
20 ms
c
Asymmetric index
3
2
1
AF
PF
0
50
Time (ms)
d
Deflection angle (degree)
200
100
0
-100
-200
AF
PF
0
50
Time (ms)

Plate 31

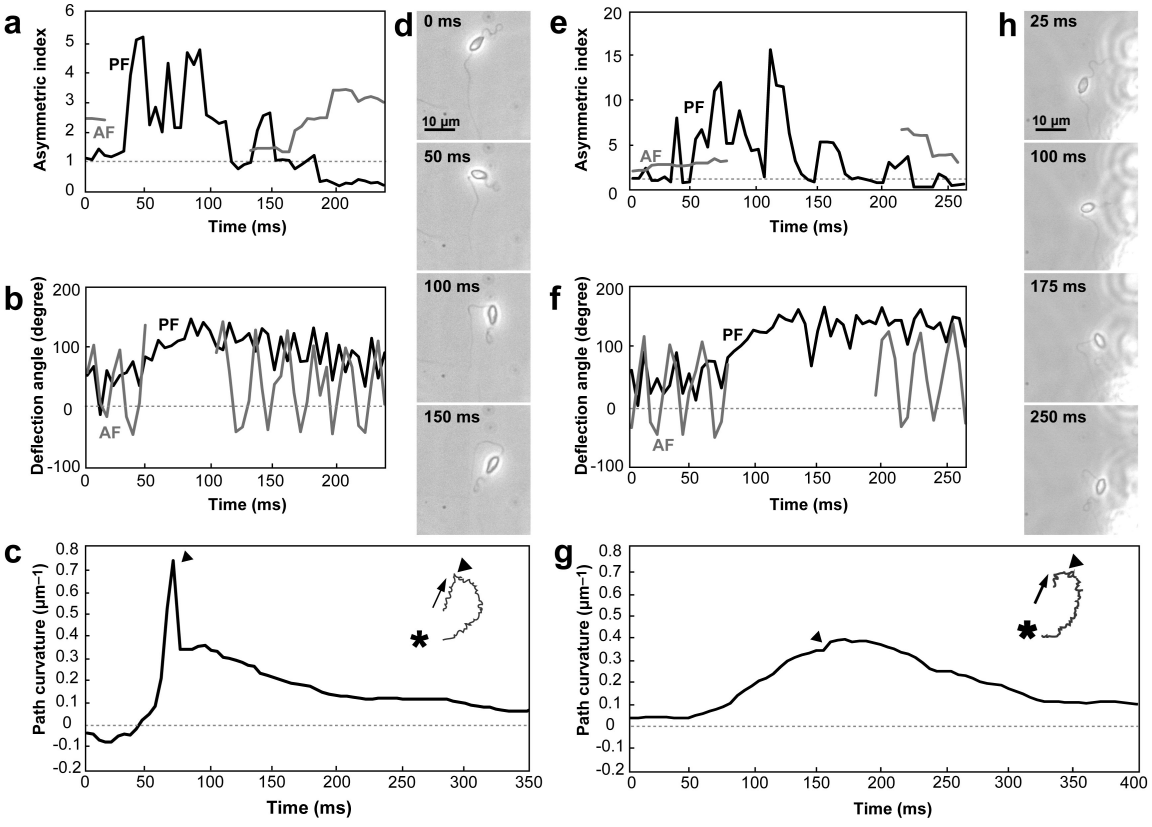
a
Asymmetric index
PF
AF
Time (ms)
b
Deflection angle (degree)
PF
AF
Time (ms)
c
Path curvature (μm−1)
Time (ms)
d
0 ms
10 μm
50 ms
100 ms
150 ms
e
Asymmetric index
PF
AF
Time (ms)
f
Deflection angle (degree)
PF
AF
Time (ms)
g
Path curvature (μm−1)
Time (ms)
h
25 ms
10 μm
100 ms
175 ms
250 ms

Plate 32

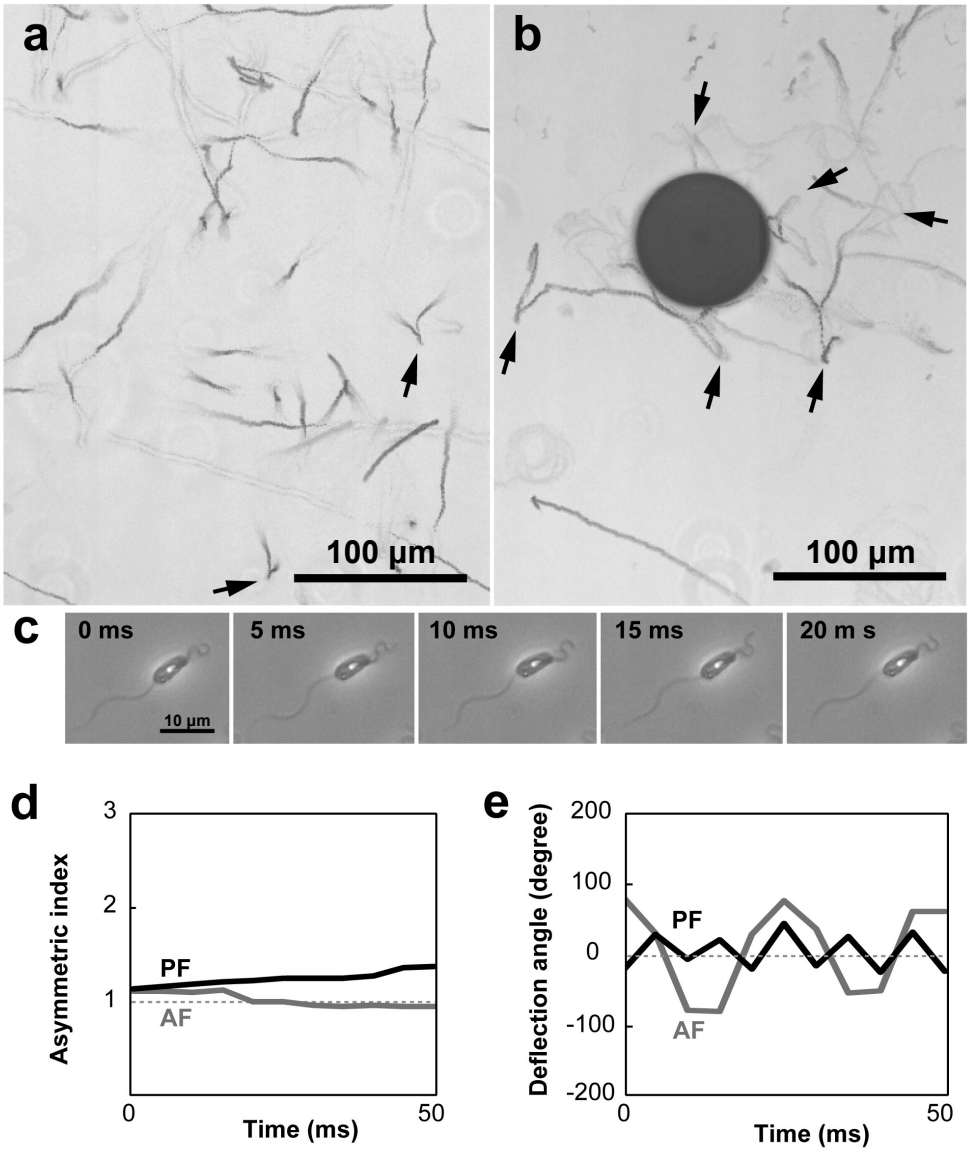
a
100 µm
b
100 µm
c
0 ms
5 ms
10 ms
15 ms
20 m s
10 µm
d
Asymmetric index
3
2
1
PF
AF
0
50
Time (ms)
e
Deflection angle (degree)
200
100
0
-100
-200
PF
AF
0
50
Time (ms)

Plate 33

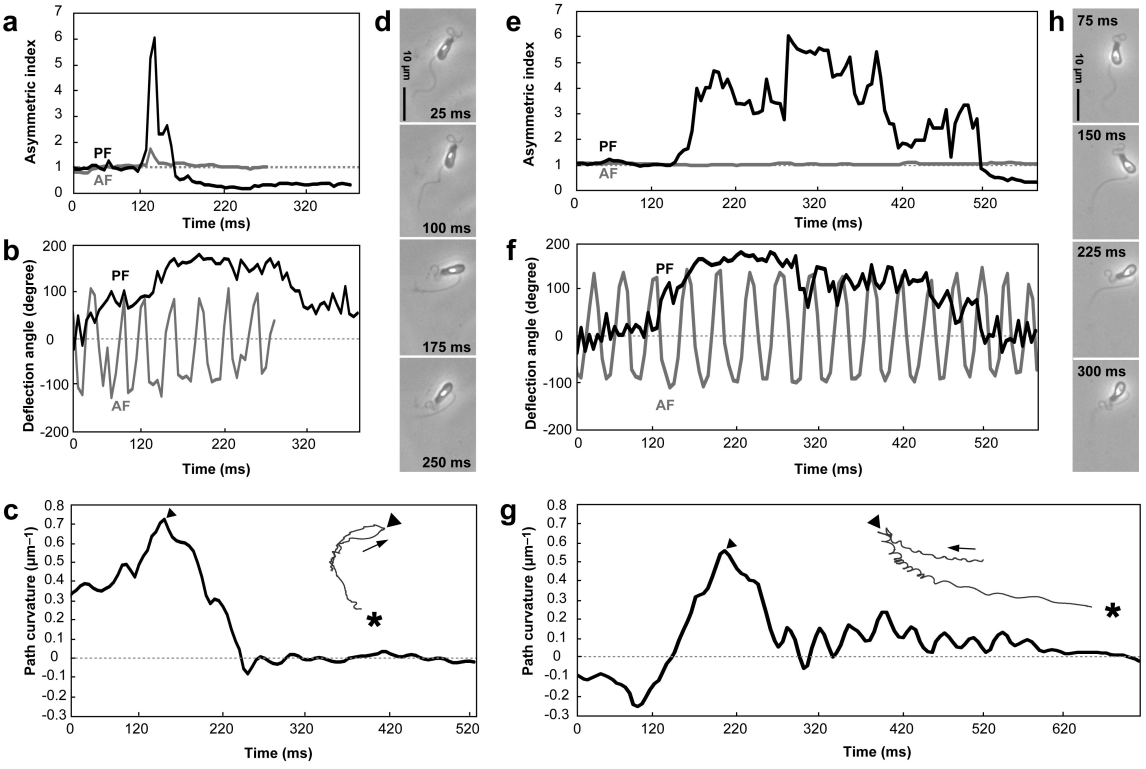
a
Asymmetric index
PF
AF
Time (ms)
b
Deflection angle (degree)
PF
AF
Time (ms)
c
Path curvature (μm⁻¹)
Time (ms)
d
10 μm
25 ms
100 ms
175 ms
250 ms
e
Asymmetric index
PF
AF
Time (ms)
f
Deflection angle (degree)
PF
AF
Time (ms)
g
Path curvature (μm⁻¹)
Time (ms)
h
75 ms
10 μm
150 ms
225 ms
300 ms

Plate 34

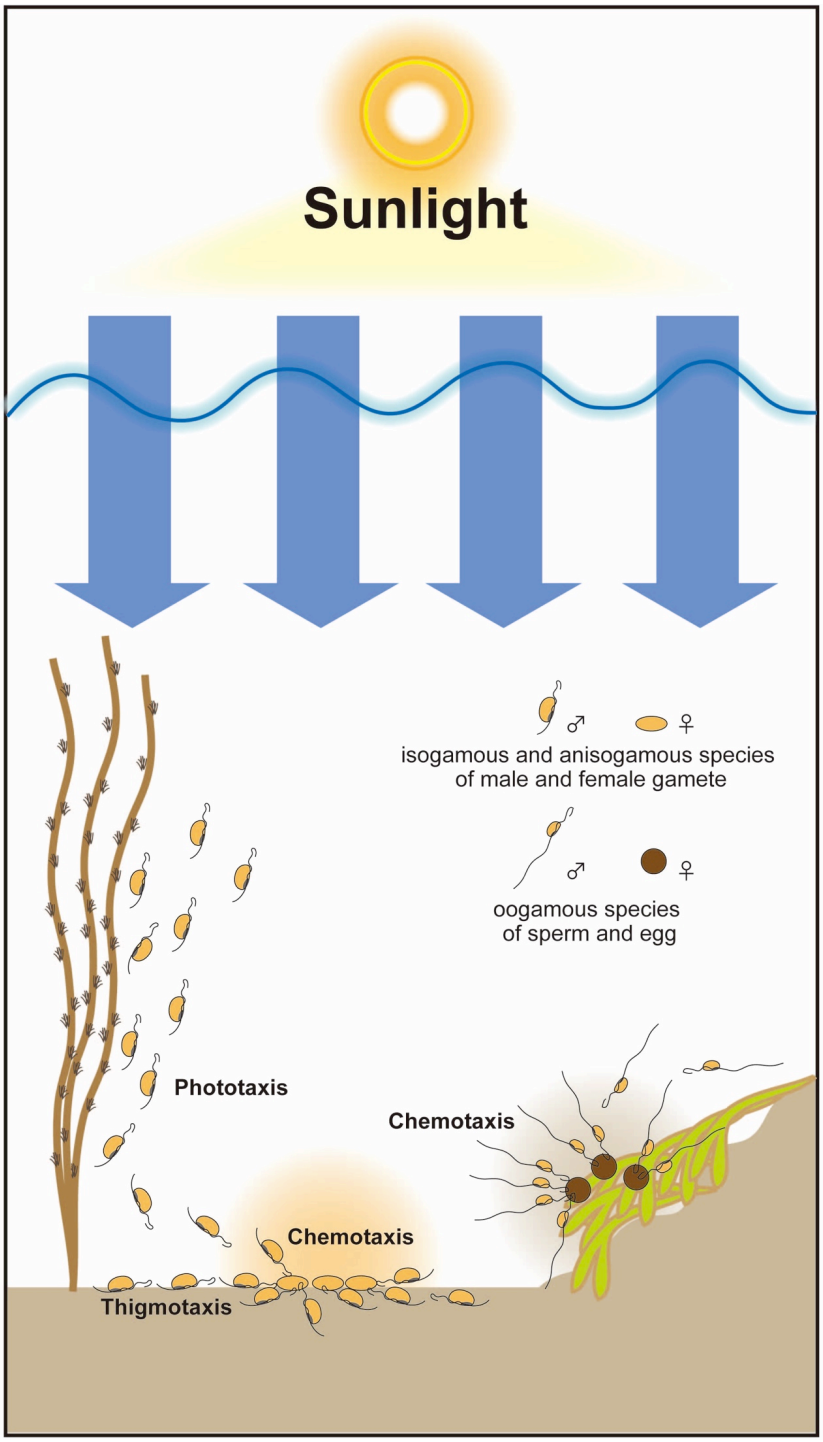
Sunlight
isogamous and anisogamous species
of male and female gamete
oogamous species
of sperm and egg
Phototaxis
Chemotaxis
Chemotaxis
Thigmotaxis

Plate 35

Isogamous and anisogamous species

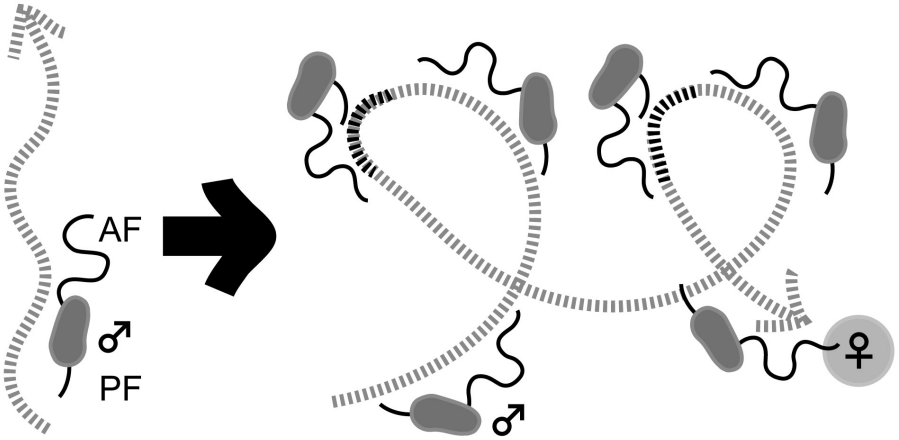

Oogamous species

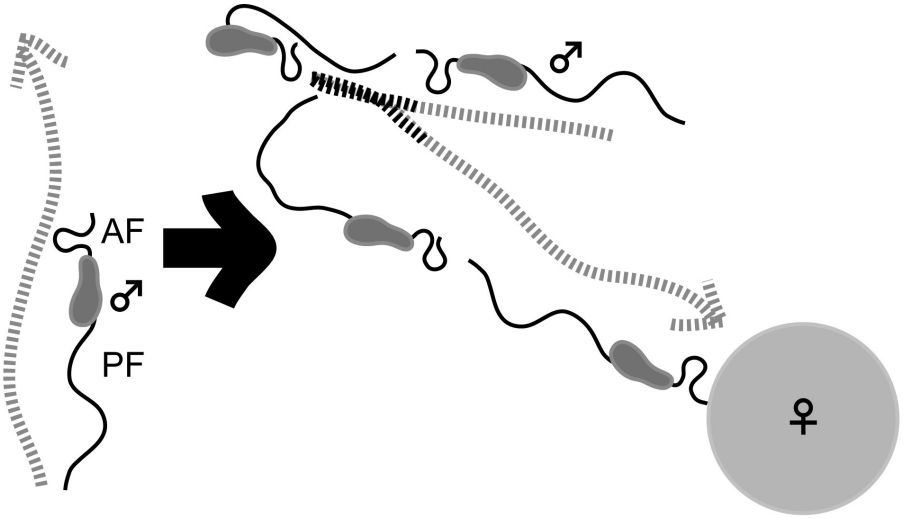

Plate 36

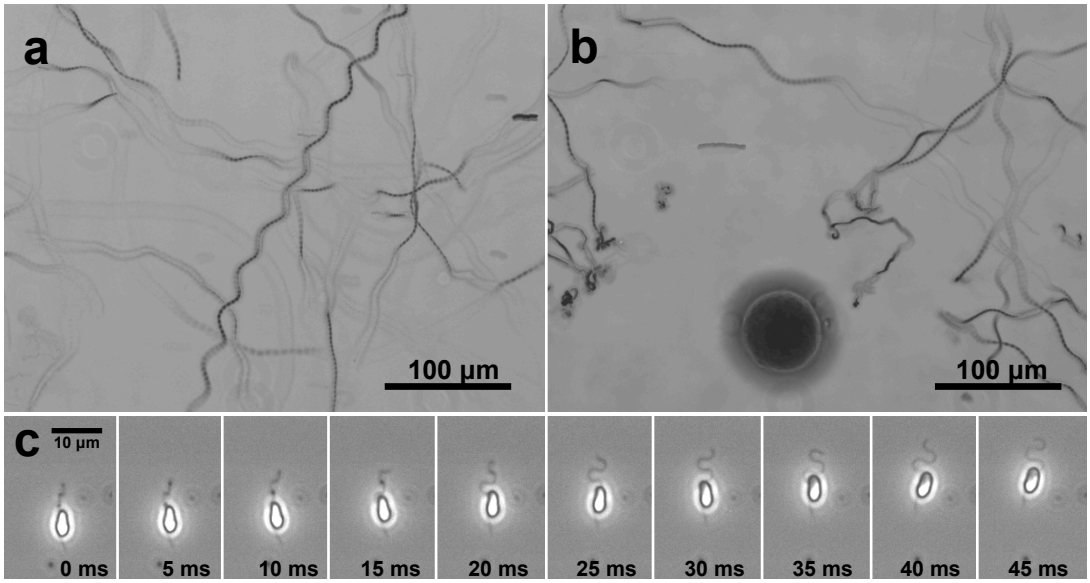
a
100 µm
b
100 µm
c
10 µm
0 ms
5 ms
10 ms
15 ms
20 ms
25 ms
30 ms
35 ms
40 ms
45 ms

Plate 37

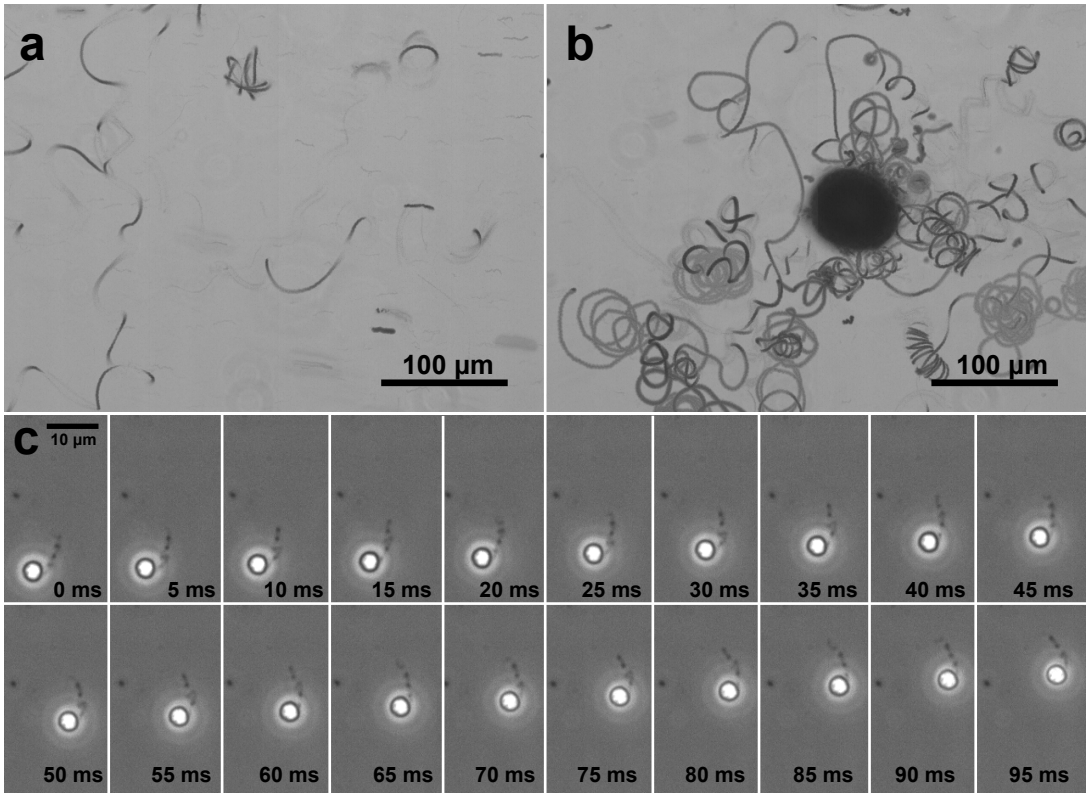
a
100 µm
b
100 µm
c
10 µm
0 ms
5 ms
10 ms
15 ms
20 ms
25 ms
30 ms
35 ms
40 ms
45 ms
50 ms
55 ms
60 ms
65 ms
70 ms
75 ms
80 ms
85 ms
90 ms
95 ms

Plate 38

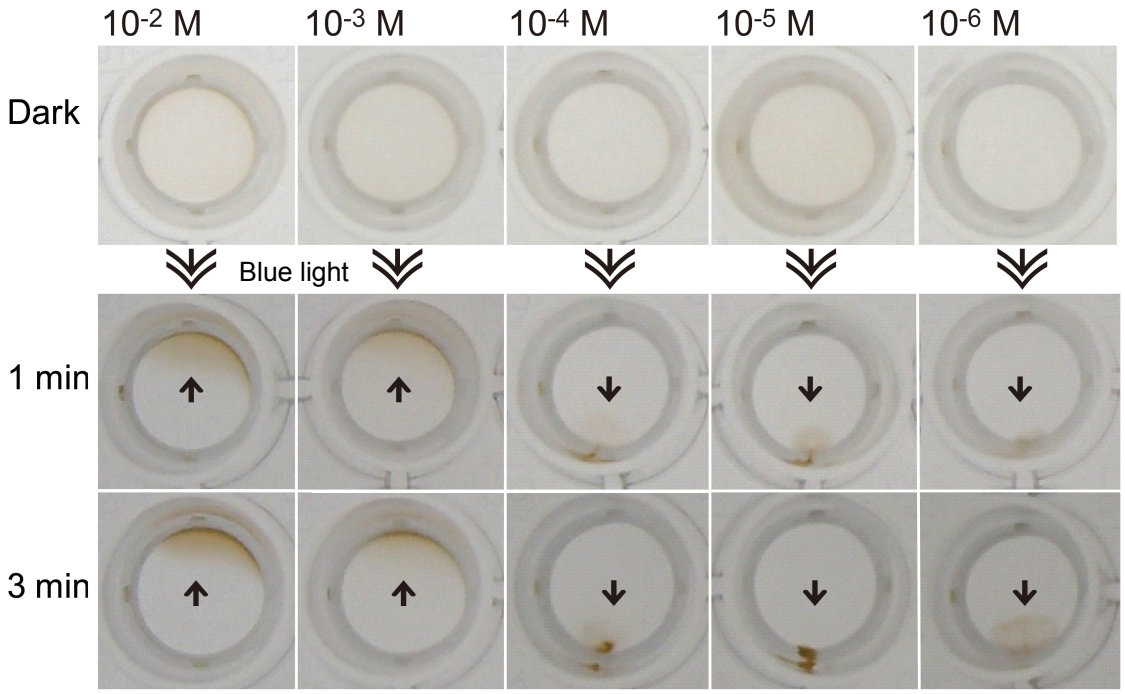

Plate 39

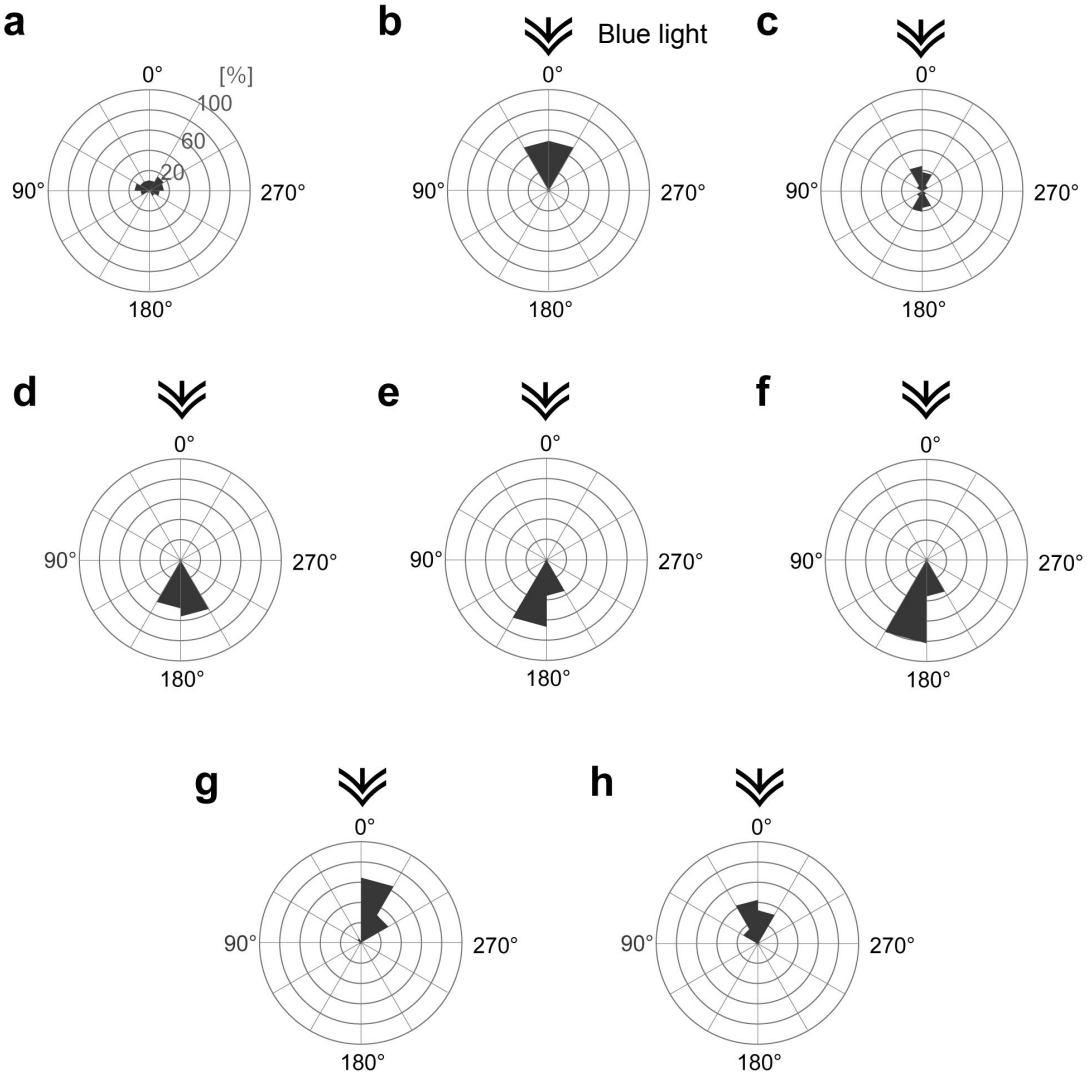
a
0°
[%]
100
60
20
90°
270°
180°
b
Blue light
0°
90°
270°
180°
c
0°
90°
270°
180°
d
0°
90°
270°
180°
e
0°
90°
270°
180°
f
0°
90°
270°
180°
g
0°
90°
270°
180°
h
0°
90°
270°
180°

Plate 40

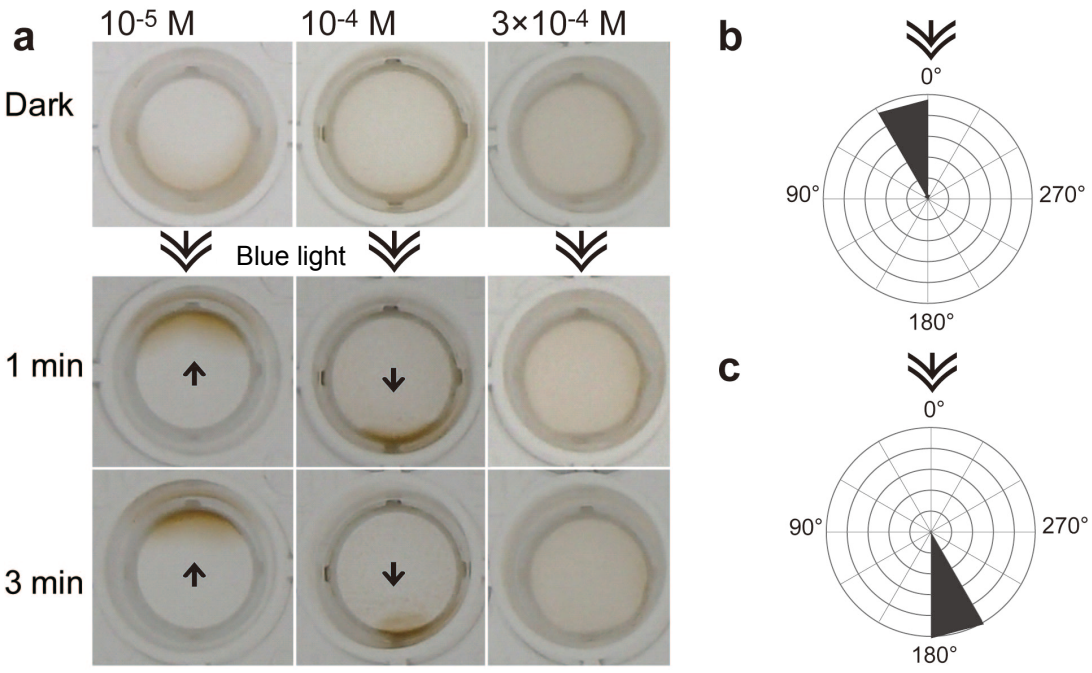
a
10-5 M
10-4 M
3×10-4 M
Dark
Blue light
1 min
3 min
b
0°
90°
270°
180°
c
0°
90°
270°
180°

Plate 41

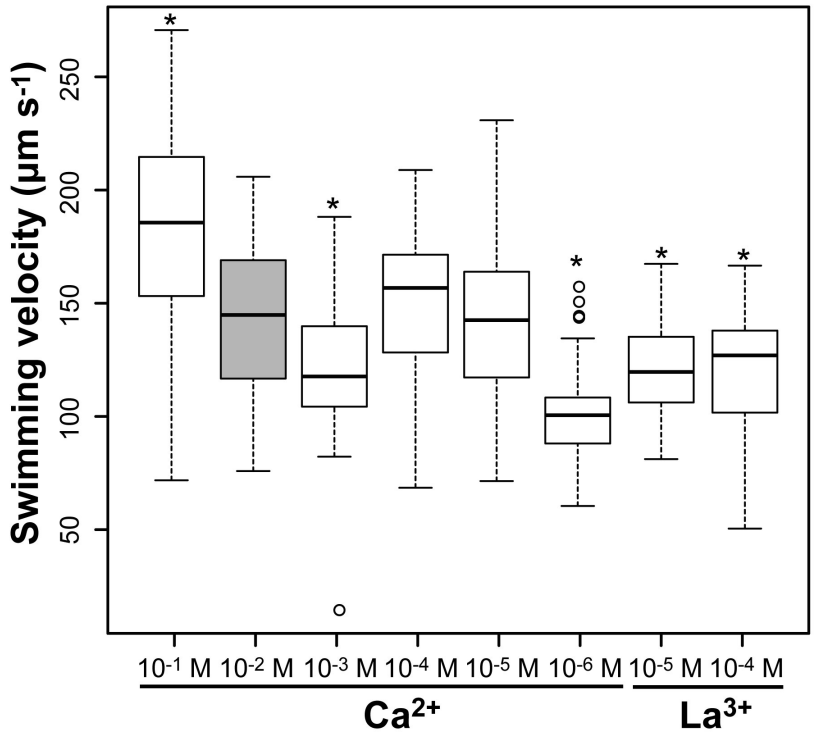
Swimming velocity (µm s-1)
50
100
150
200
250
10-1 M
10-2 M
10-3 M
10-4 M
10-5 M
10-6 M
10-5 M
10-4 M
Ca2+
La3+

Plate 42

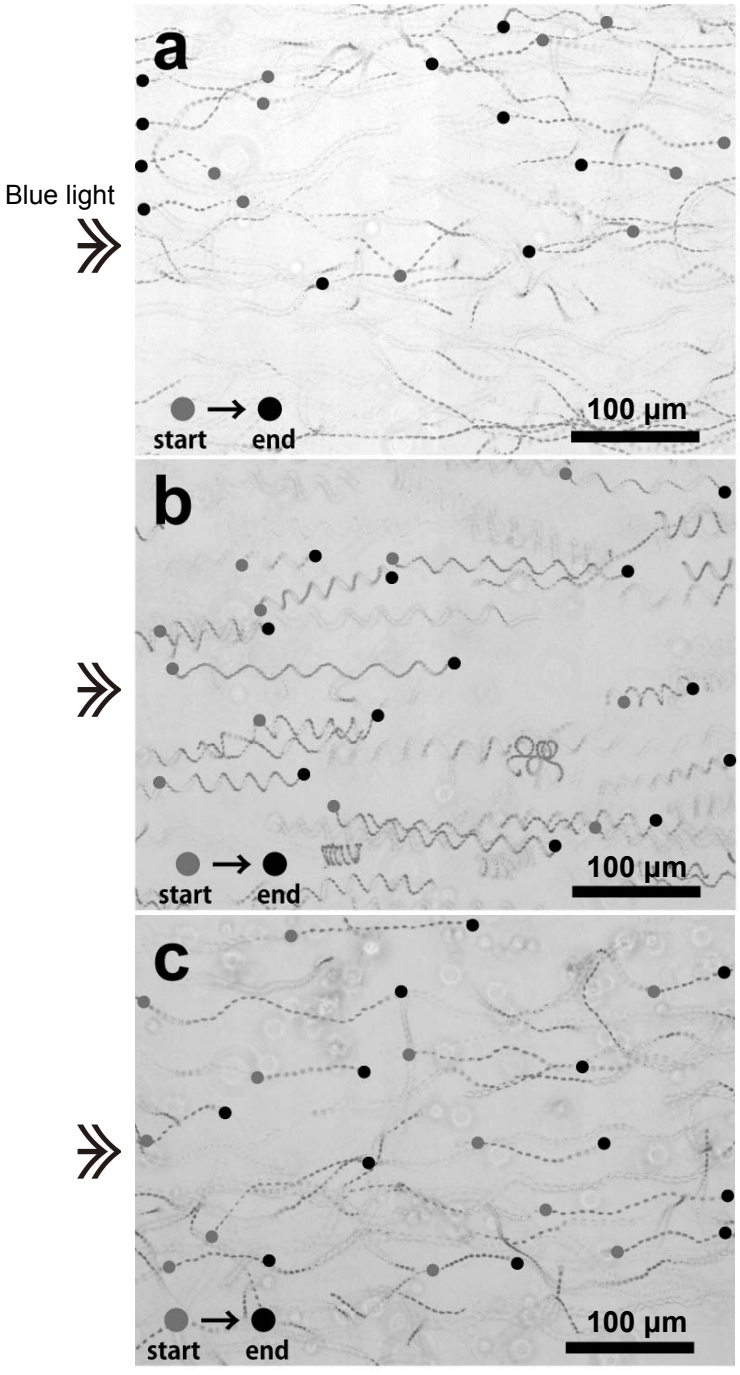
Blue light
a
start
end
100 µm
b
start
end
100 µm
c
start
end
100 µm

Plate 43

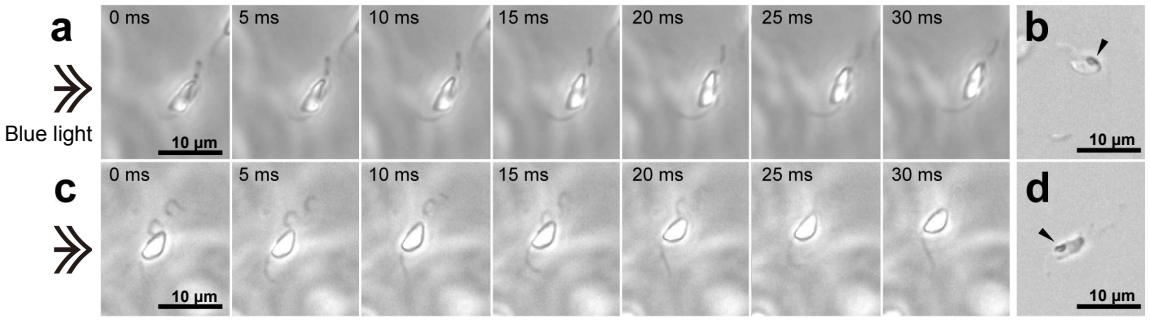
a
Blue light
0 ms
5 ms
10 ms
15 ms
20 ms
25 ms
30 ms
10 µm
b
10 µm
c
0 ms
5 ms
10 ms
15 ms
20 ms
25 ms
30 ms
10 µm
d
10 µm

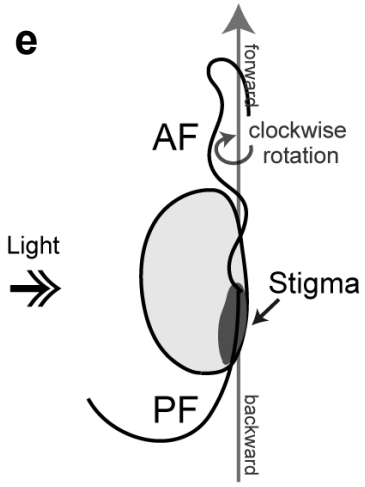
e
forward
AF
clockwise
rotation
Light
Stigma
PF
backward

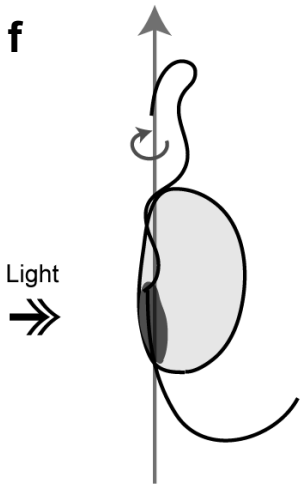
f
Light

Plate 44

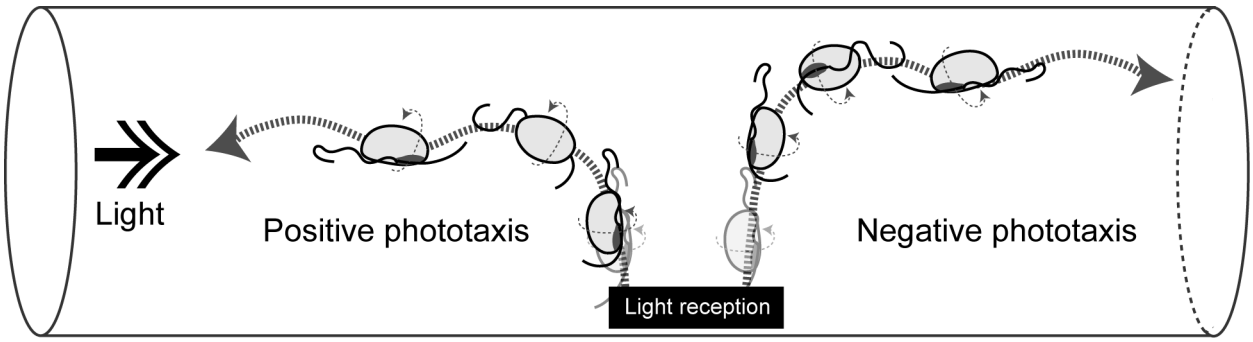
Light
Positive phototaxis
Light reception
Negative phototaxis

Plate 45

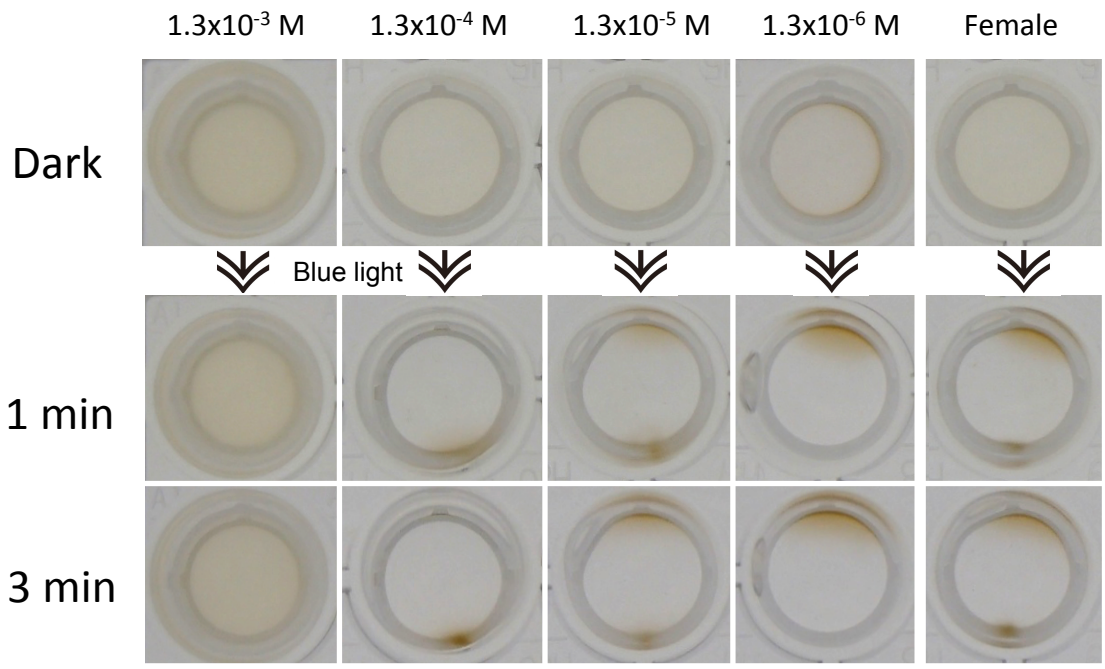
1.3x10-3 M
1.3x10-4 M
1.3x10-5 M
1.3x10-6 M
Female
Dark
Blue light
1 min
3 min

Plate 46

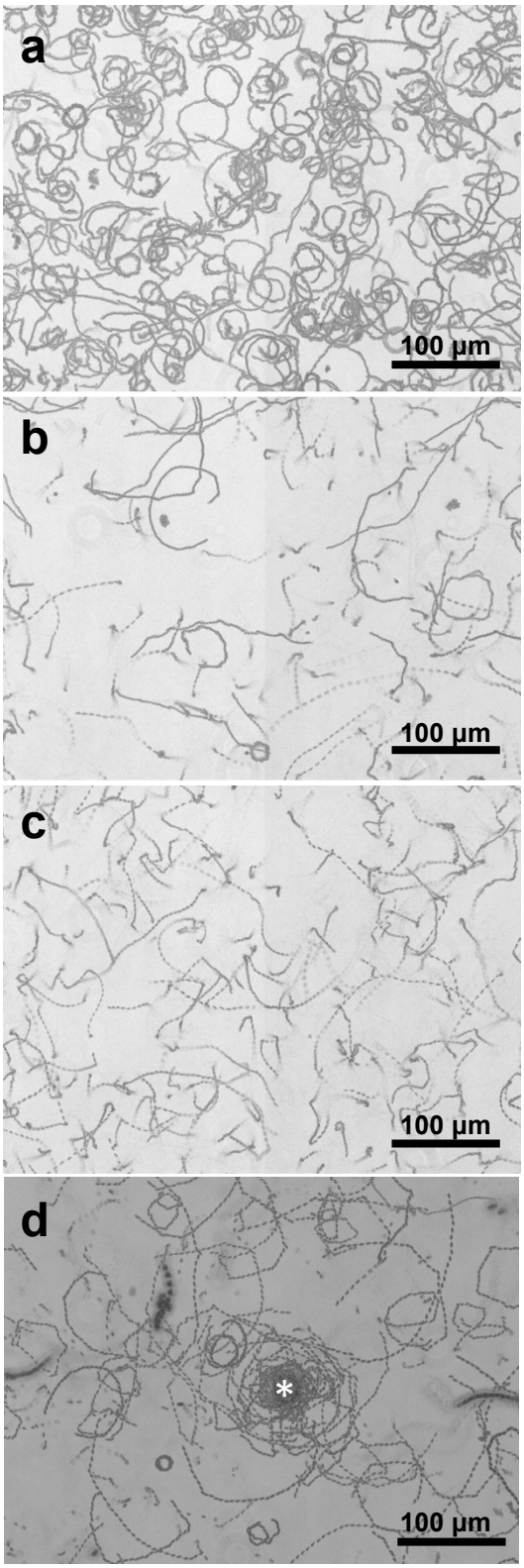

Plate 47

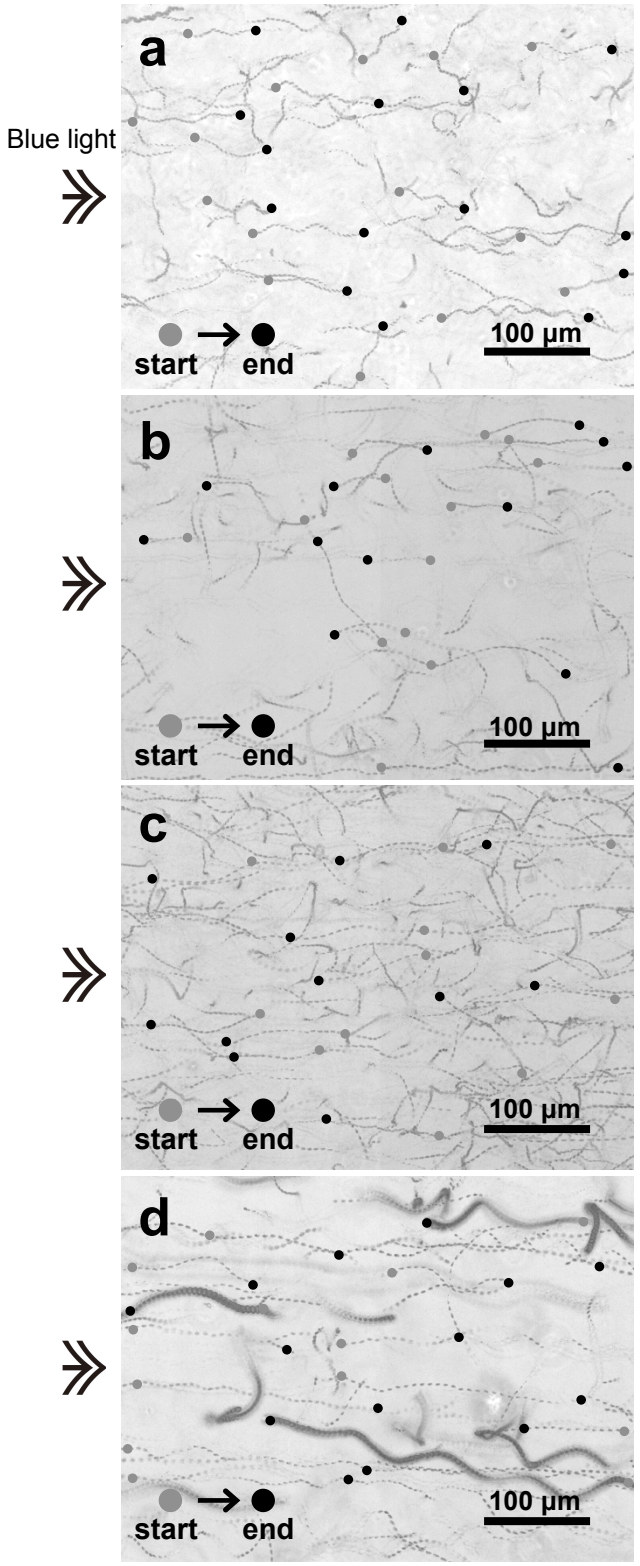
Blue light
a
start
end
100 µm
b
start
end
100 µm
c
start
end
100 µm
d
start
end
100 µm

Plate 48

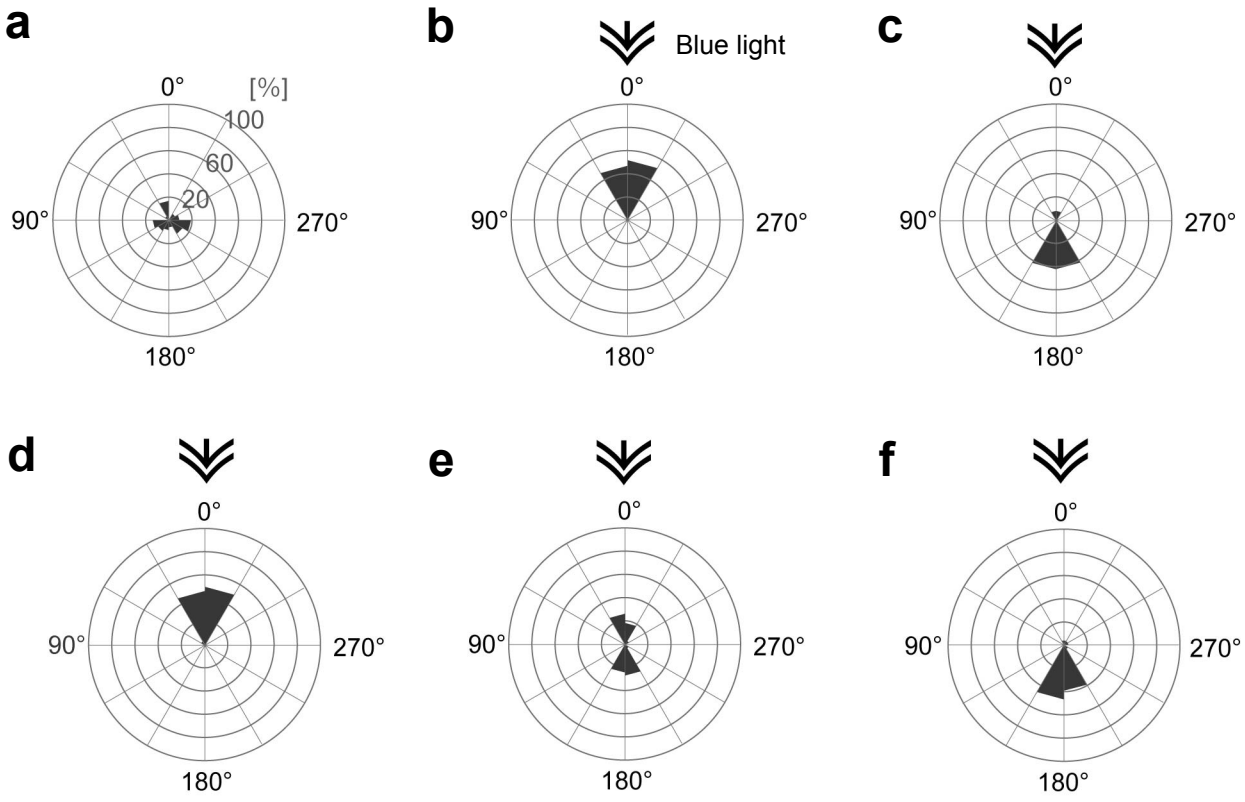
a
0°
[%]
100
60
20
90°
270°
180°
b
Blue light
0°
90°
270°
180°
c
0°
90°
270°
180°
d
0°
90°
270°
180°
e
0°
90°
270°
180°
f
0°
90°
270°
180°

Plate 49

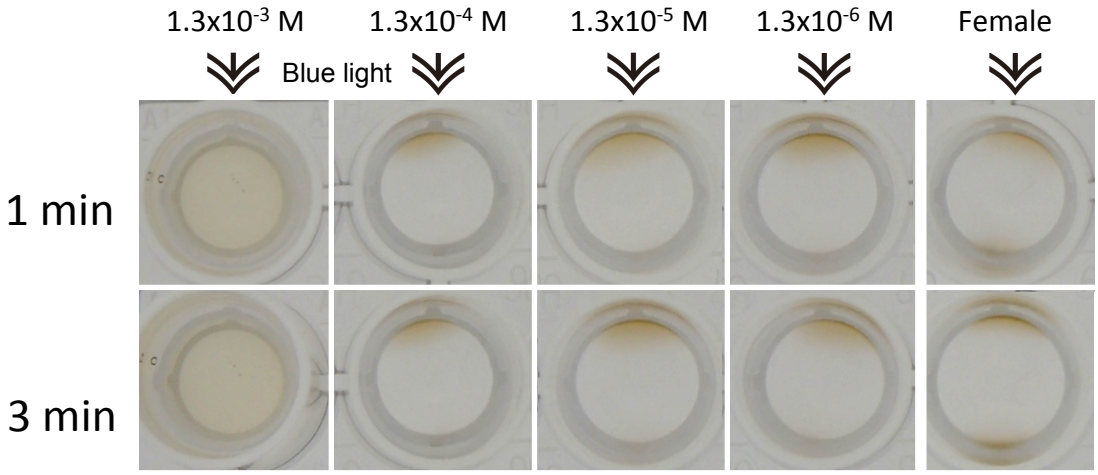
1.3x10-3 M
1.3x10-4 M
1.3x10-5 M
1.3x10-6 M
Female
Blue light
1 min
3 min

Plate 50

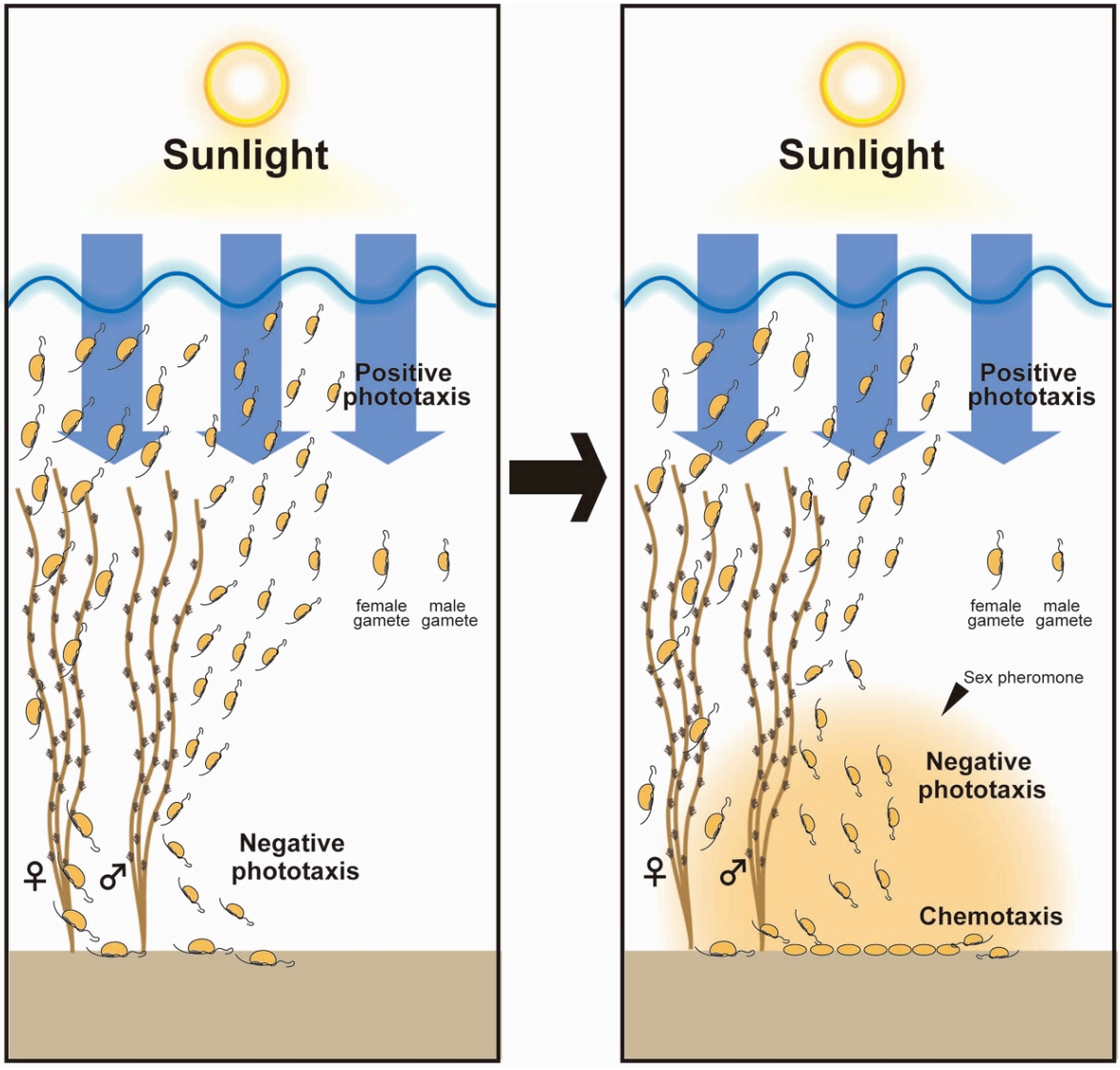

Without sex pheromone **With sex pheromone**

Plate 51

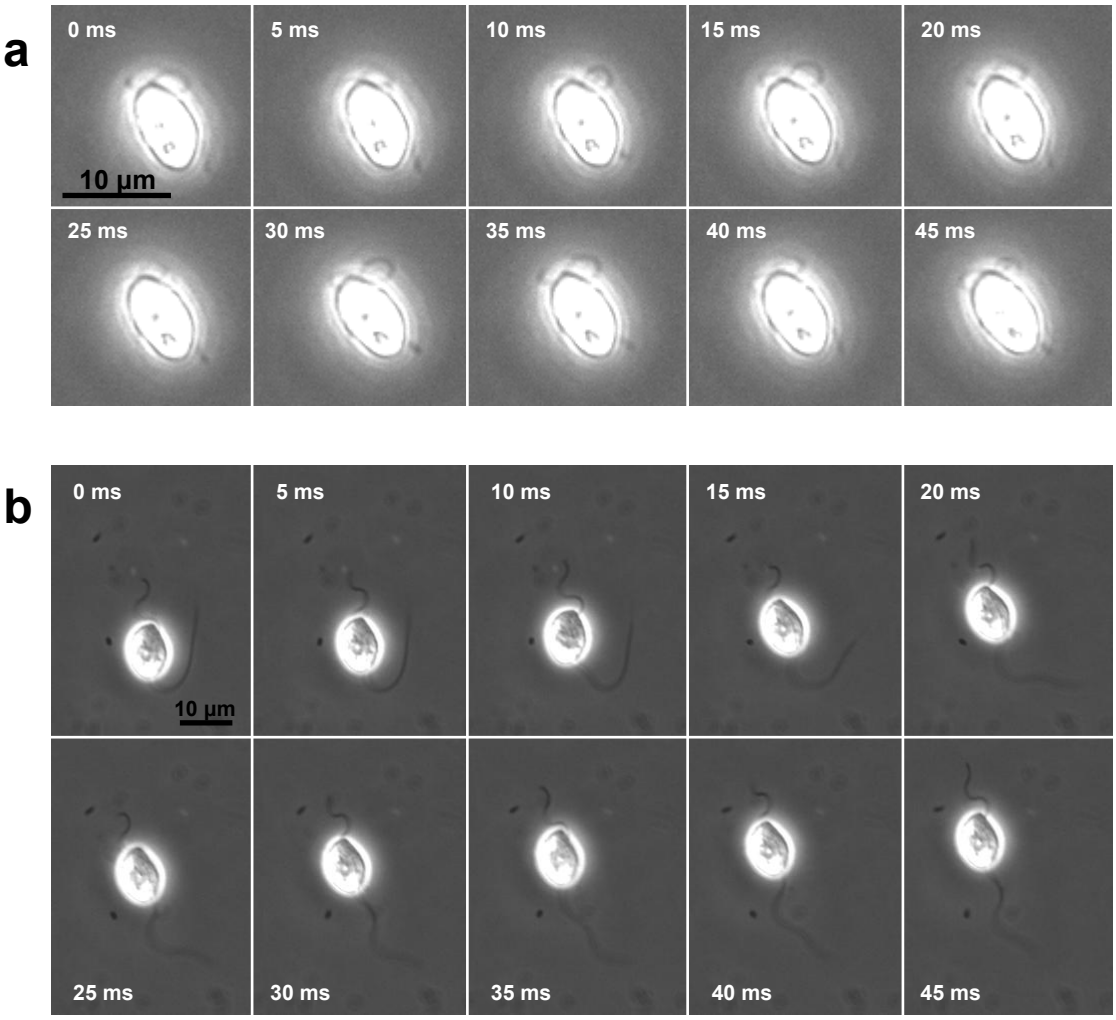
a
0 ms
5 ms
10 ms
15 ms
20 ms
10 µm
25 ms
30 ms
35 ms
40 ms
45 ms
b
0 ms
5 ms
10 ms
15 ms
20 ms
10 µm
25 ms
30 ms
35 ms
40 ms
45 ms

Plate 52

a

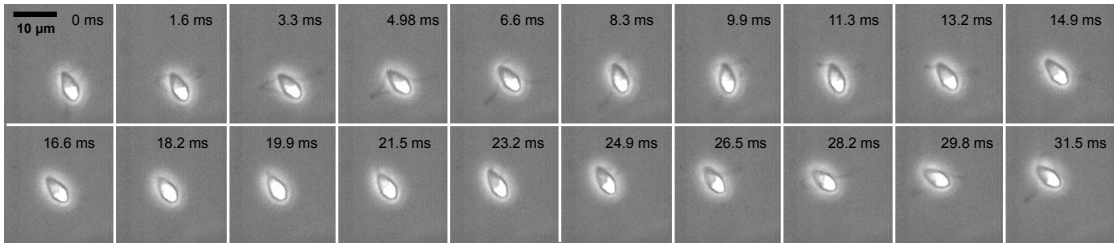
10 µm
0 ms
1.6 ms
3.3 ms
4.98 ms
6.6 ms
8.3 ms
9.9 ms
11.3 ms
13.2 ms
14.9 ms
16.6 ms
18.2 ms
19.9 ms
21.5 ms
23.2 ms
24.9 ms
26.5 ms
28.2 ms
29.8 ms
31.5 ms

b

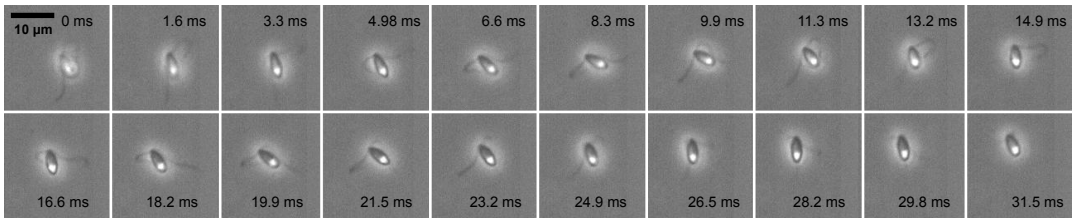
10 µm
0 ms
1.6 ms
3.3 ms
4.98 ms
6.6 ms
8.3 ms
9.9 ms
11.3 ms
13.2 ms
14.9 ms
16.6 ms
18.2 ms
19.9 ms
21.5 ms
23.2 ms
24.9 ms
26.5 ms
28.2 ms
29.8 ms
31.5 ms

c

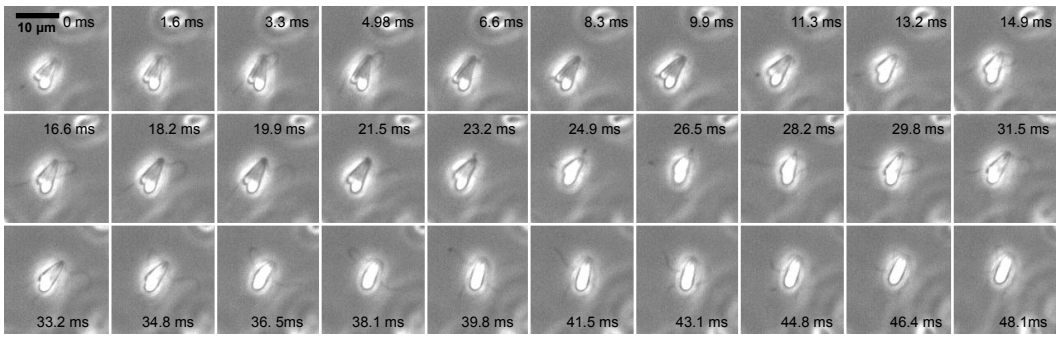
10 µm
0 ms
1.6 ms
3.3 ms
4.98 ms
6.6 ms
8.3 ms
9.9 ms
11.3 ms
13.2 ms
14.9 ms
16.6 ms
18.2 ms
19.9 ms
21.5 ms
23.2 ms
24.9 ms
26.5 ms
28.2 ms
29.8 ms
31.5 ms
33.2 ms
34.8 ms
36. 5ms
38.1 ms
39.8 ms
41.5 ms
43.1 ms
44.8 ms
46.4 ms
48.1ms